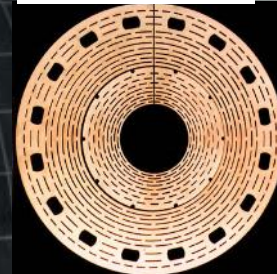


National High Magnetic Field Laboratory



Florida State University

45T Hybrid DC Magnet



1.4 GW Generator

Los Alamos National Laboratory



101T Pulse Magnet
10mm bore

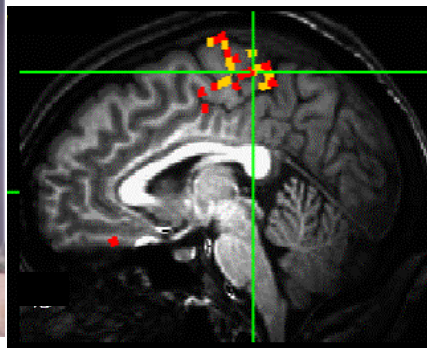


University of Florida

Advanced Magnetic Resonance Imaging and Spectroscopy Facility



11.4T MRI Magnet
400mm warm bore

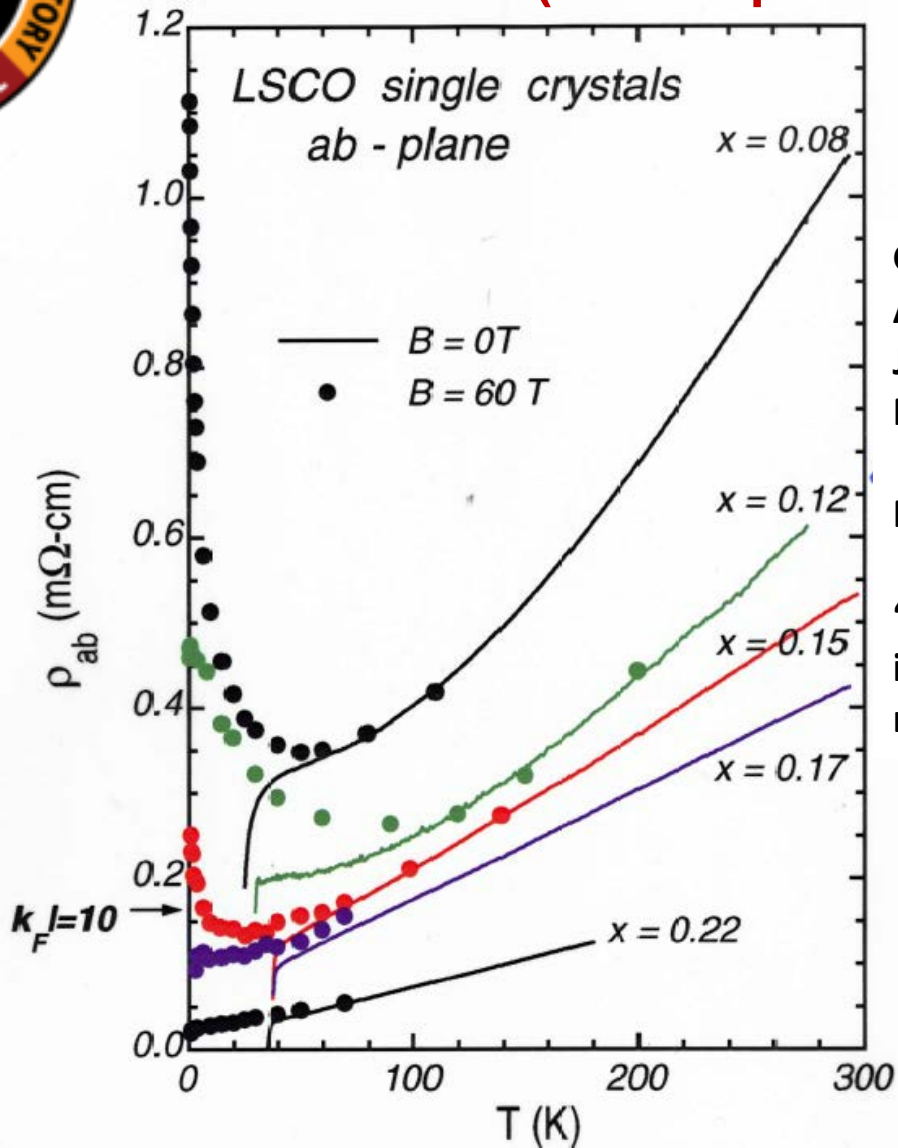


High B/T Facility
17T, 6weeks at 1mK

900MHz, 105mm bore
21T NMR/MRI Magnet



Evidence for a Phase Transition Near Optimum Doping in the Cuprates (1995 to present)



G.S. Boebinger, Yoichi Ando,
A. Passner, T. Kimura, M. Okuya,
J. Shimoyama, K. Kishio, K. Tamasaku,
N. Ichikawa, and S. Uchida,

Phys. Rev. Lett. 77, 5417 (1996)

“Insulator-to-metal crossover
in the normal state of $\text{La}_{2-x}\text{Sr}_x\text{CuO}_4$
near optimum doping.”



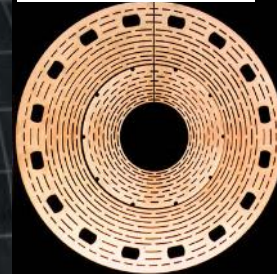
Overview of the MagLab User Program

National High Magnetic Field Laboratory



Florida State University

45T Hybrid DC Magnet



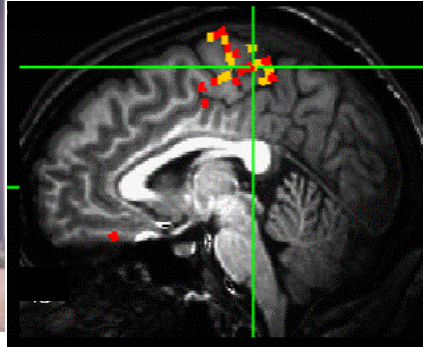
University of Florida

Advanced Magnetic Resonance Imaging and Spectroscopy Facility



High B/T Facility
17T, 6weeks at 1mK

900MHz, 105mm bore
21T NMR/MRI Magnet

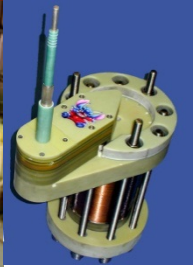


11.4T MRI Magnet
400mm warm bore

Los Alamos National Laboratory



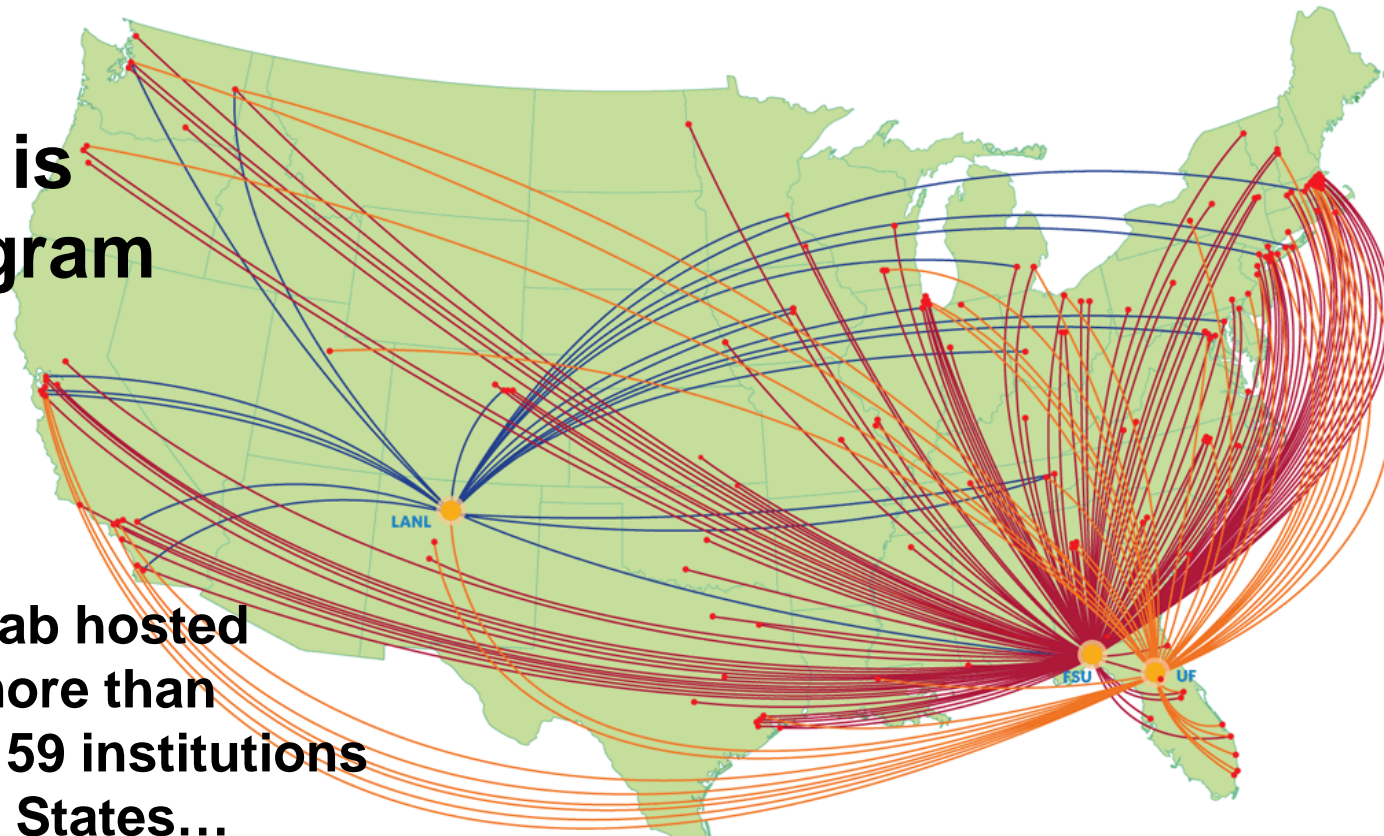
101T Pulse Magnet
10mm bore



1.4 GW Generator

The MagLab is its User Program

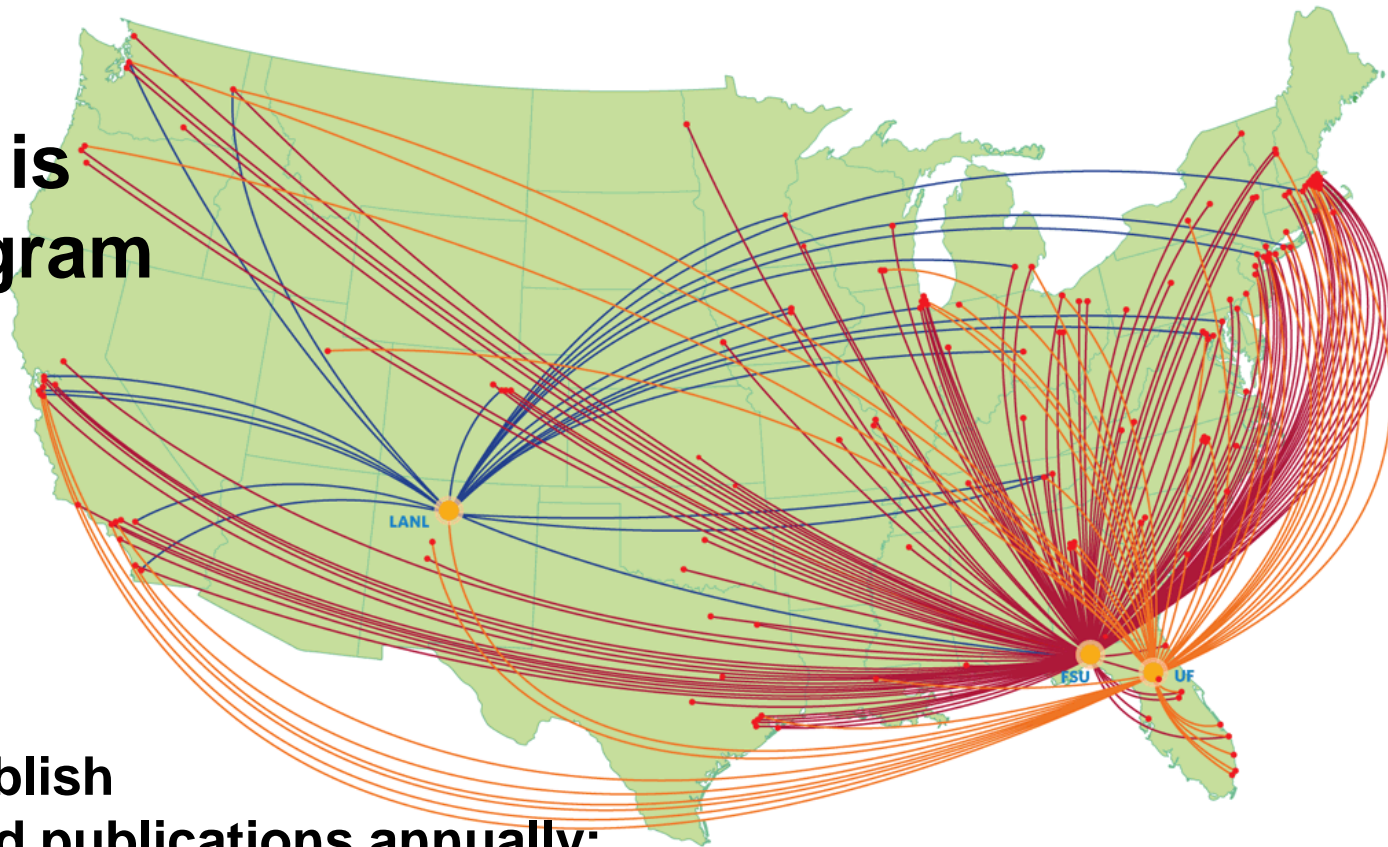
In 2012, the MagLab hosted experiments by more than 1350 users from 159 institutions across the United States...



...and a total of 277 institutions throughout the world.



The MagLab is its User Program



MagLab users publish
about 440 refereed publications annually:

2009-2013 Publications

2200 Total Publications

28 PNAS

63 Nature Journals

147 Physical Review Letters

318 Physical Review B

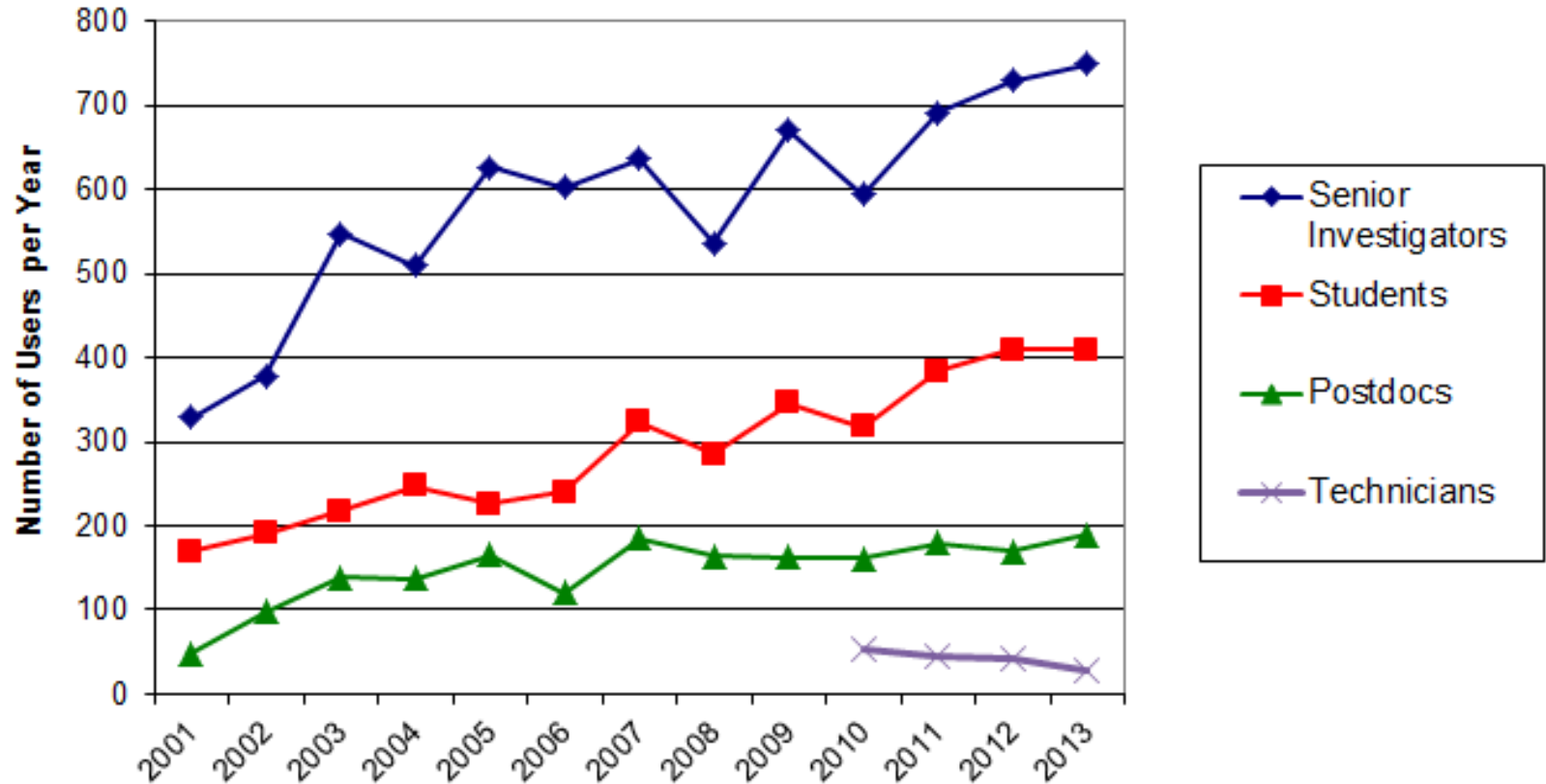
47 PRB (Rapid Comm)

59 JACS



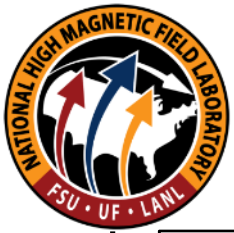


Magnet Lab User Profile 2001-2013 as of 2/3/2014

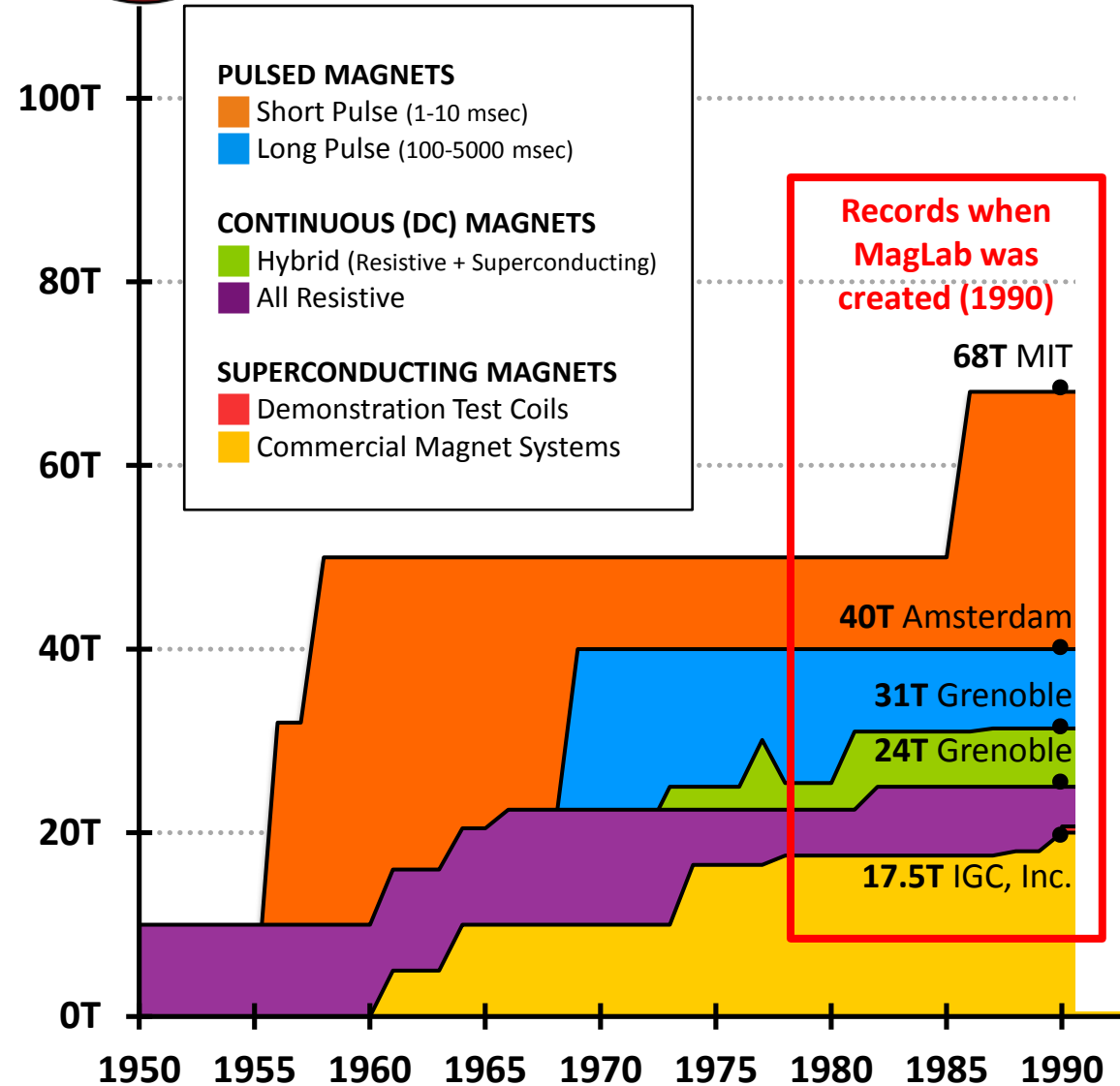


Hosting ~ 1350 Users annually: 55% senior investigators, 15% postdocs, 30% students

Hosting ~ 425 Principal Investigators annually, approximately 20% are new every year

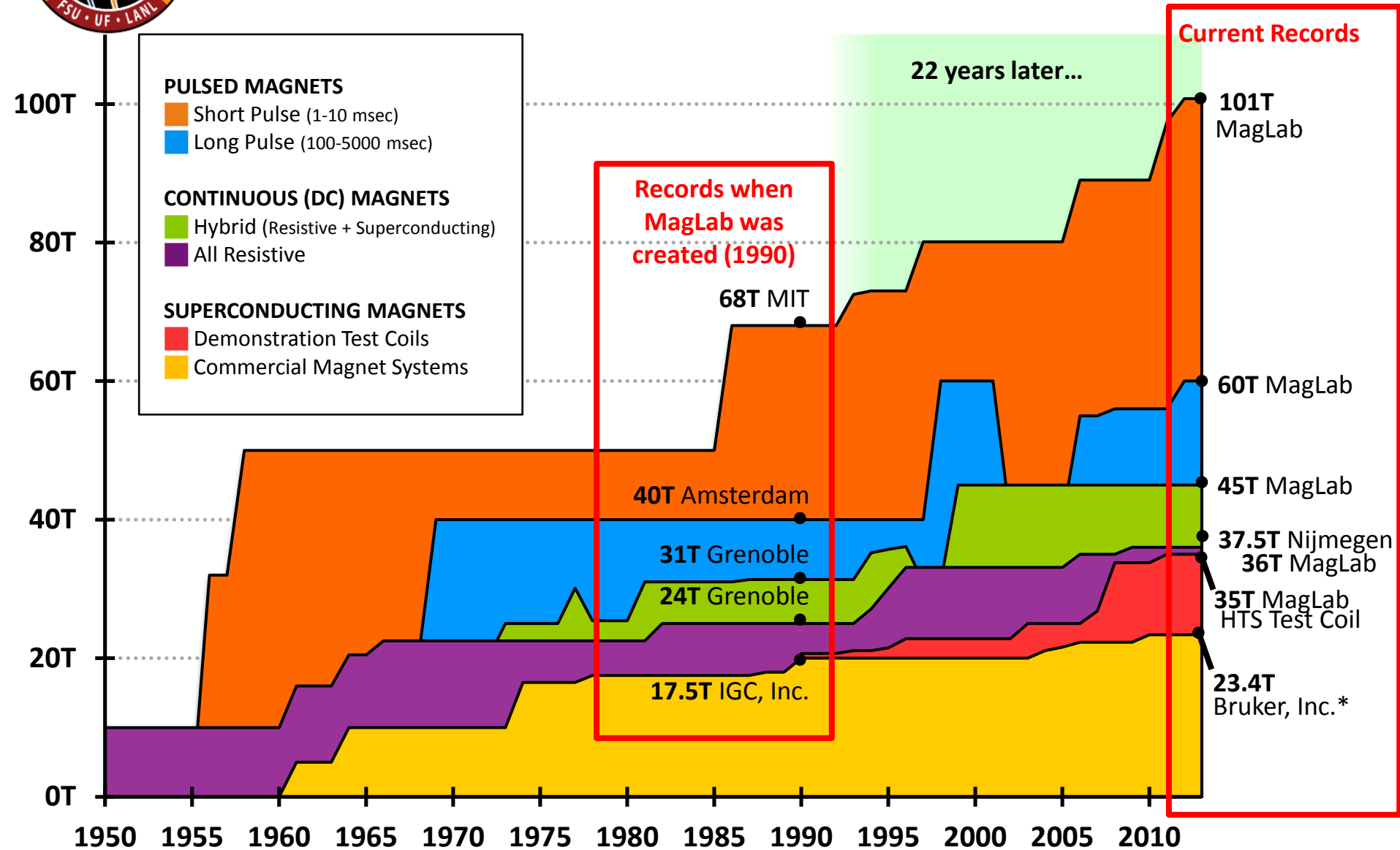


MagLab Technology Leads the World





MagLab Technology Leads the World





Welcome to our
laboratory
Watch the video

User Center
Request Magnet Time

[Vol 18 issue 4](#)



Mag Lab
Reports

[Issue 8](#)



▶ Join a MagLab geochemist on her journey to Tibet and discover why a MagLab engineer is thrilled to be working on one of the most complex machines ever built in our latest edition of *flux*. [Read more.](#)

[About us](#)



▶ Each year, our facilities support the science and engineering research projects of over 1000 users from all over the world. [Read more.](#)

◀◀ Previous News Item

Next News Item ▶▶

[Scientists at Work](#)



Today:

▶ **Kang Wang (UCLA)**

PROJECT: **Investigation of magnetic-field effect on topological insulator surface states**

WHEN: Monday, March 12 - Friday, March 16

WHERE: DC Field Facility

[Publications](#) — [Visitors](#) — [Seminars, Workshops & Conferences](#)

[Diversity initiatives](#)



▶ Learn about the Dependent Care travel program and the lab's other innovative diversity initiatives here. [Read more.](#)

MagLab Website:
magnet.fsu.edu

Click on **“Search Pubs”** for all refereed publications from the user program

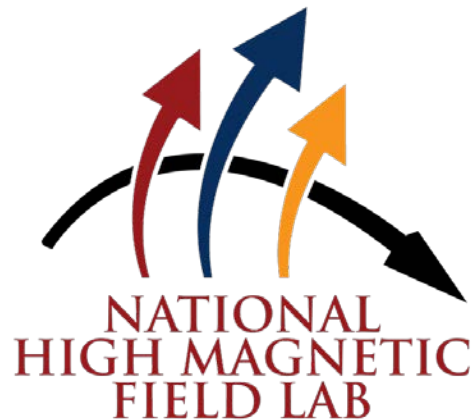
Click on **“Publications & Reports”** for :

MagLab Reports, our scientific outreach magazine

and **Flux**, our outreach magazine for the general public



**...we look forward to hosting you
at the MagLab**



**We host ~ 1400 magnet users annually
...20% of our Principal Investigators are first-timers.**



To request magnet time, apply online: www.magnet.fsu.edu



The Cuprates: The Early Years



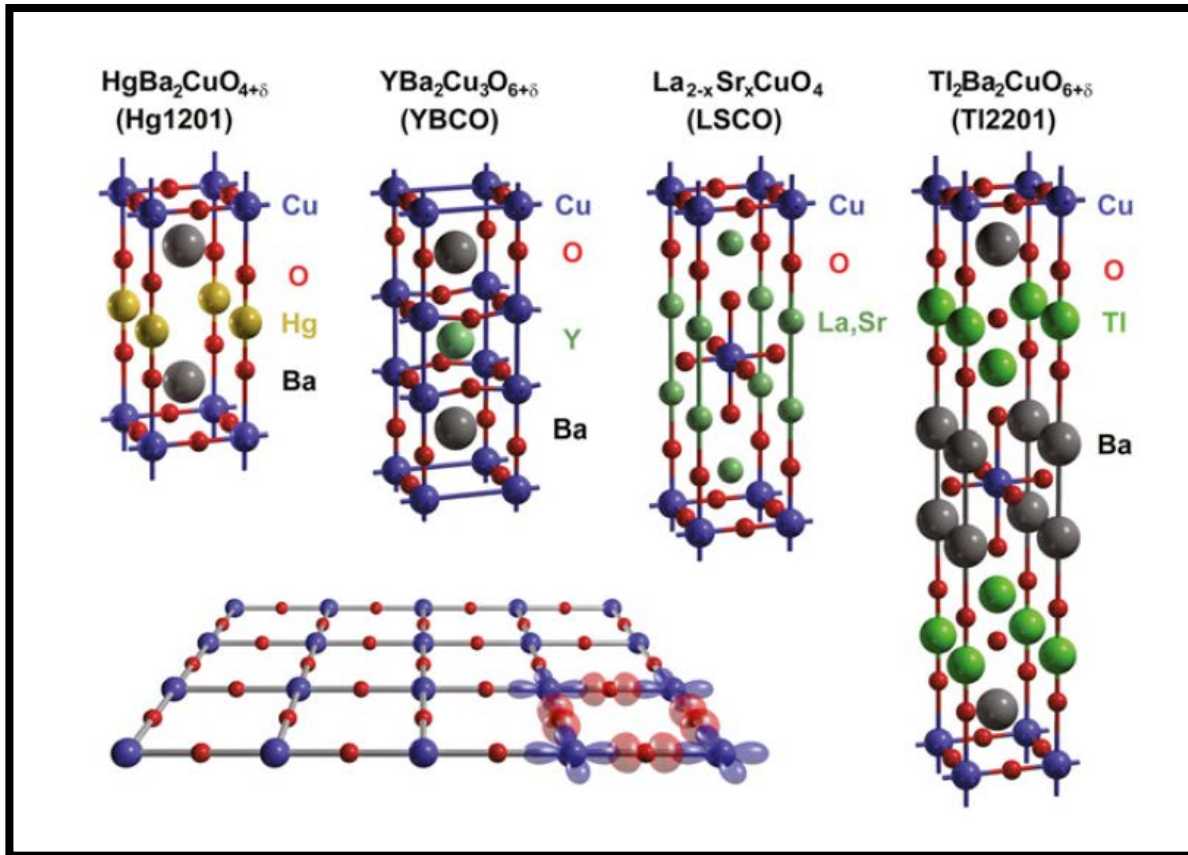
Key Ingredients for Cuprate Superconductivity

$T_c=94$ K

$T_c=94$ K

$T_c=39$ K

$T_c=90$ K

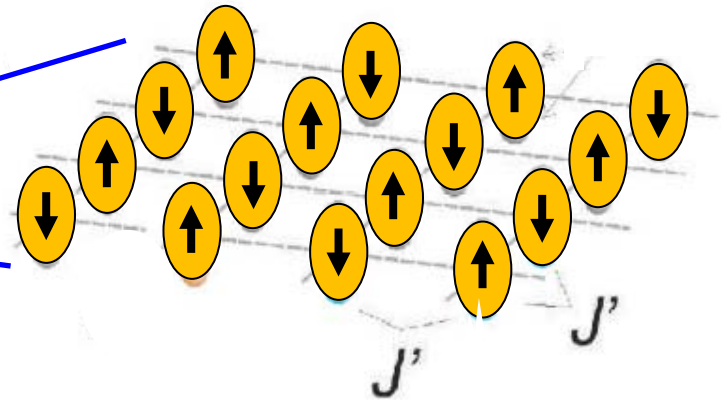
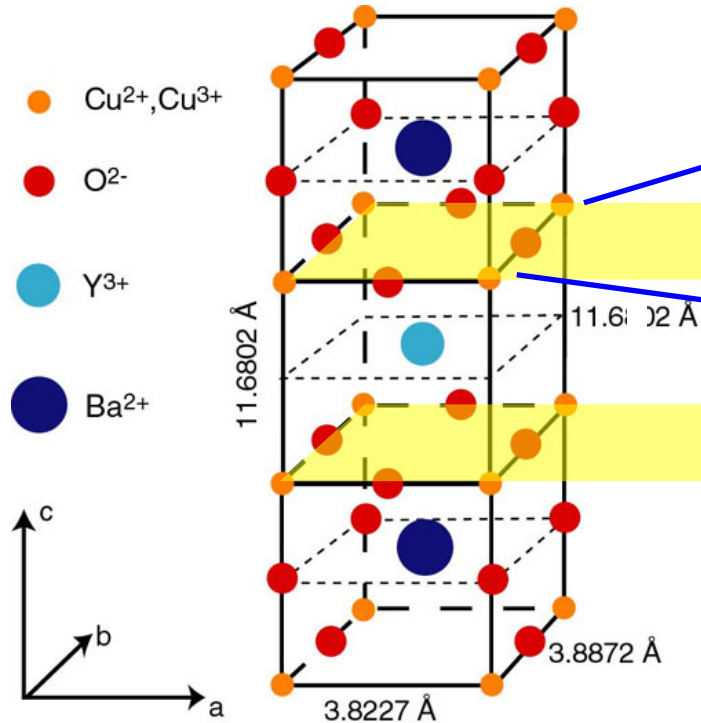


Barisic, N *et al.*, PNAS (2013)



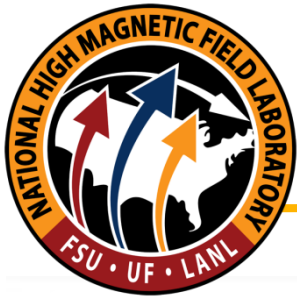
First Key Ingredient for ('Cuprate') High-Temperature Superconductors:

the Copper – Oxygen Plane



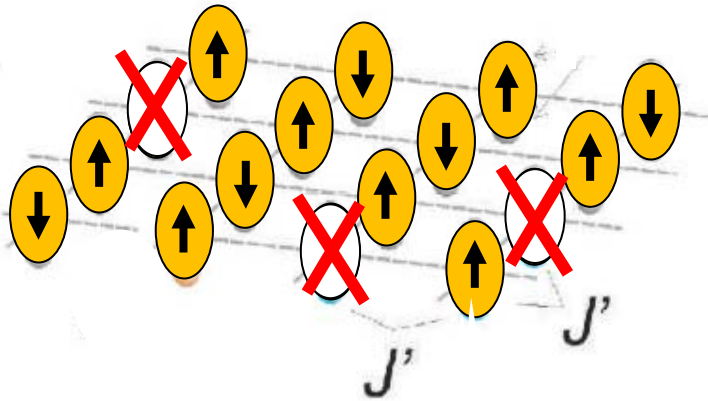
The 2D Copper-Oxygen Plane...
*...the playground of high-temperature
superconductivity*

**With one electron on each Copper atom,
the electrons cannot move
...and you have an insulator**



Second Key Ingredient for ('Cuprate') High-Temperature Superconductors:

Removing electrons from the Copper – Oxygen Plane

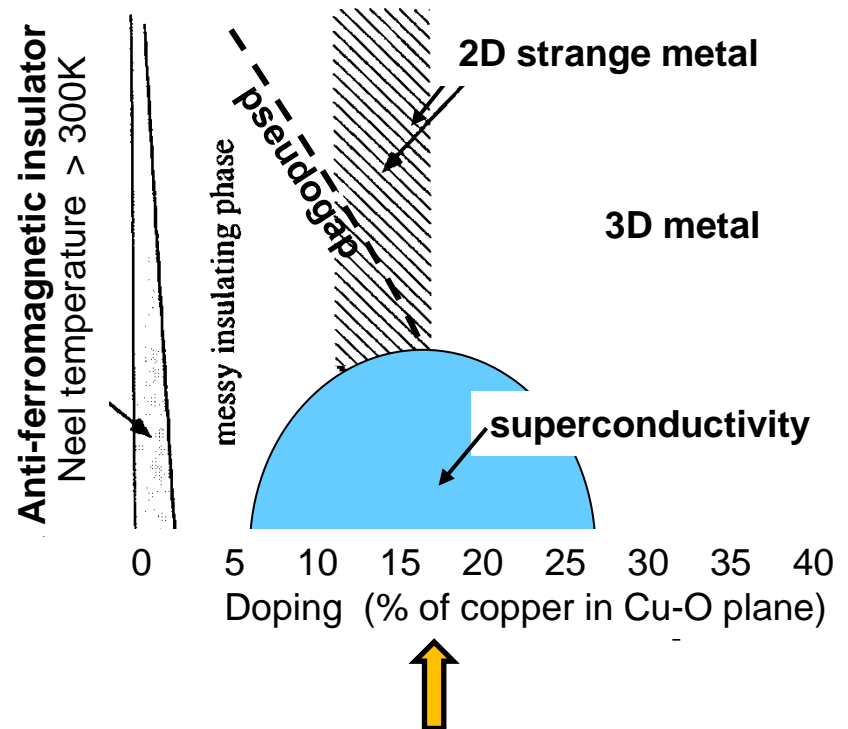


With one electron on each Copper atom,
the electrons cannot move
...and you have an insulator

However, remove ~5% to ~27%

of the electrons...

...and you have a High-Tc Superconductor

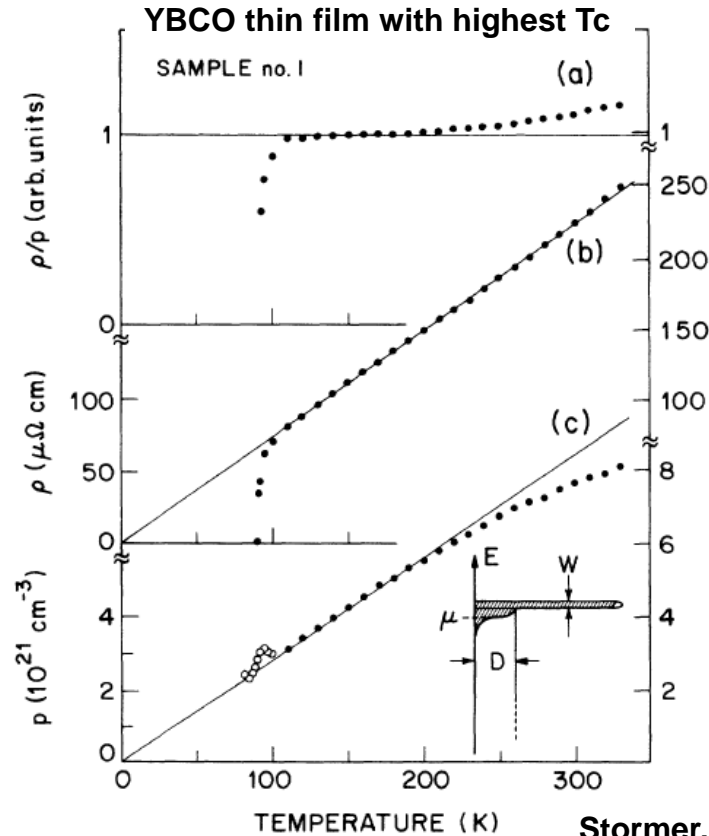


For more than a dozen different materials, the same 16% doping
...*optimizes superconductivity (highest transition temperature)*

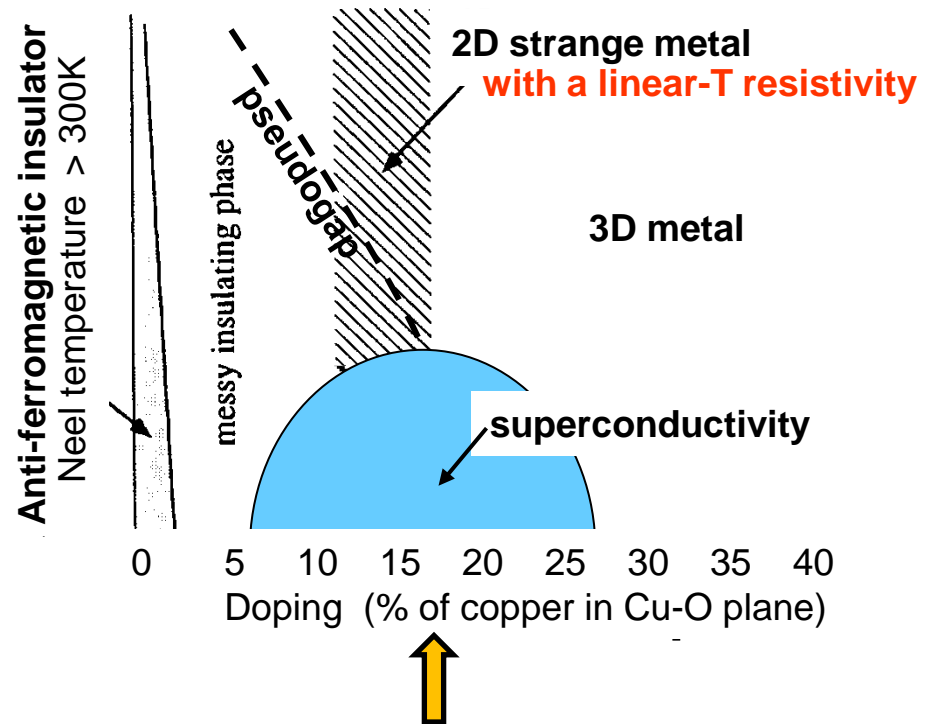


Second Key Ingredient for ('Cuprate') High-Temperature Superconductors:

Removing electrons from the Copper – Oxygen Plane



Storner, et al. PR B38, 2472 (1988)



For more than a dozen different materials, the same 16% doping
 ...*optimizes superconductivity (highest transition temperature)*
 ...*optimizes linear-T resistivity*

Phase Diagram of the High- T_c Superconductors

July 7, 2014, c.9:30am

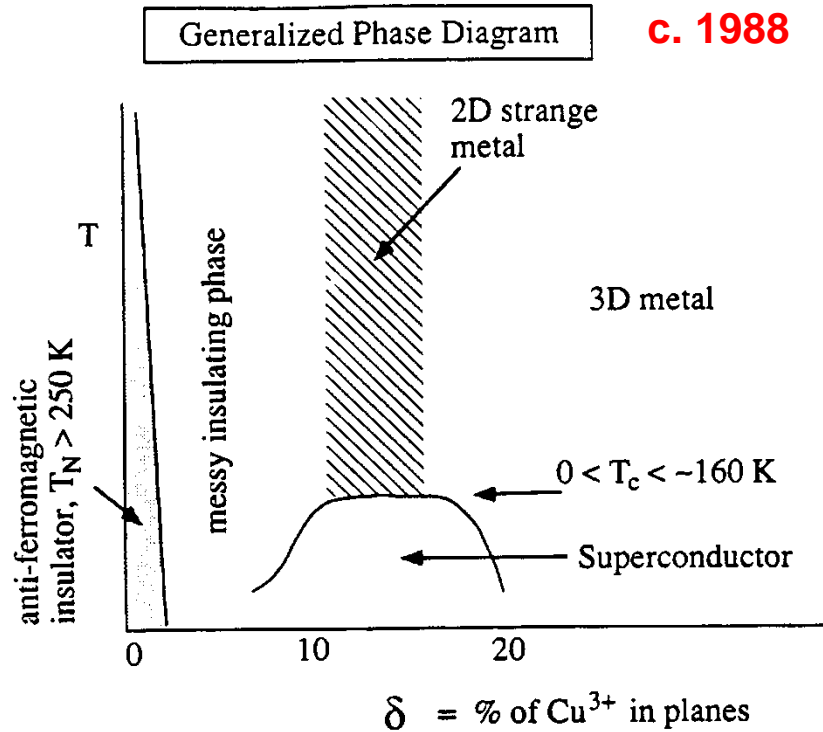
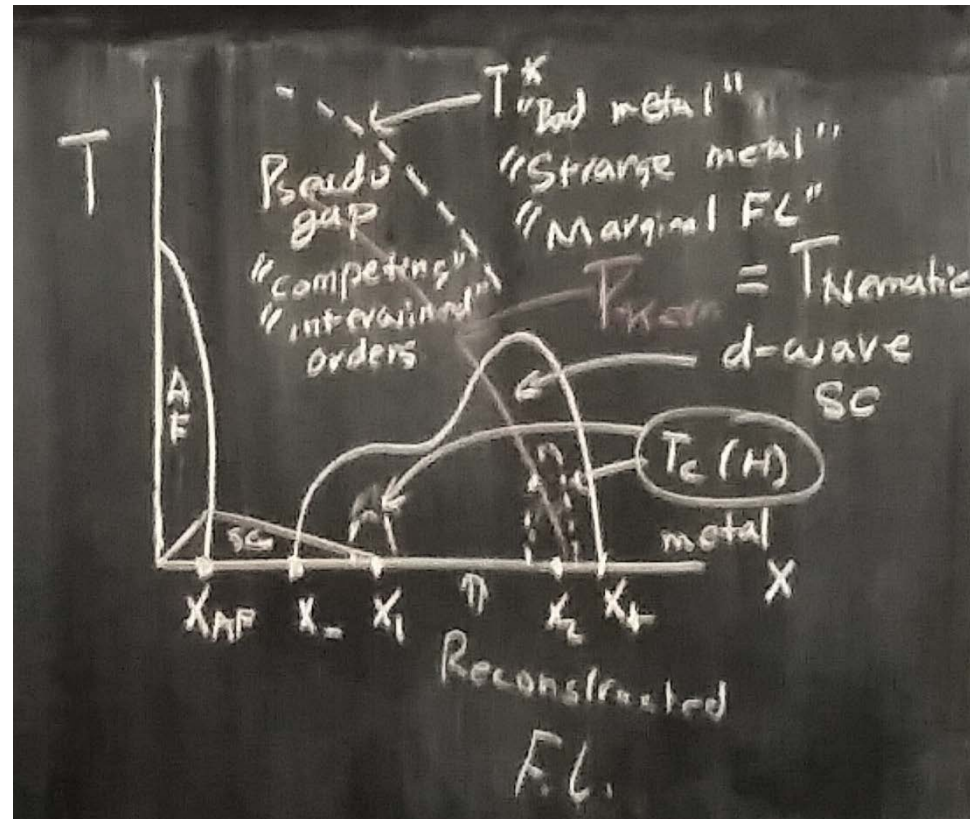


Figure 3.26. "Generalized Phase Diagram" as seen (roughly) in $(\text{La} - \text{Sr})\text{CuO}_4$.





Suppressing Superconductivity with Magnetic Fields

**to Probe the Abnormal Normal State
in the Zero-Temperature Limit**

The Abnormal Normal State of the High- T_c Superconductors

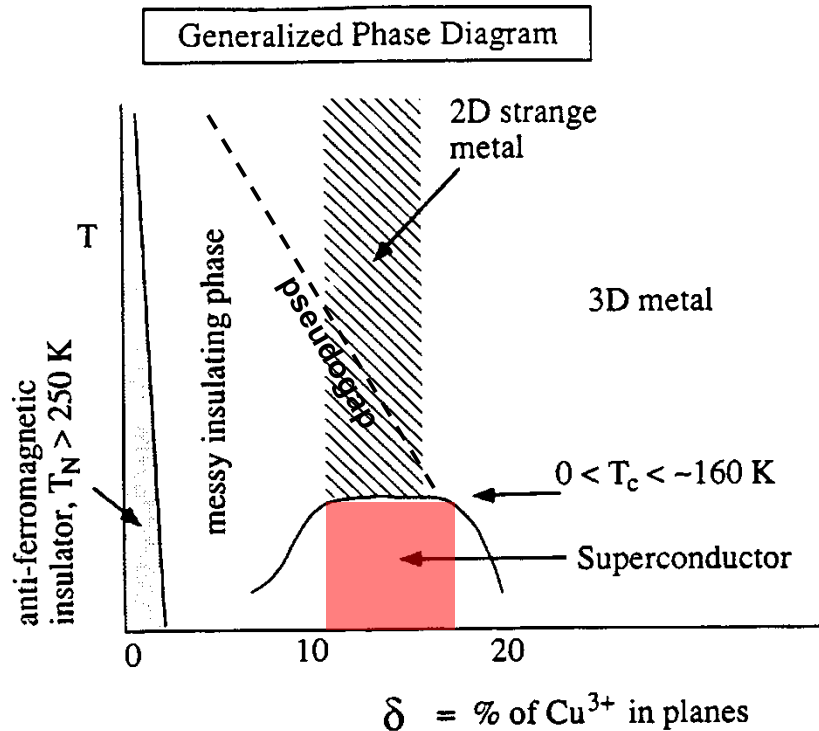


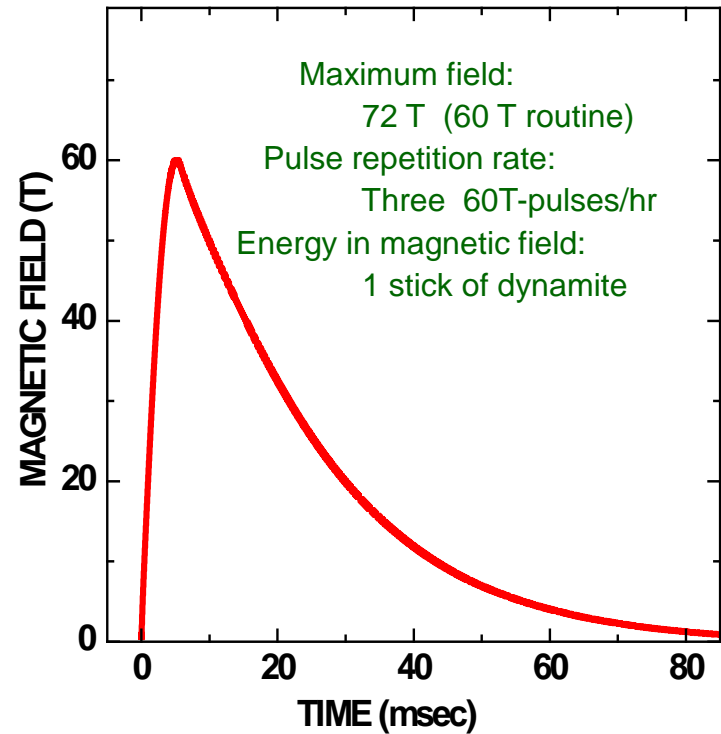
Figure 3.26. "Generalized Phase Diagram" as seen (roughly) in $(La - Sr)CuO_4$.

SUPERCONDUCTORS IN THE NORMAL STATE		
Experiment	Cuprates	BCS Superconductors
Optical conductivity	Metallic in C-O plane	Metallic in all directions
Resistivity	Increases linearly with temperature	Linear increase with temp. at high temp. Faster at low temp.
Hall effect	Temperature-dependent	Non-temperature-dependent
Neutron scattering	Temperature-dependent magnetic signature	Non-temperature-dependent
NMR spin relaxation rate	Increases nonlinearly with temp. above T_c	Increases linearly with temp. above T_c
NMR spin susceptibility	Pseudogap	No pseudogap
Specific heat	Pseudogap	No pseudogap
Photoemission	D-wave pseudogap	No pseudogap
Electron tunneling	Pseudogap, superconducting gap same size	No pseudogap
Electronic Raman scattering	Pseudogap	No pseudogap
Phonon frequency shift	Pseudogap	No pseudogap

Anderson, Science 256, 1526 (1992) and Research News, Science 278, 1879 (1997)

Using 60 teslas....to suppress the superconducting state and reveal the normal-state phase diagram

Pulsed Magnet Facility, Bell Laboratories (1990-1998)



Energy = 1 stick of dynamite

Energy = 1 jelly doughnut

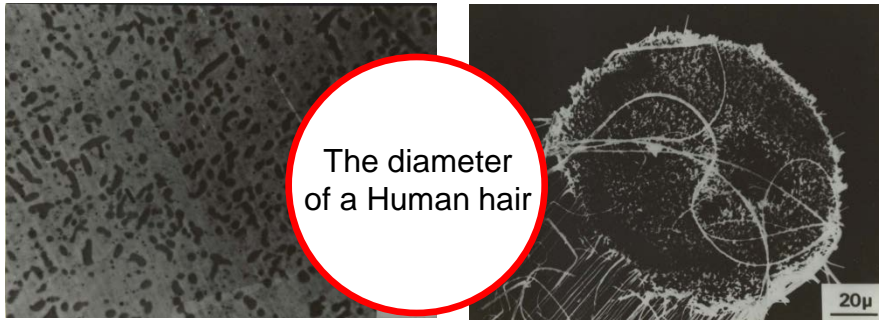
Challenges in Producing High Magnetic Fields

Pressure Under Water

12 feet	Ears	6 pounds per square inch
2000 feet	Submarine	1000 psi
12,000 feet	Ocean Floor	6000 psi

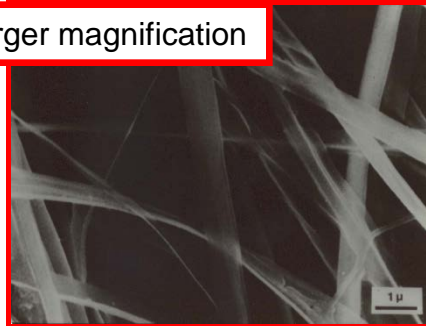
Pressure inside NHMFL Pulsed Magnets

800,000 gauss Pulsed Magnet 200,000 psi
 (which equals 1.4GPa or 130 kg per square millimeter)
 (which is more pressure than most materials can handle)



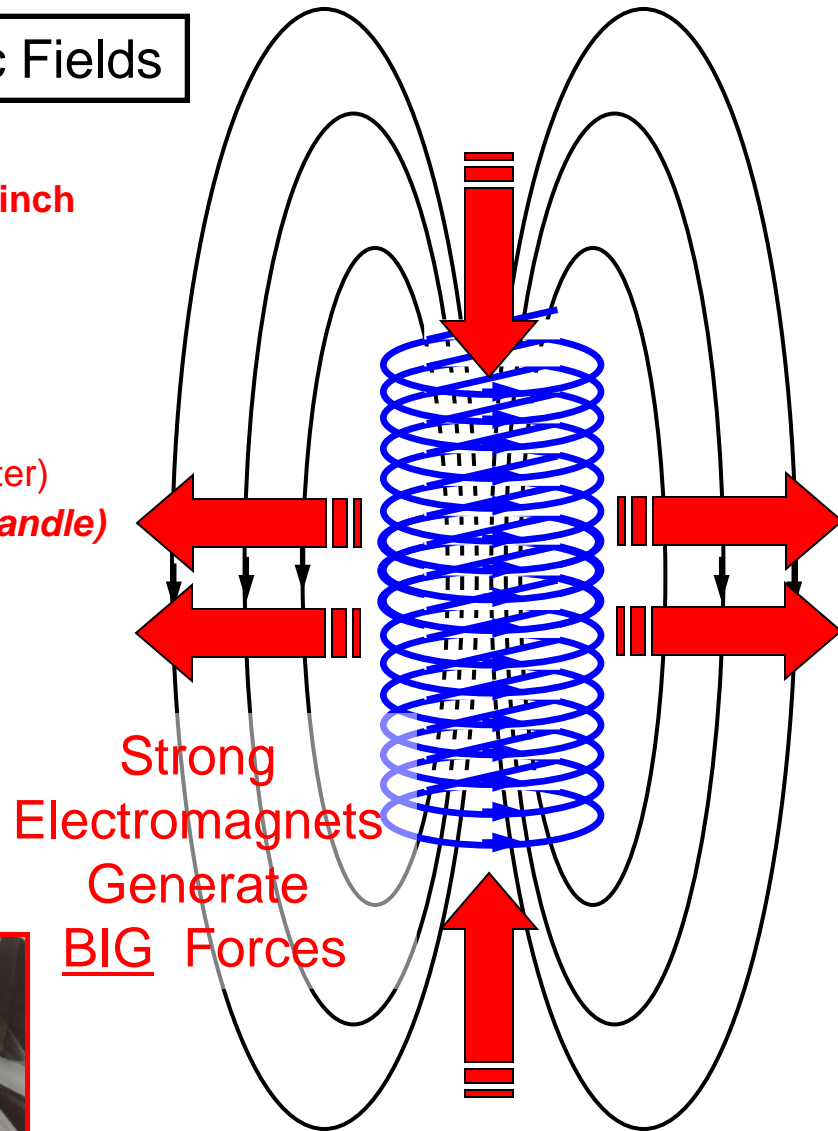
20% Niobium Droplets in 80% Copper Matrix

20 times larger magnification



The Niobium ribbons work (sort of) like steel bars in cement...

...except the nano-composite is five times stronger than either constituent



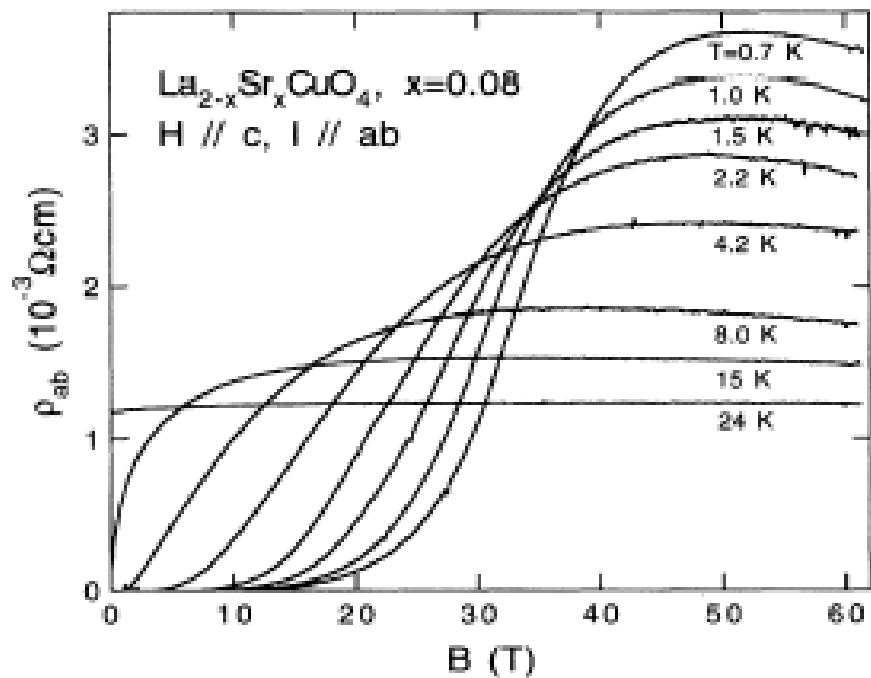


FIG. 1. In-plane resistivity ρ_{ab} versus magnetic field for the $x = 0.08$ $\text{La}_{2-x}\text{Sr}_x\text{CuO}_4$ single crystal at various temperatures.

$(\text{LaSr})_2\text{CuO}_4$

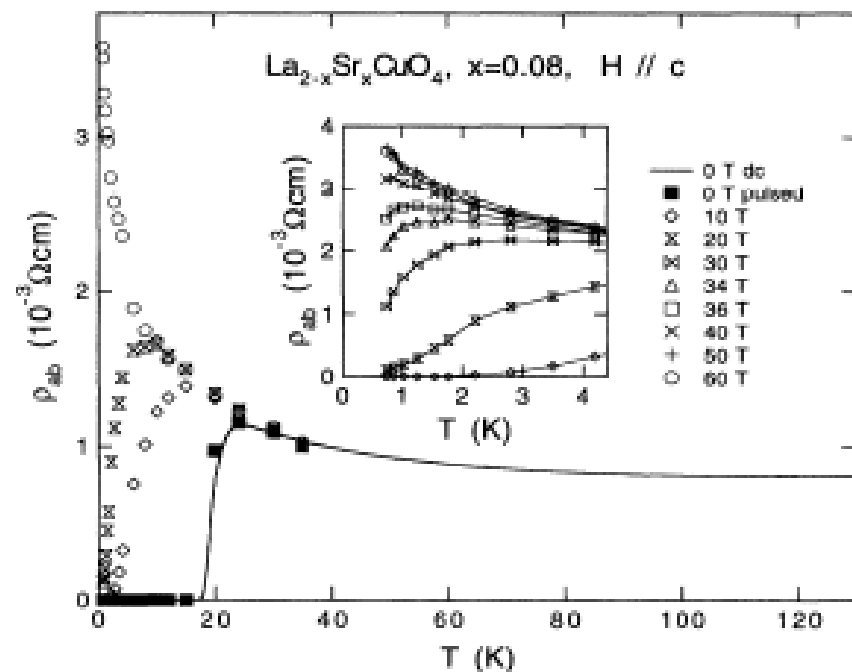
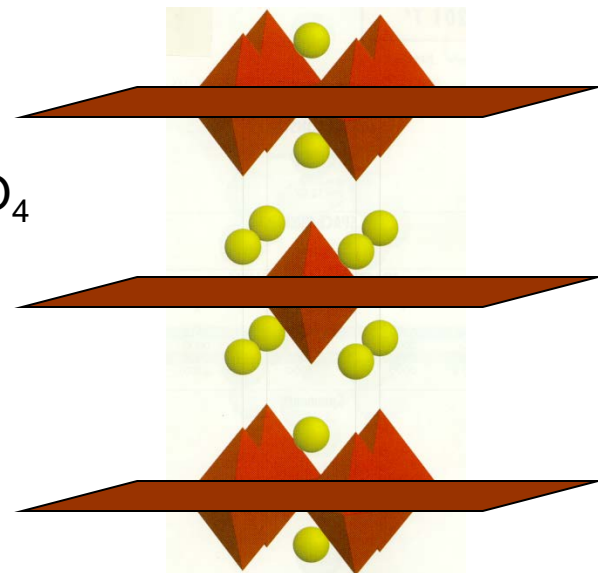


FIG. 2. Temperature dependence of ρ_{ab} in 0, 10, 20, and 60 T, obtained from the pulsed magnetic field data. The solid line shows the zero-field resistive transition. The inset contains the low-temperature data.

Logarithmic Divergence of both In-Plane and Out-of-Plane Normal-State Resistivities of Superconducting $\text{La}_{2-x}\text{Sr}_x\text{CuO}_4$ in the Zero-Temperature Limit

$\text{La}_{1.92}\text{Sr}_{0.08}\text{CuO}_4$

Yoichi Ando,* G. S. Boebinger, and A. Passner

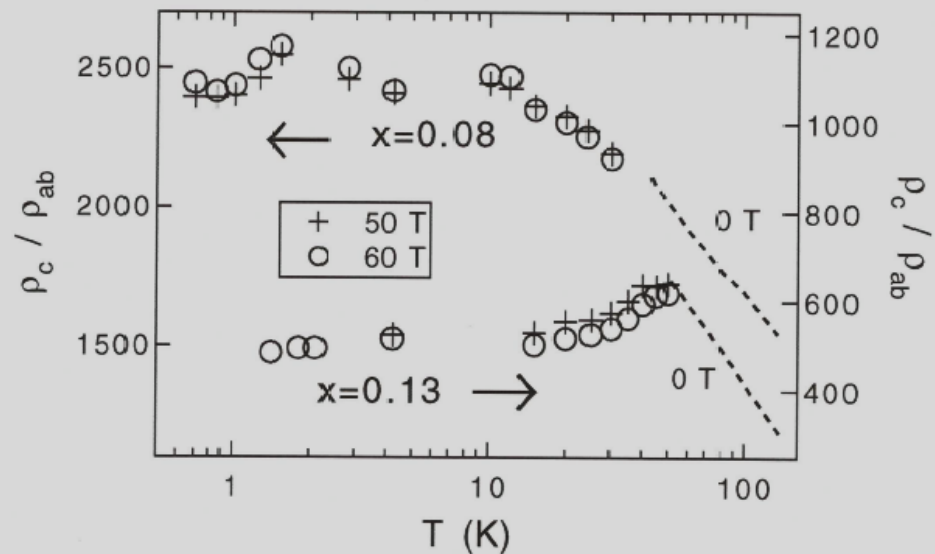
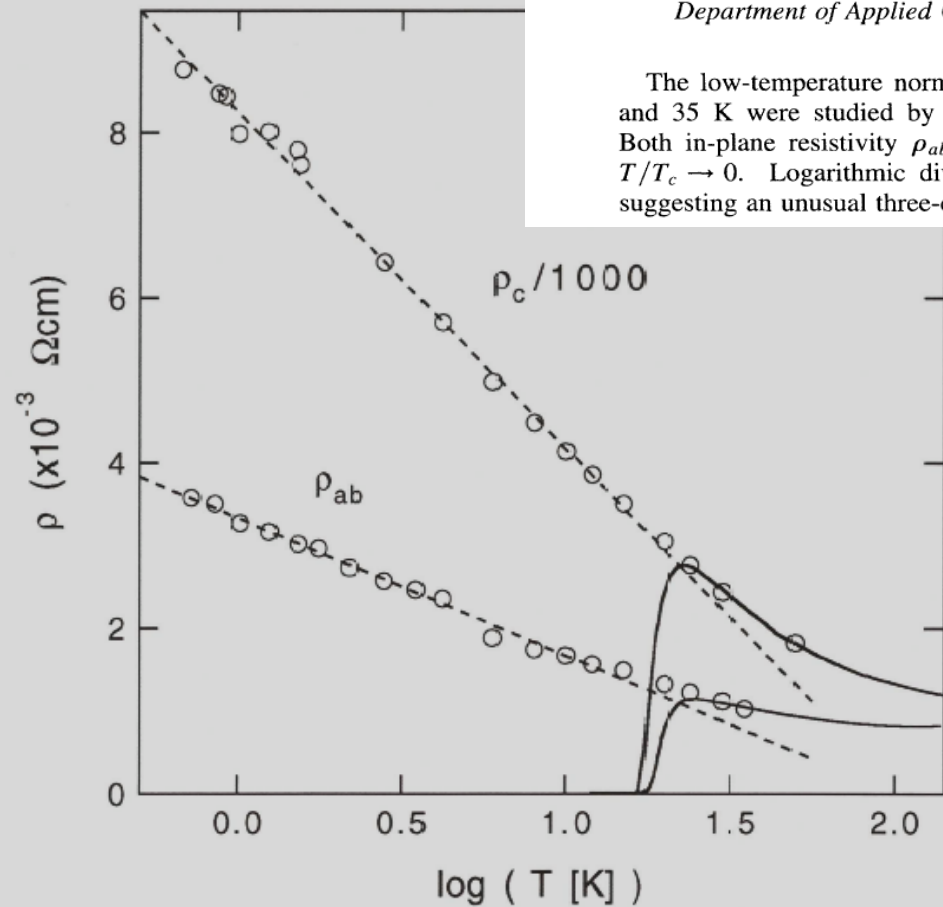
AT&T Bell Laboratories, 600 Mountain Avenue, Murray Hill, New Jersey 07974

Tsuyoshi Kimura and Kohji Kishio

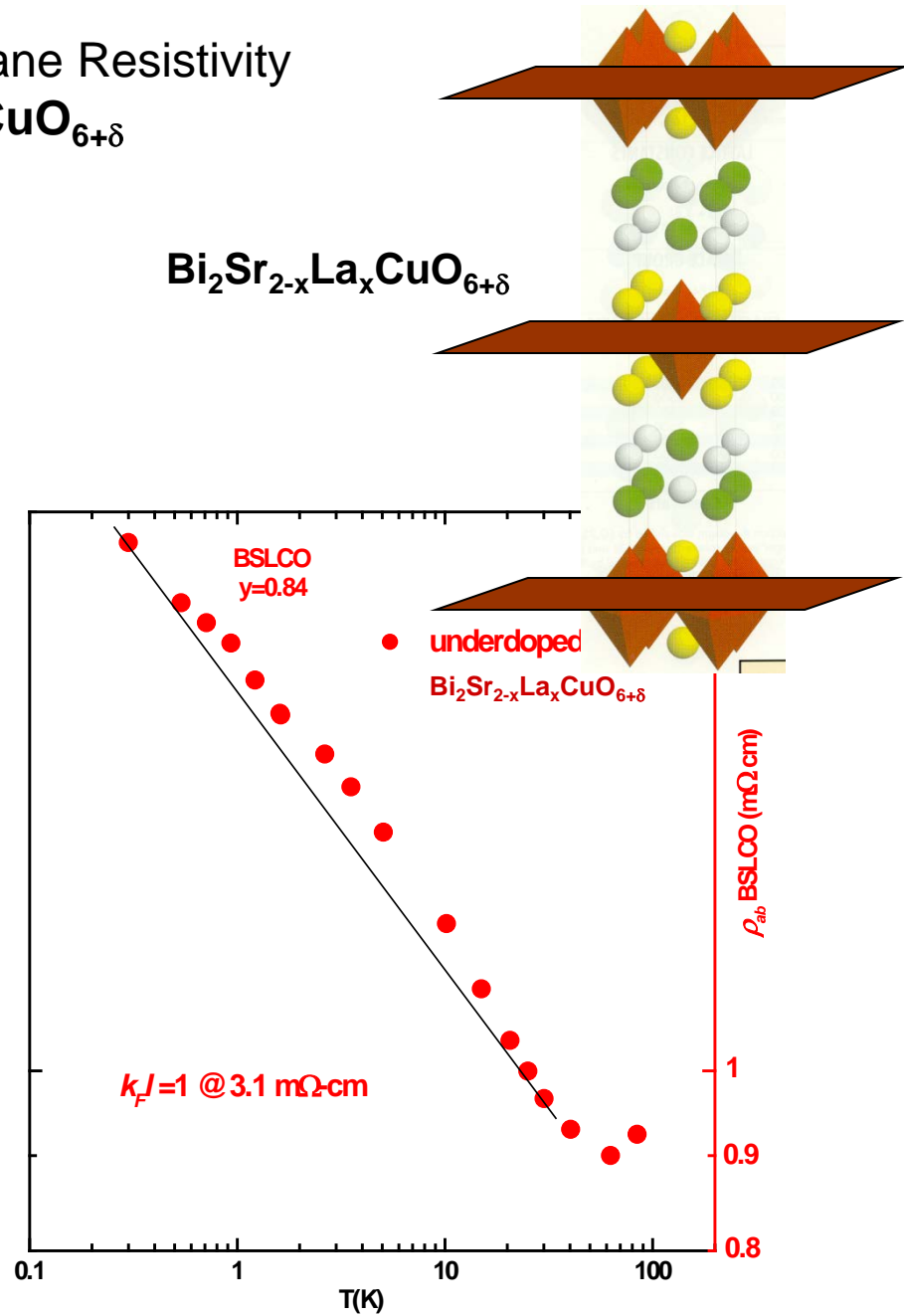
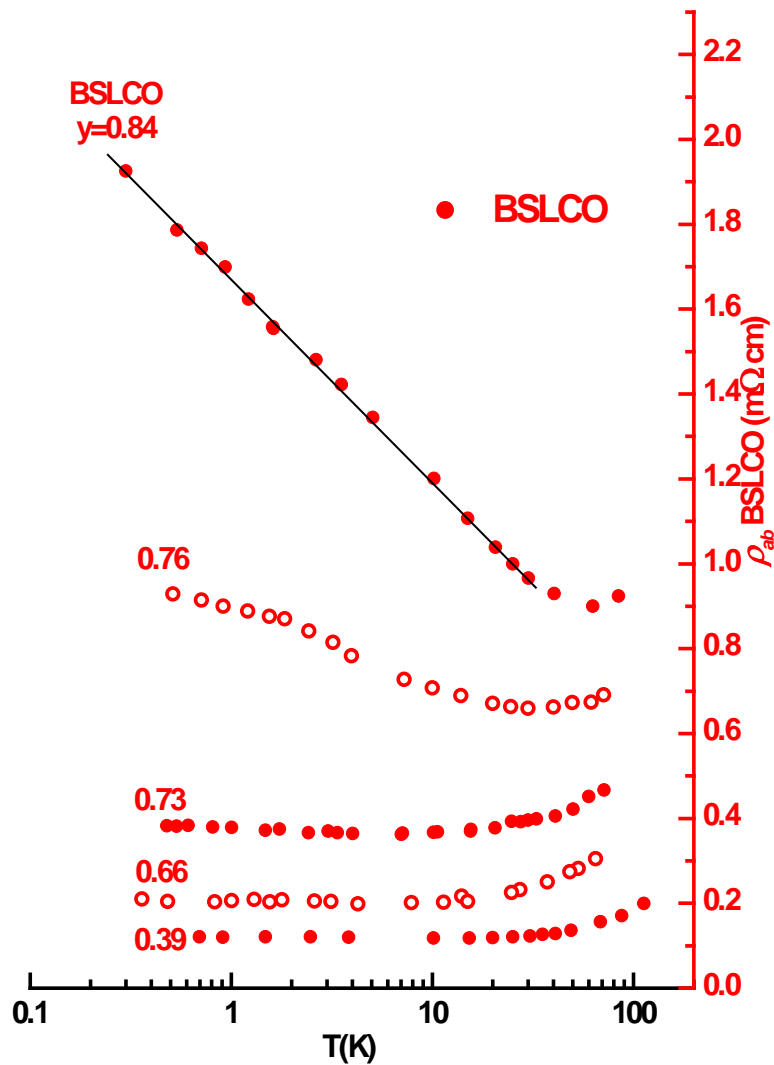
Department of Applied Chemistry, University of Tokyo, Hongo, Bunkyo-ku, Tokyo 113, Japan

(Received 18 August 1995)

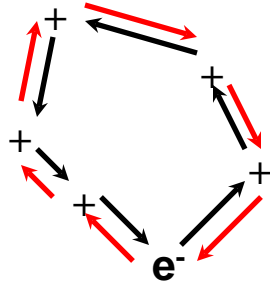
The low-temperature normal-state resistivities of underdoped $\text{La}_{2-x}\text{Sr}_x\text{CuO}_4$ crystals with T_c of 20 and 35 K were studied by suppressing the superconductivity with pulsed magnetic fields of 61 T. Both in-plane resistivity ρ_{ab} and out-of-plane resistivity ρ_c are found to diverge logarithmically as $T/T_c \rightarrow 0$. Logarithmic divergence is accompanied by a nearly constant anisotropy ratio, ρ_c/ρ_{ab} , suggesting an unusual three-dimensional insulator.



Logarithmic Divergence of the In-Plane Resistivity of Underdoped $\text{Bi}_2\text{Sr}_{2-x}\text{La}_x\text{CuO}_{6+\delta}$



LOGARITHMIC DIVERGENCES....WHAT THIS IS NOT

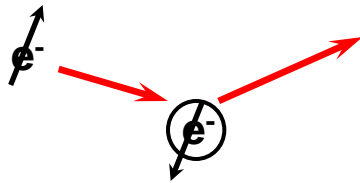


Weak Anderson Localization

*Time-reversed scattering sequences give rise to coherent backscattering
Small logarithmic decrease in conductivity in two dimensional systems.*

NOT LIKELY, because...

Large effect seen in resistivity. Persists even in 60T magnetic field.



Kondo Scattering

*Spin-flip scattering of conduction electrons from local magnetic moments
Logarithmic increase in resistivity in three dimensions*

NOT LIKELY, because...

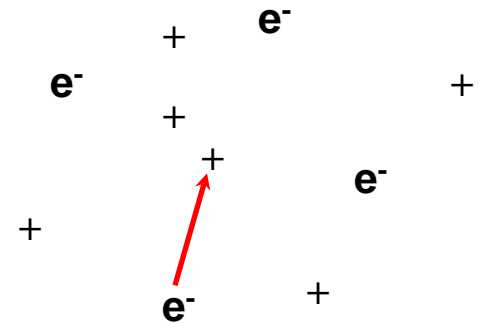
Persists in 60T magnetic field even for temperatures $k_B T < g\mu_B H$

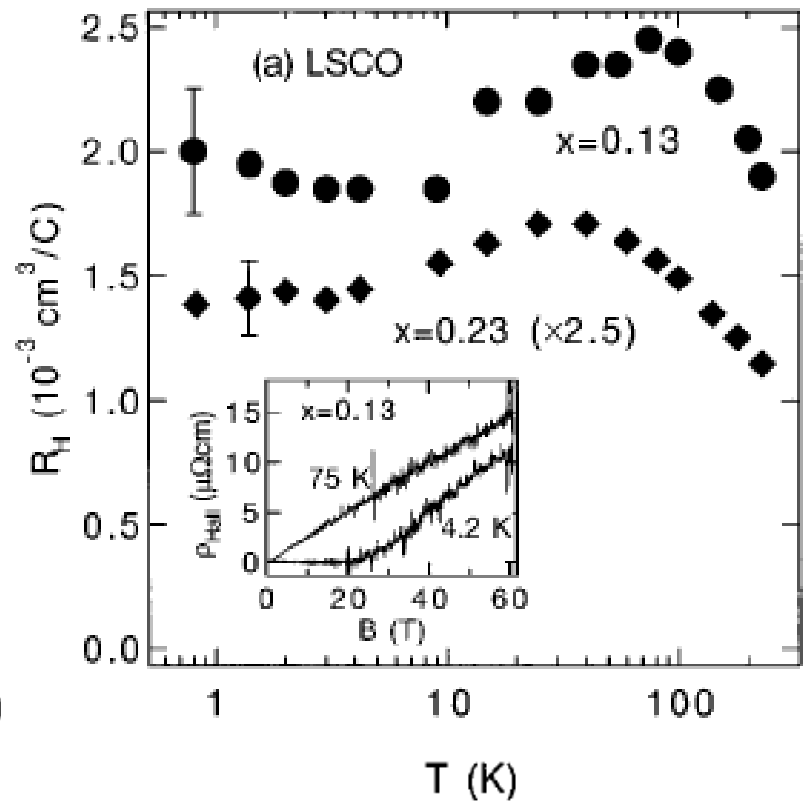
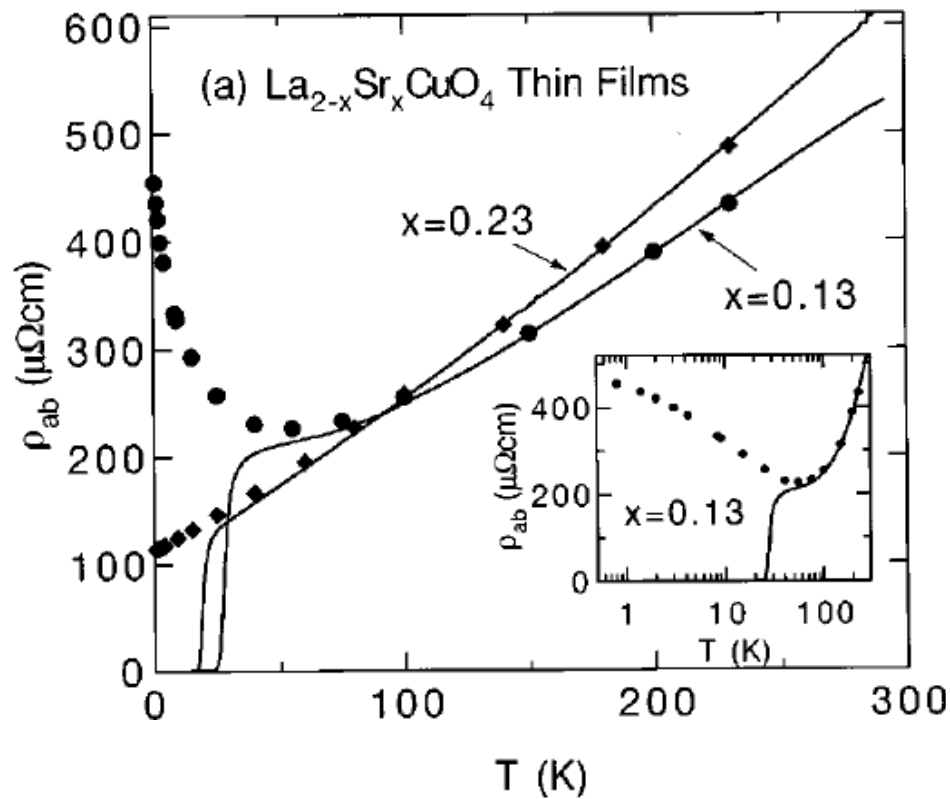
Enhanced Localization due to Electron Interactions

*Logarithmic decrease in the density of states near the Fermi energy
Logarithmically suppressed conductivity in two-dimensional systems
and carrier concentration due to reduced density of states*

NOT LIKELY, because...

Large effect seen in resistivity. No divergence seen in Hall effect.



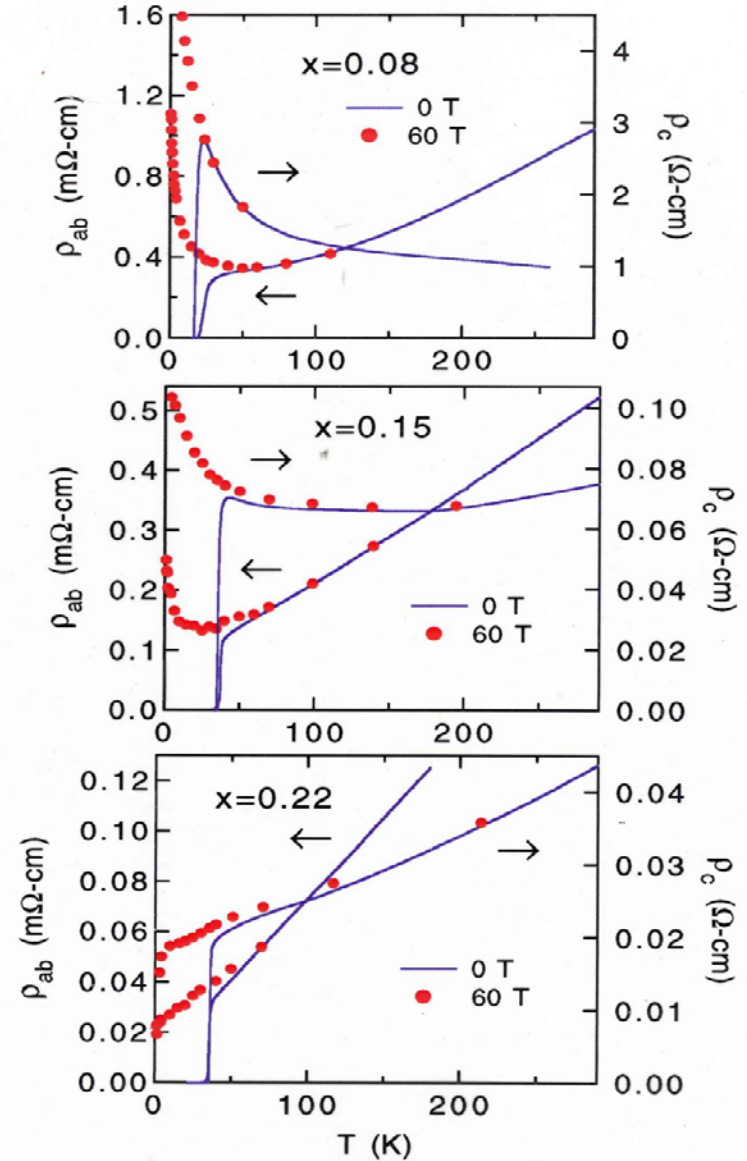
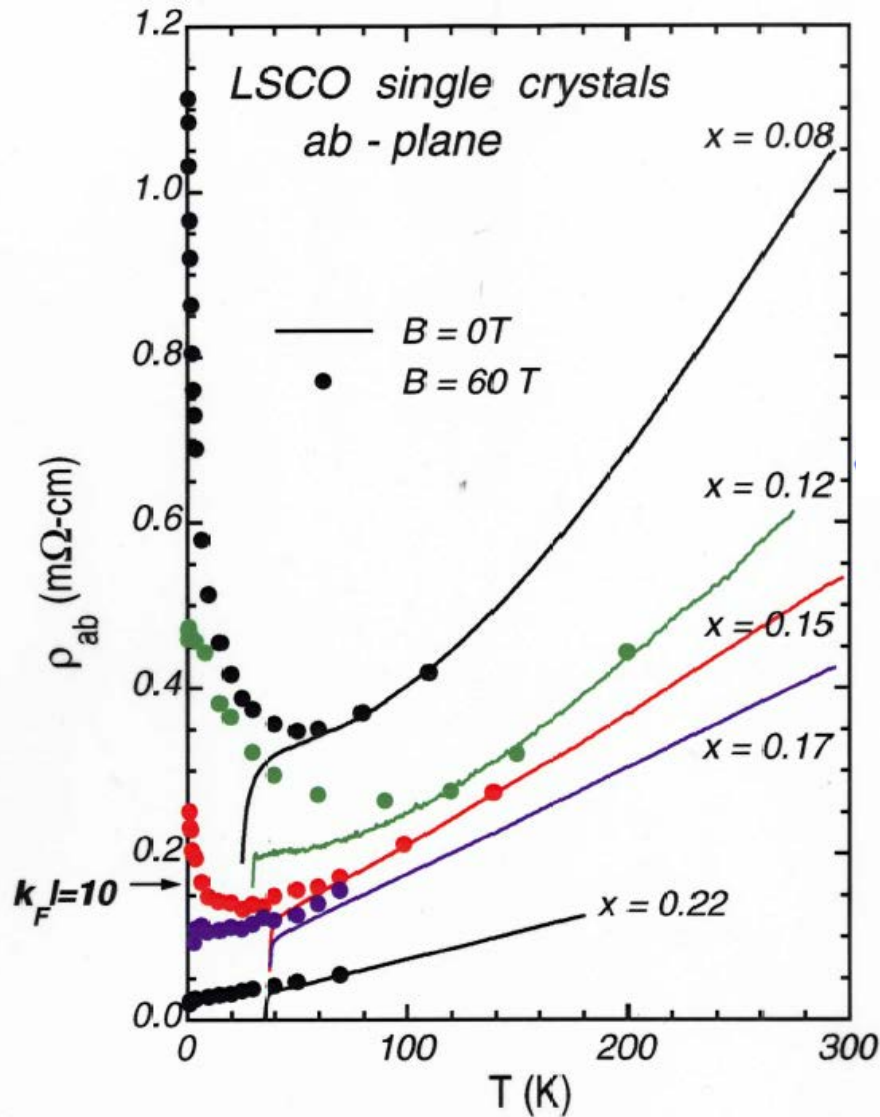


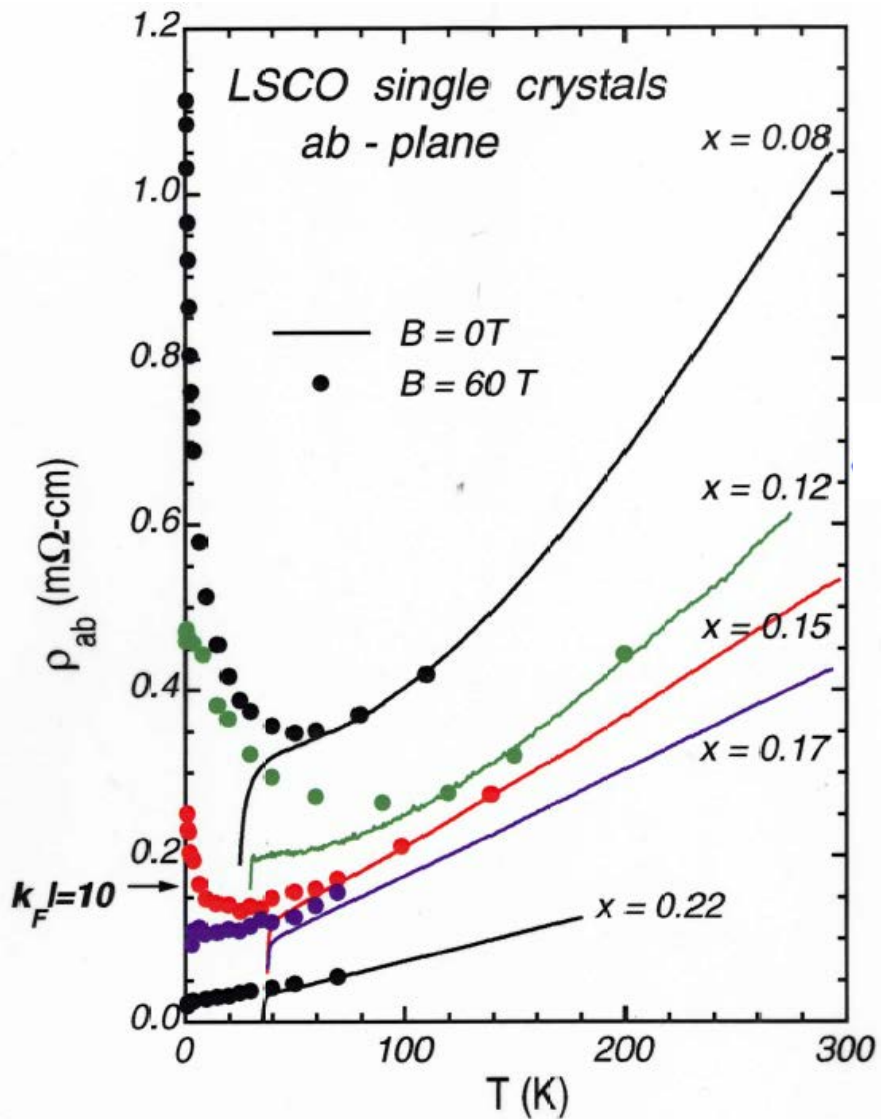
Ando, Boebinger, et al. PRB 56 R8530 (1997)

“Insulator-to-metal crossover in the normal state of $\text{La}_{2-x}\text{Sr}_x\text{CuO}_4$ near optimum doping.”

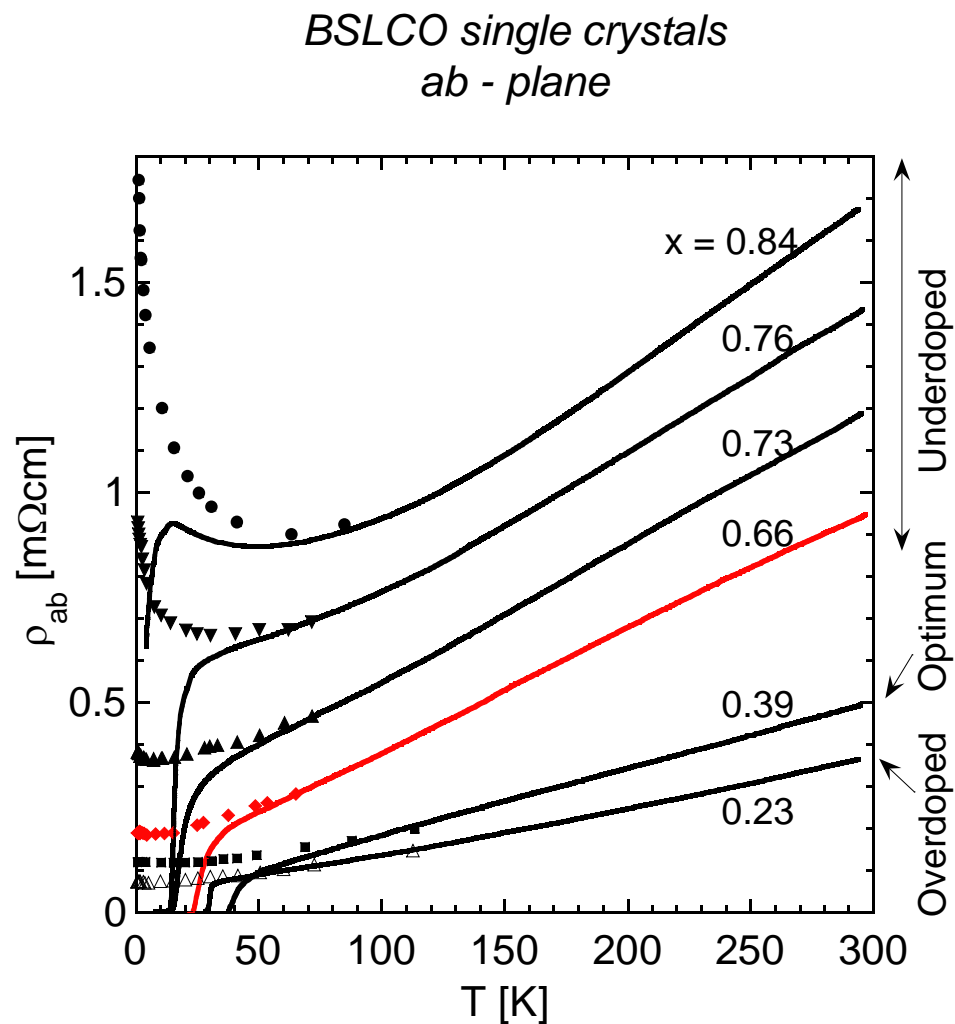
G.S. Boebinger, Yoichi Ando, A. Passner, T. Kimura, M. Okuya,

J. Shimoyama, K. Kishio, K. Tamasaku, N. Ichikawa, and S. Uchida, *Phys. Rev. Lett.* **77**, 5417 (1996).





PRL **77**, 5417 (1996)



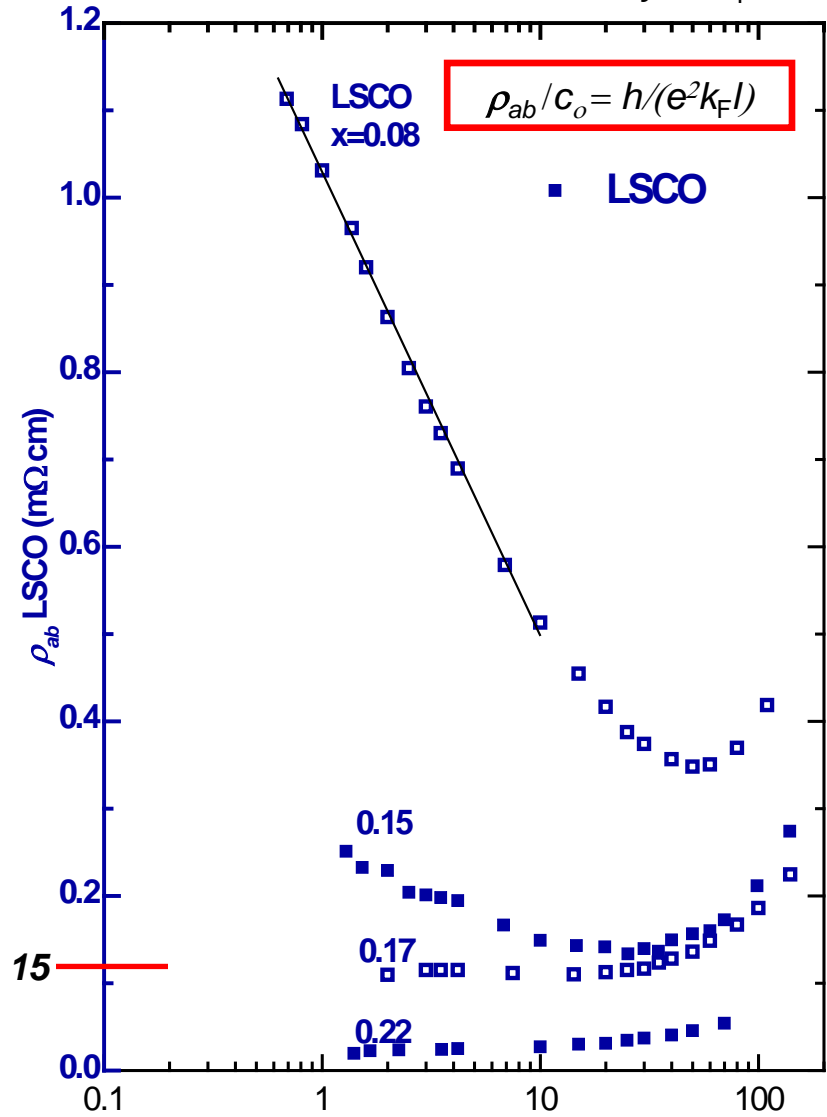
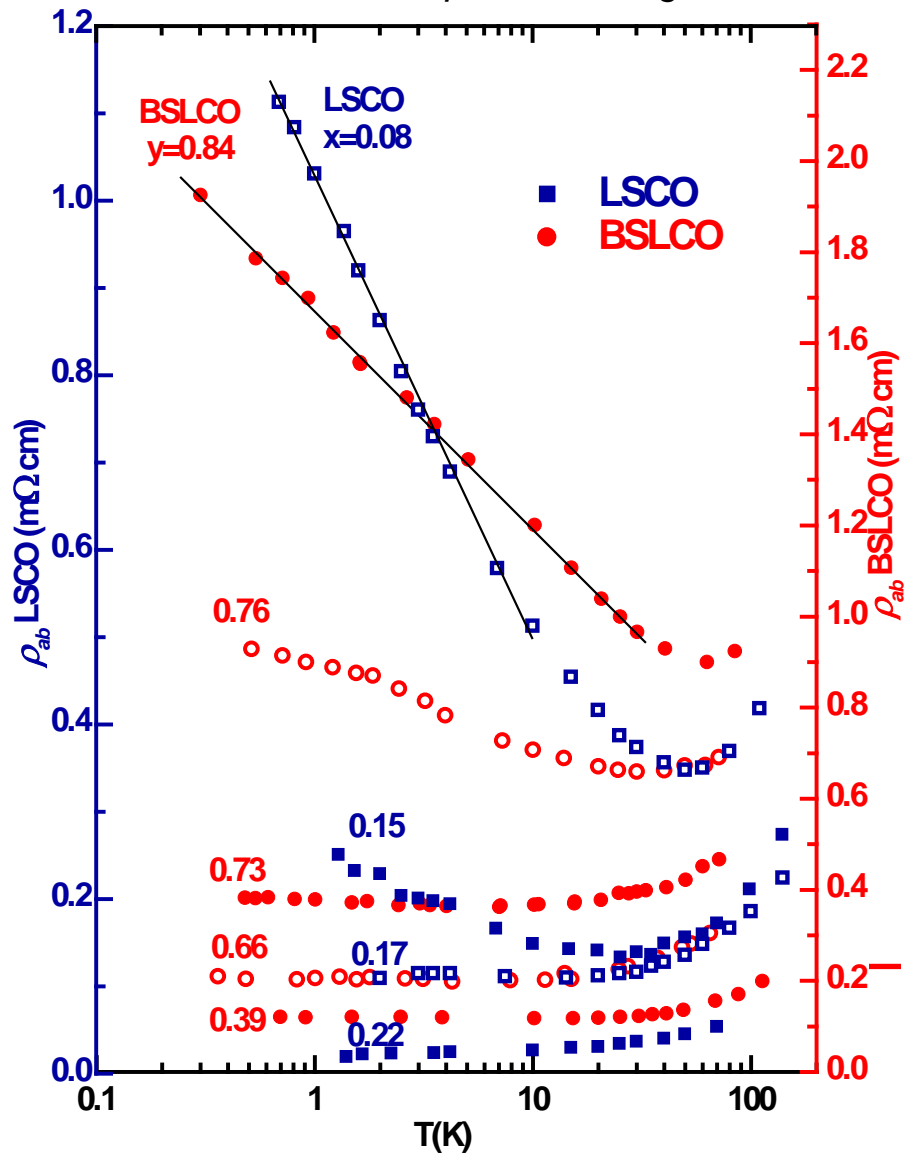
PRL **85**, 638 (2000)

Logarithmically Divergent Resistivity in Underdoped Cuprates

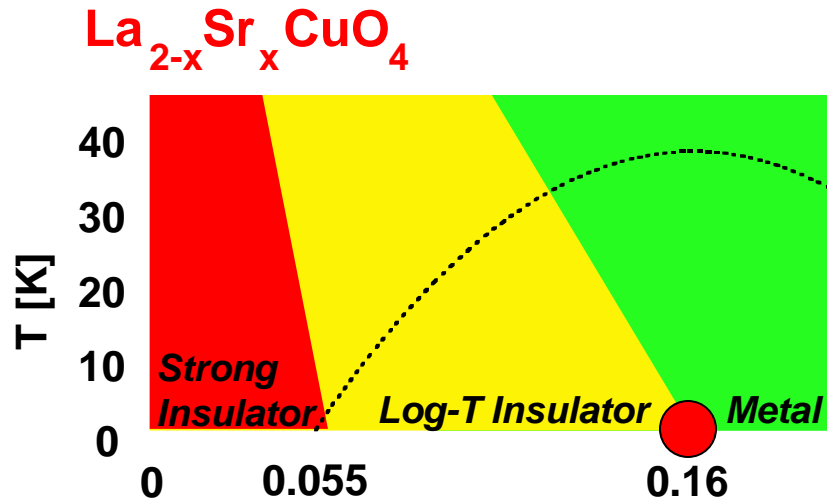
Similarities between the Insulator-to-Metal crossover in BSLCO and LSCO:

--- occurs under the superconducting 'dome'

--- occurs at the same normalized resistivity, at $k_F l \sim 15$.

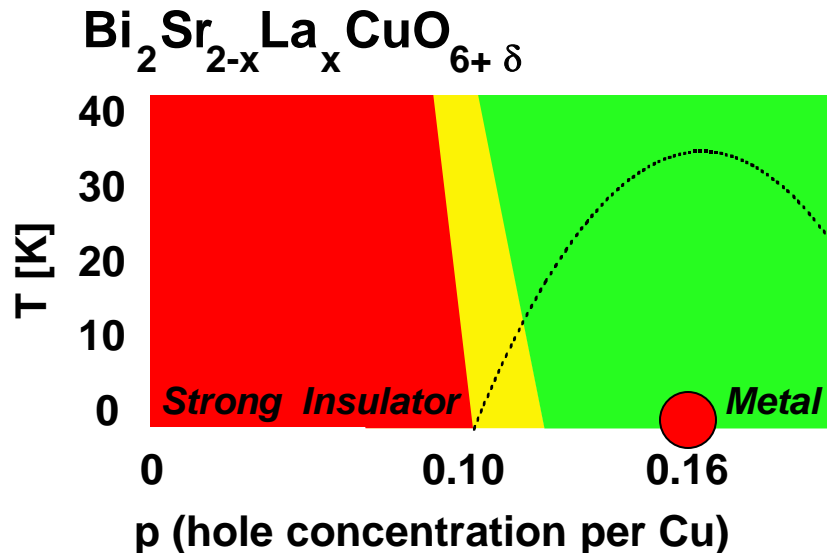


Questions: Metal-Insulator Crossover in the Low-Temperature Normal State



Sharp Insulator-to-Metal Crossover
---at optimum doping

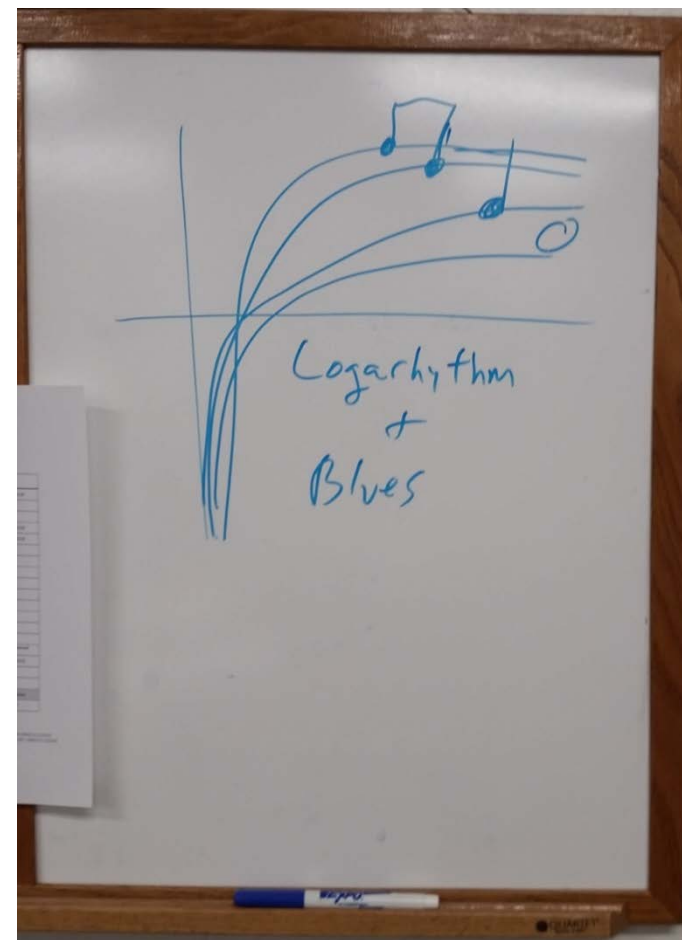
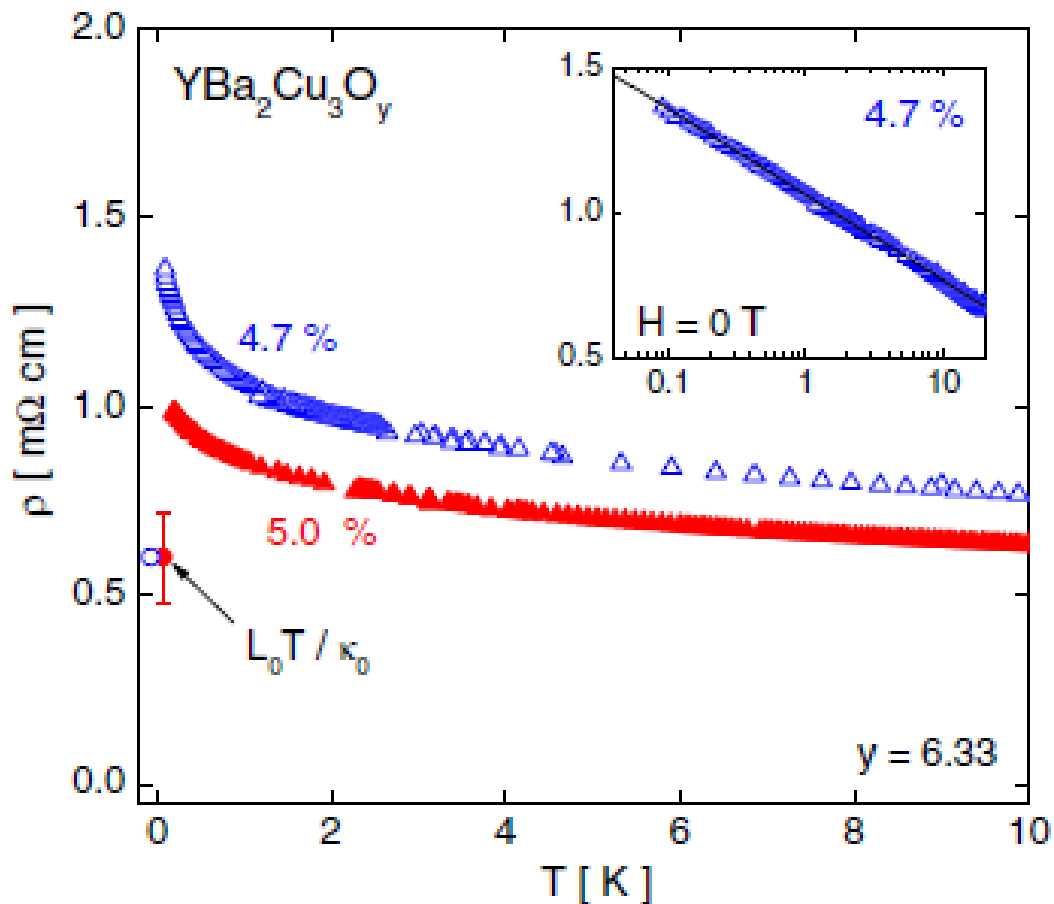
Evidence of a Quantum Critical Point ?
---near optimum doping
---where linear-T resistivity
has been attributed to critical behavior



No evidence of weird resistivity behavior
at optimum doping in BSLCO...
other than the usual linear-T resistivity.

If there were a Quantum Critical Point
at optimum doping in BSLCO
---between two metallic states.
---underdoped metal exhibits
unusual scattering or localization.
---would like to find experimental evidence
in transport.

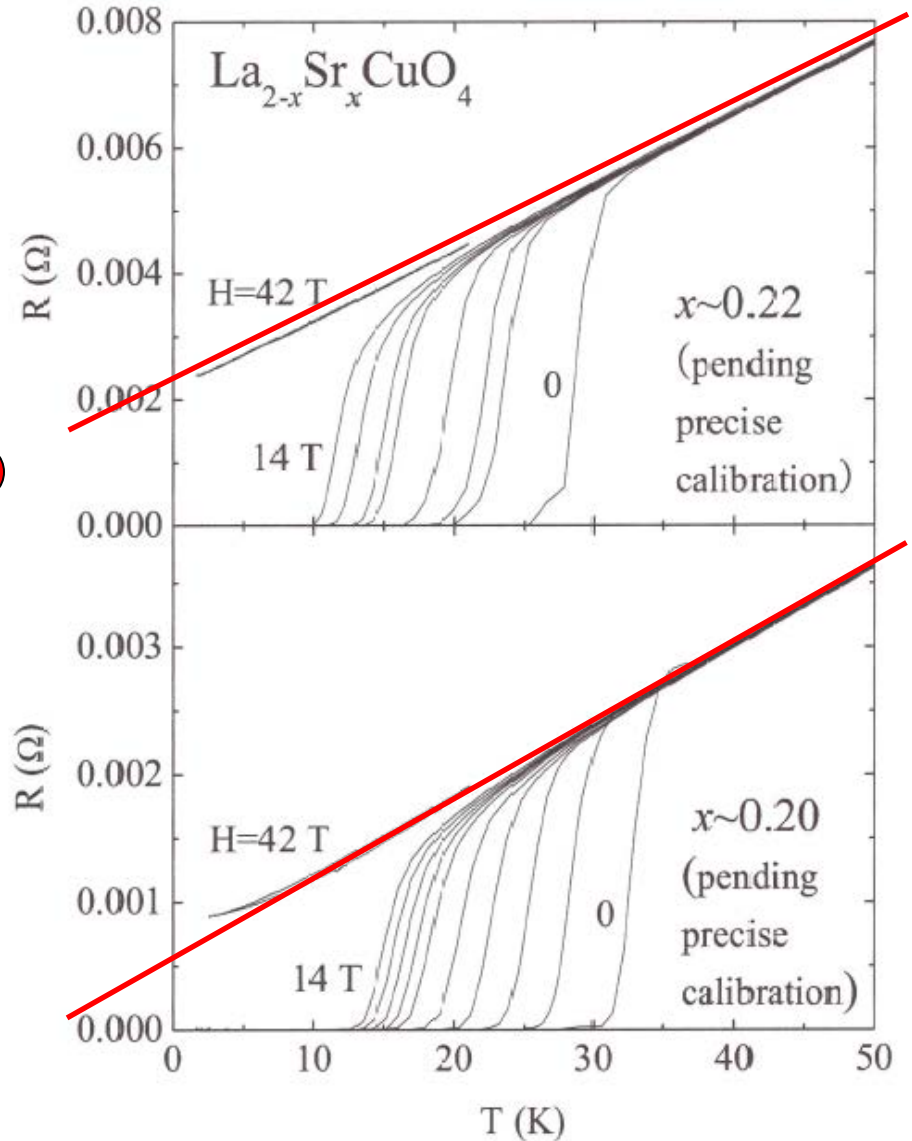
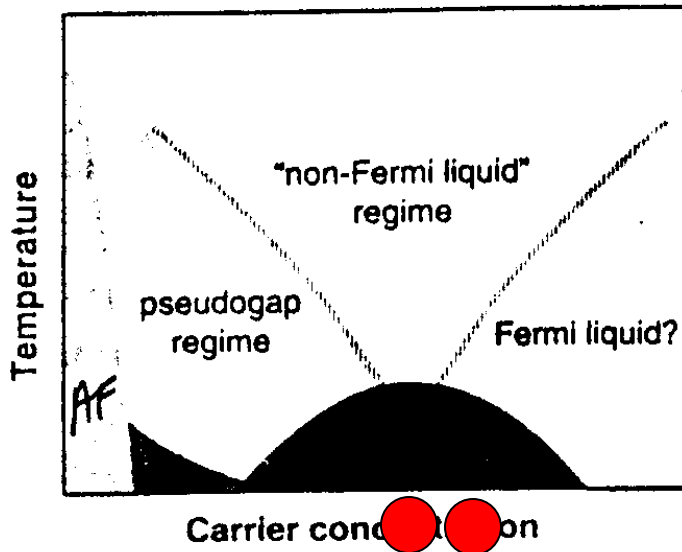
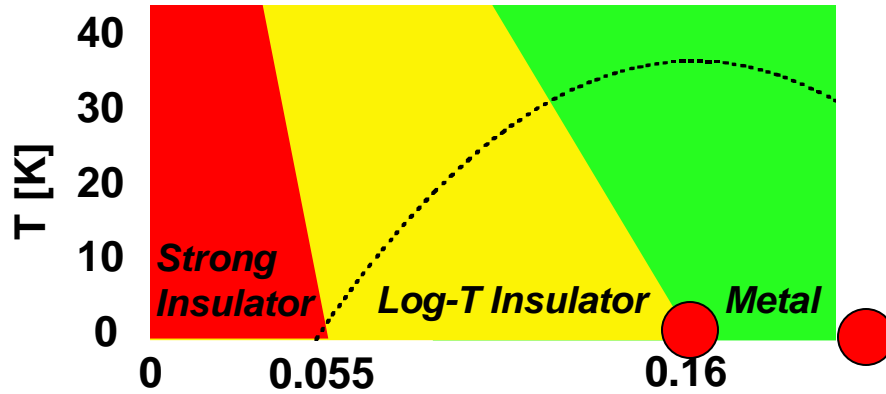
Logarithmic upturn in resistivity in underdoped, non-superconducting YBCO



Nicolas Doiron-Leyraud,¹ Mike Sutherland,² S. Y. Li,¹ Louis Taillefer,^{1,3,*} Ruixing Liang,^{4,3}
D. A. Bonn,^{4,3} and W. N. Hardy^{4,3}

PRL 97, 207001 (2006)

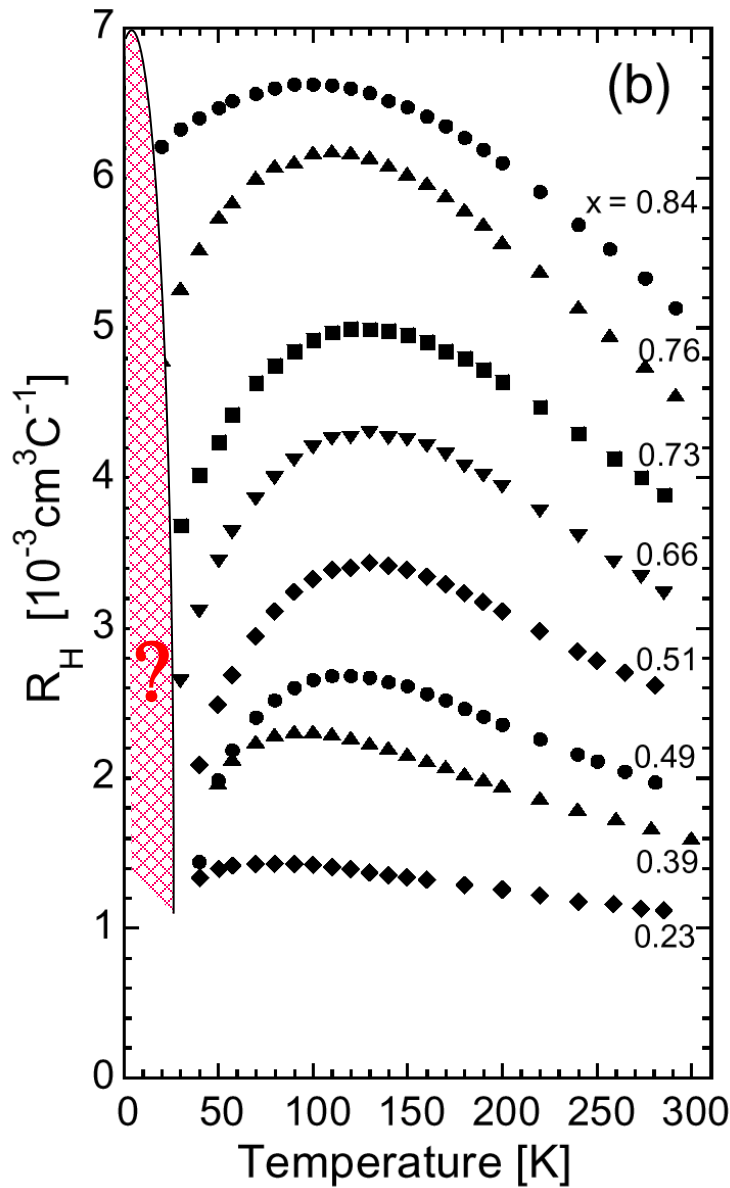
Linear-T to zero temperature as evidence of a quantum critical point



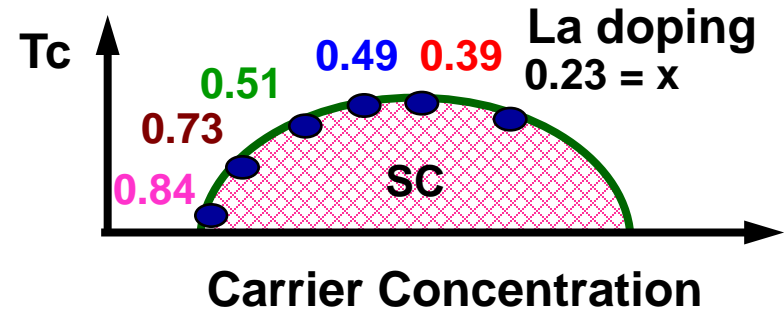
K.H. Kim, N. Harrison, G.S. Boebinger (Los Alamos);
S. Komiyama, S. Ono, Y. Ando (CRIEPI) (unpublished 2003)



Switching from Resistivity to Hall Measurements



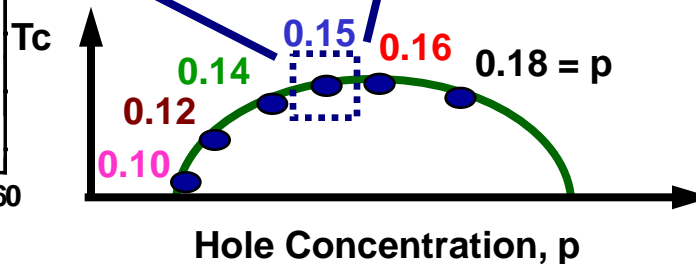
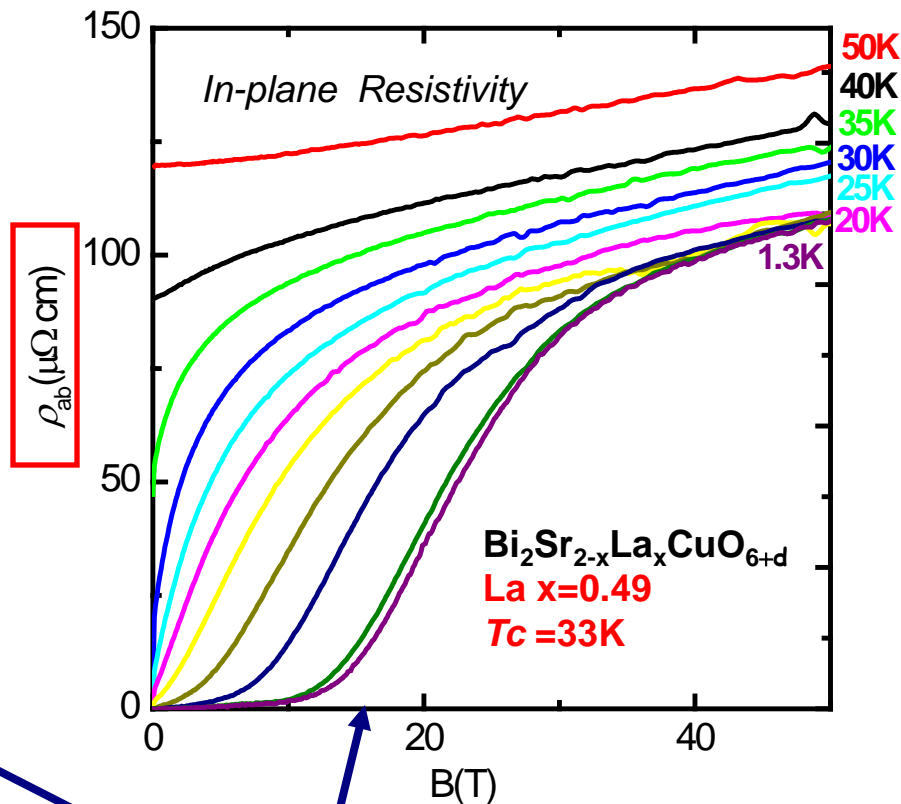
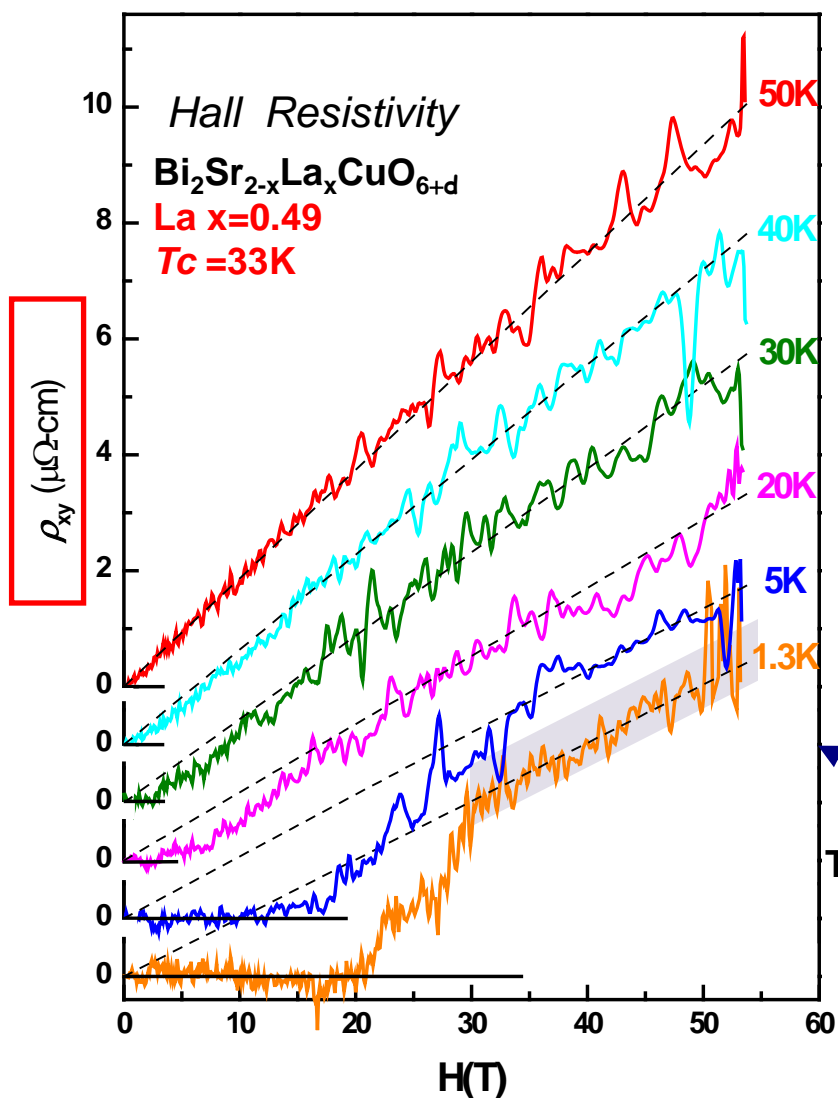
Hall Effect in $\text{Bi}_2\text{Sr}_{2-x}\text{La}_x\text{CuO}_{6+d}$



- Unusual Temperature-dependence of Hall coefficient not understood

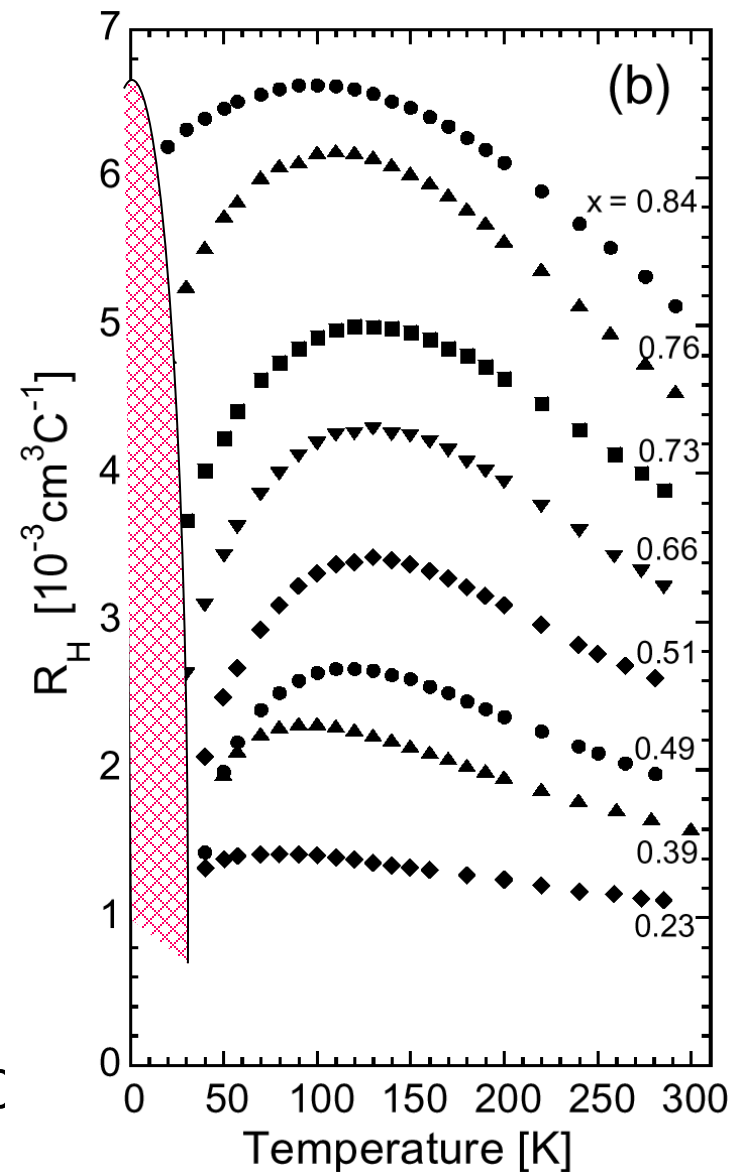
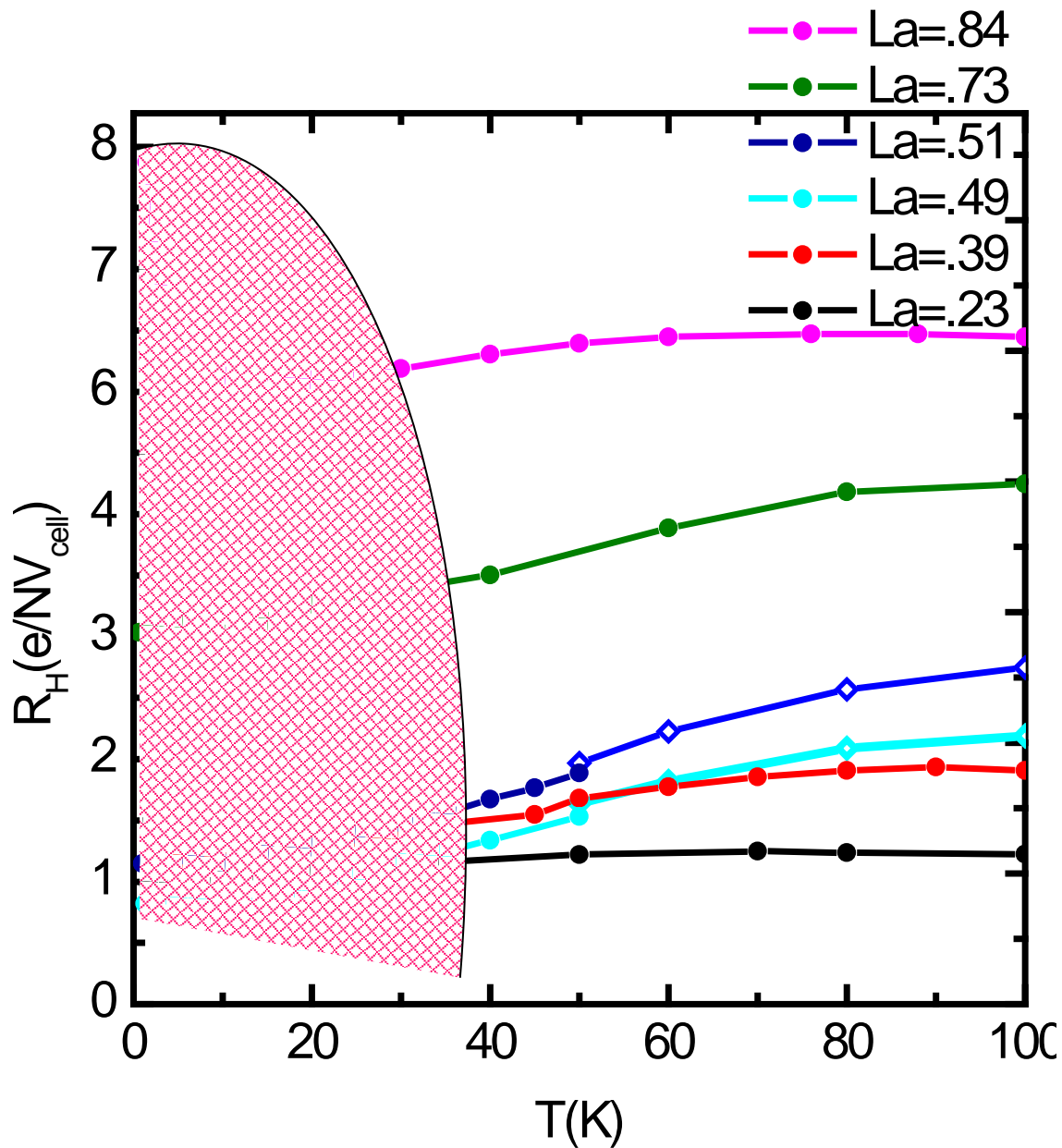
- What happens below T_c ?

Low Temperature Normal State Hall Effect

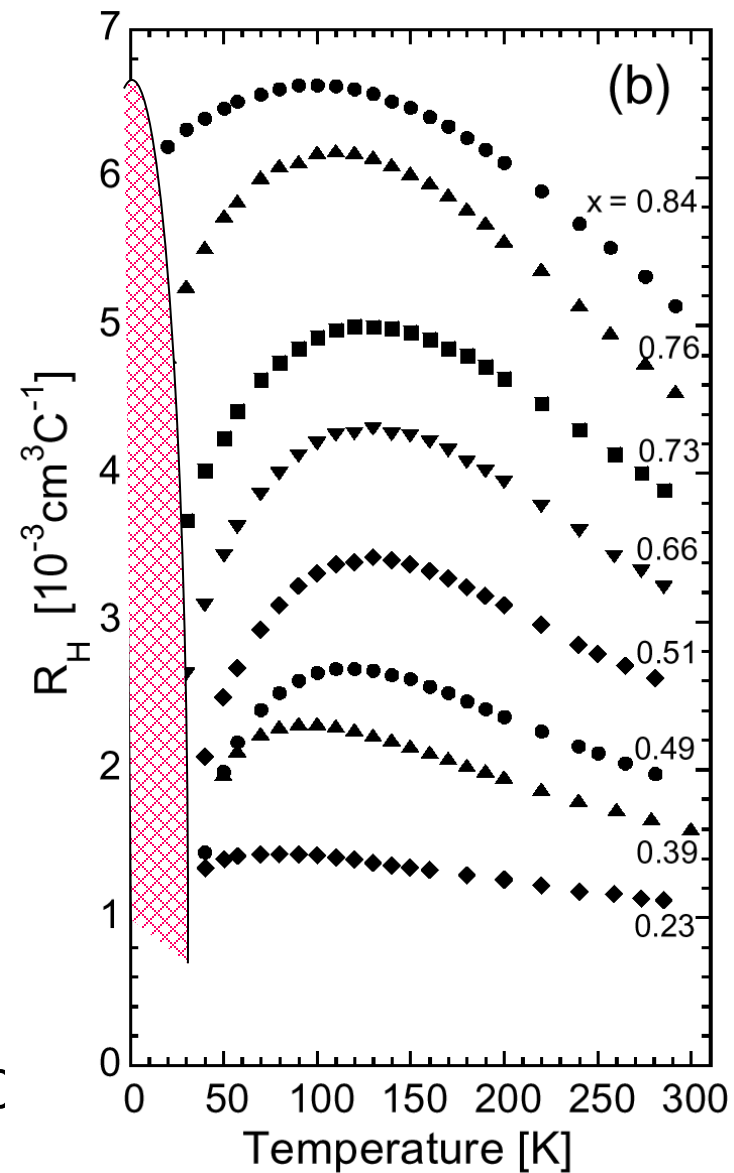
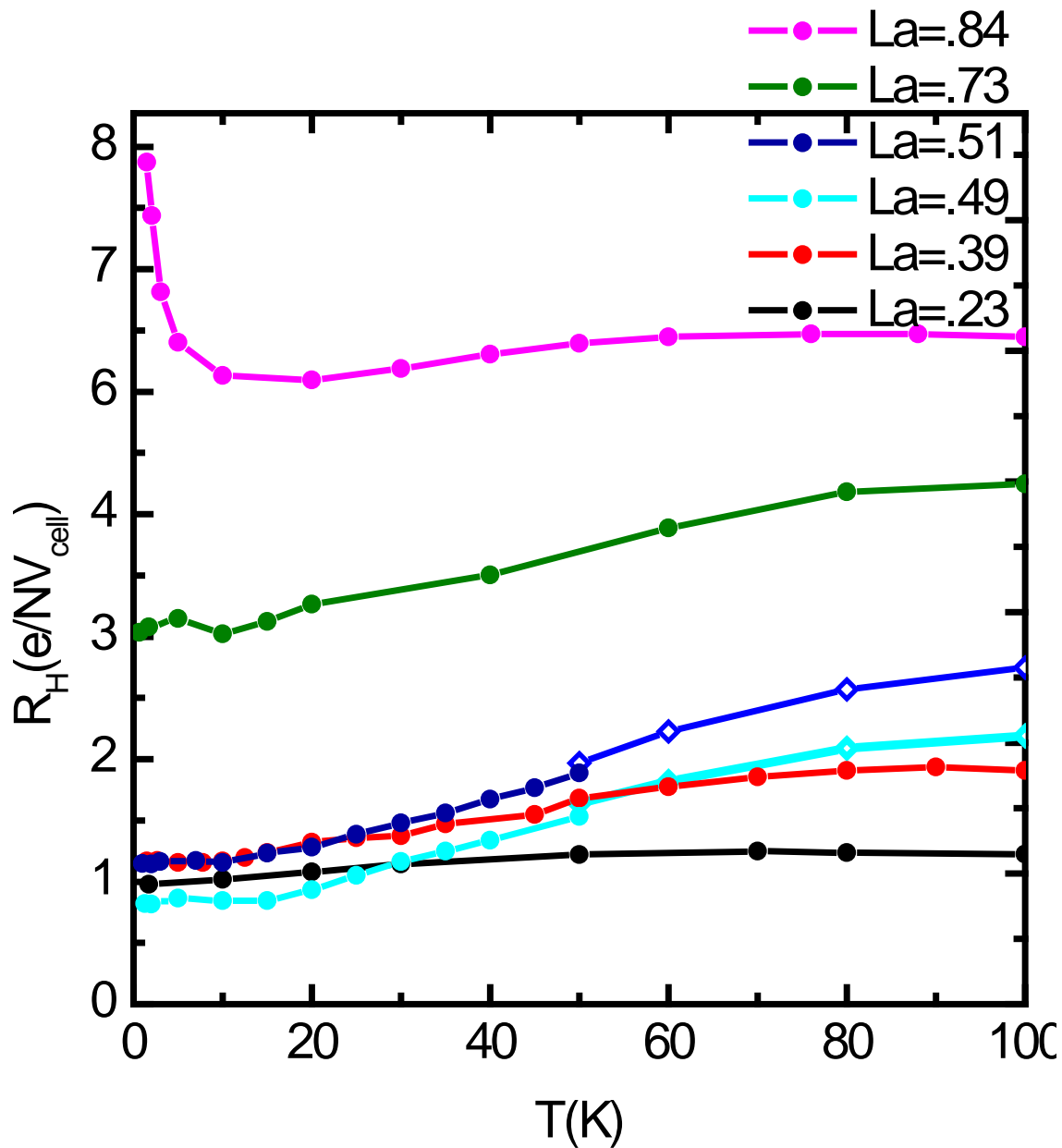


High-field Hall voltage is linear in field

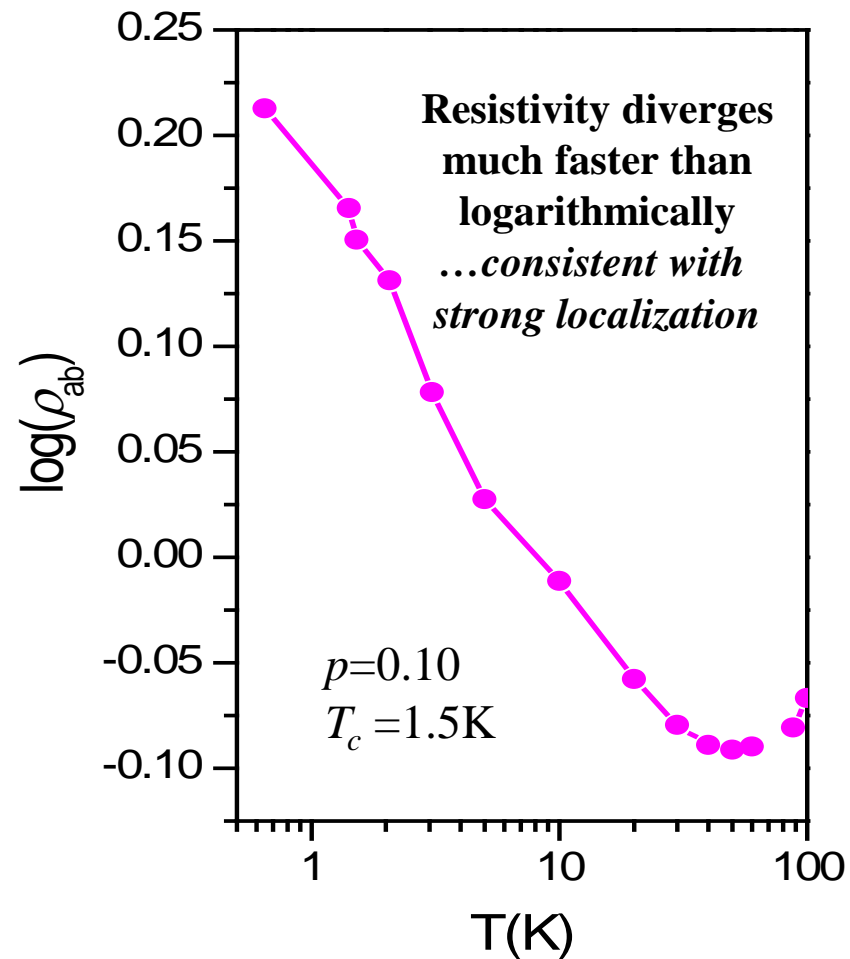
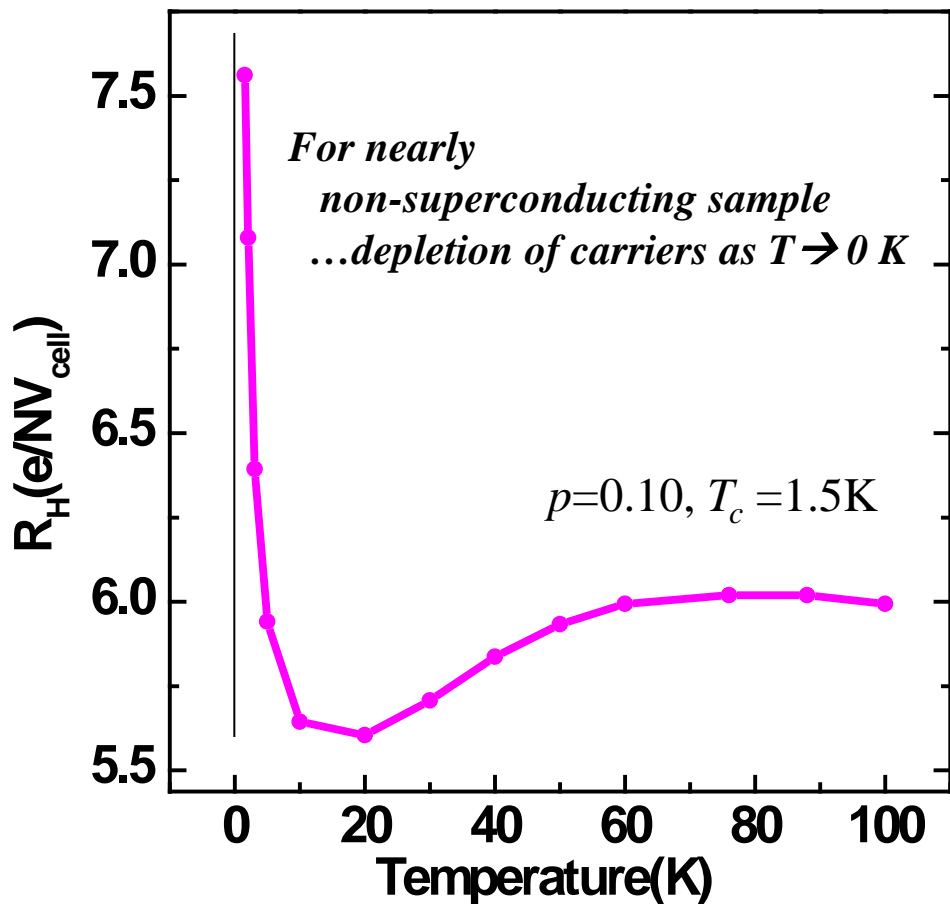
Low Temperature Hall Effect



Low Temperature Hall Effect



Insulator-to-Superconductor boundary (the Underdoped Side of the Superconducting Dome)



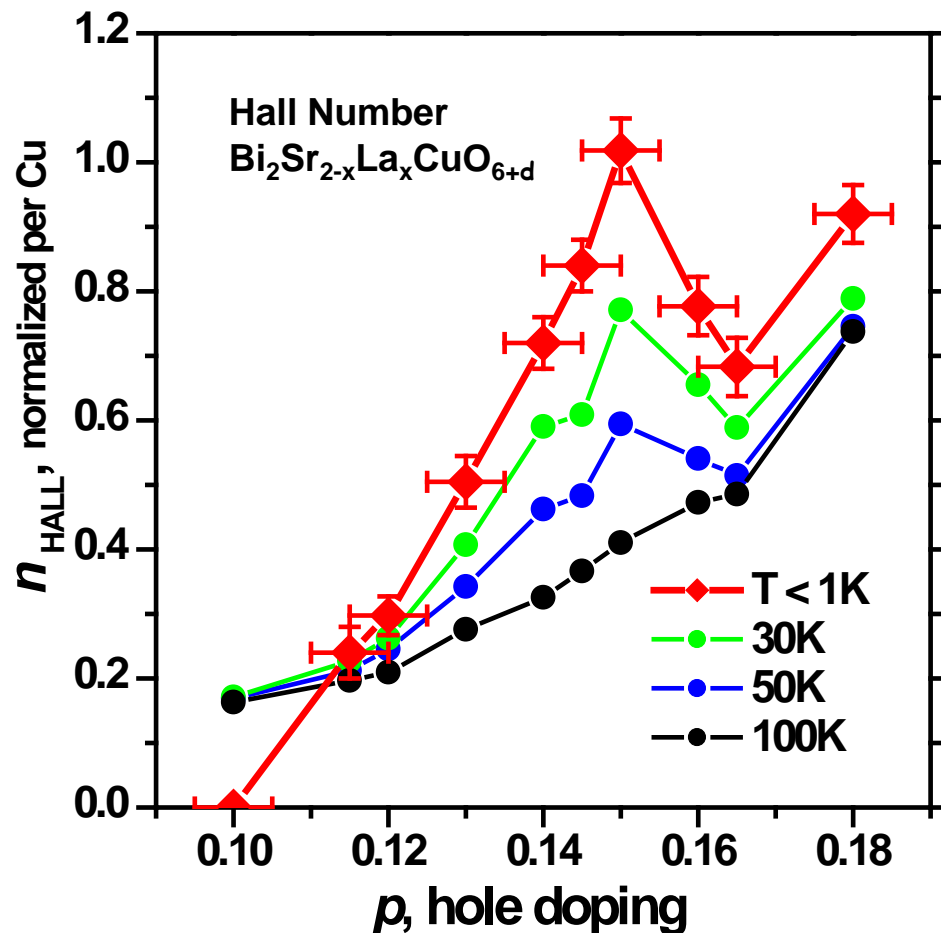
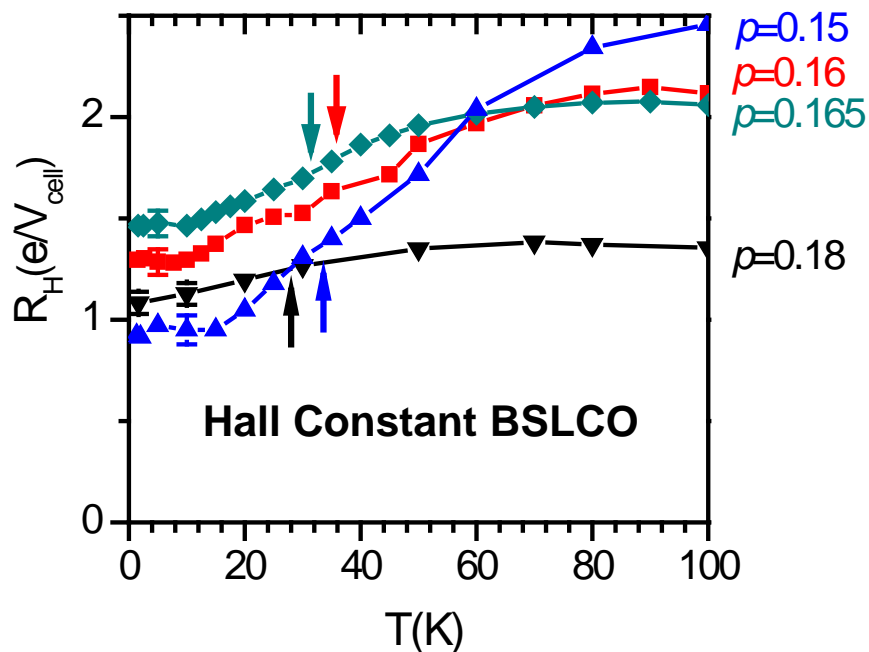
“Signature of optimal doping in Hall-effect measurements on a high-temperature superconductor”

Fedor F. Balakirev, Jonathan B. Betts, Albert Migliori, S. Ono, Yoichi Ando & Gregory S. Boebinger, Nature 424, 912 (2003).

Change in T -dependence

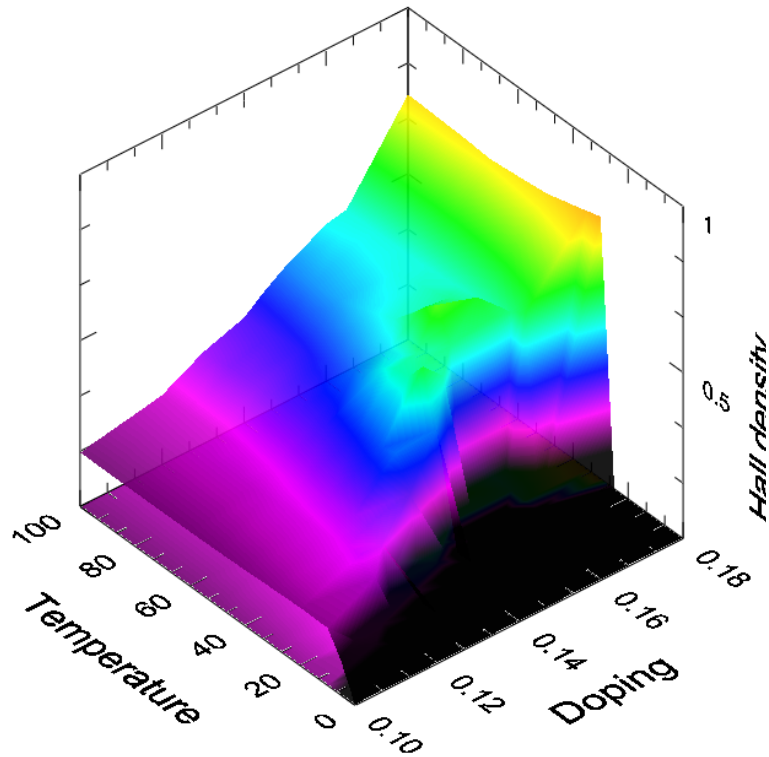
...no feature at zero-field T_c

...lose temperature dependence as $T \rightarrow 0$



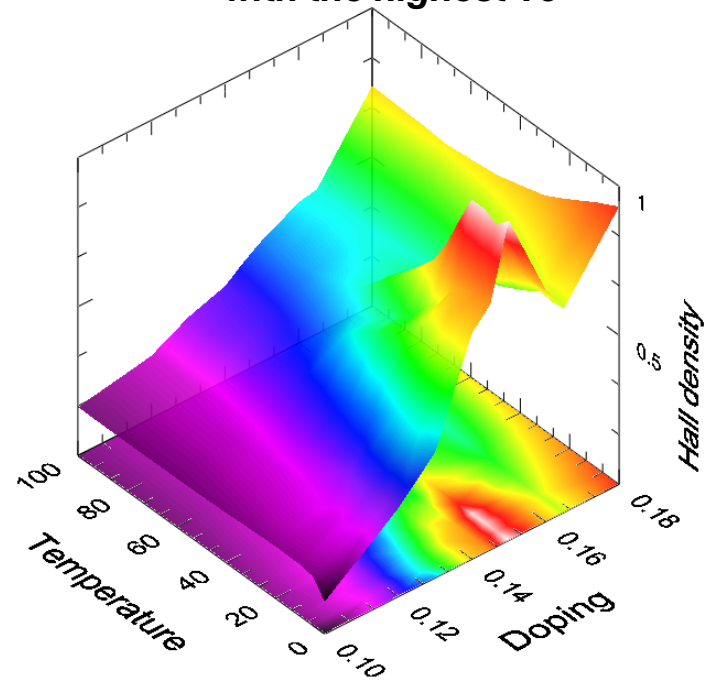
...gives an anomaly at doping corresponding to the at highest T_c

We may understand the high-temperature behavior of the Hall number...



...but not the peak at low temperatures

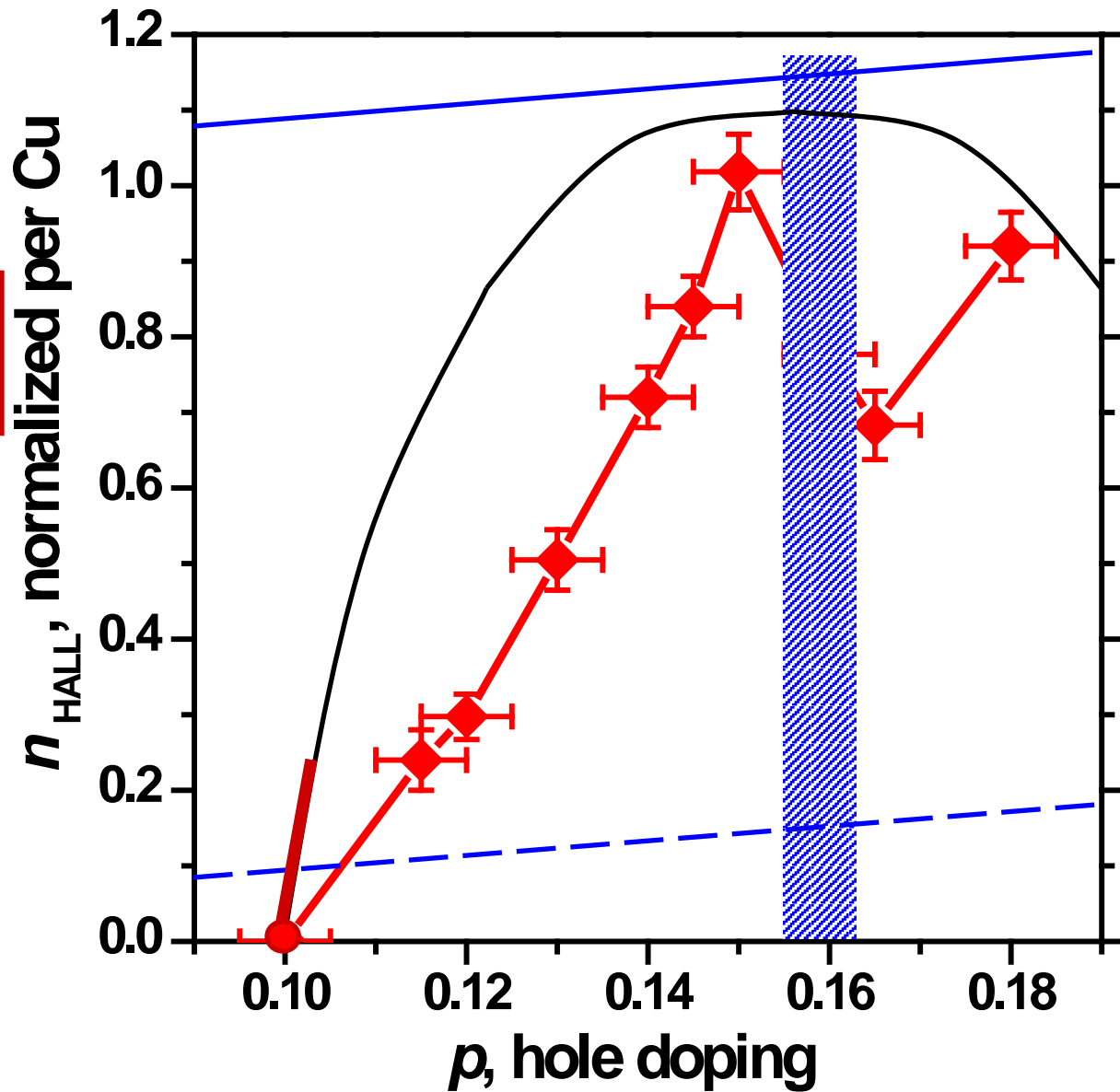
**...at temperatures below T_c
...and centered on the sample
with the highest T_c**



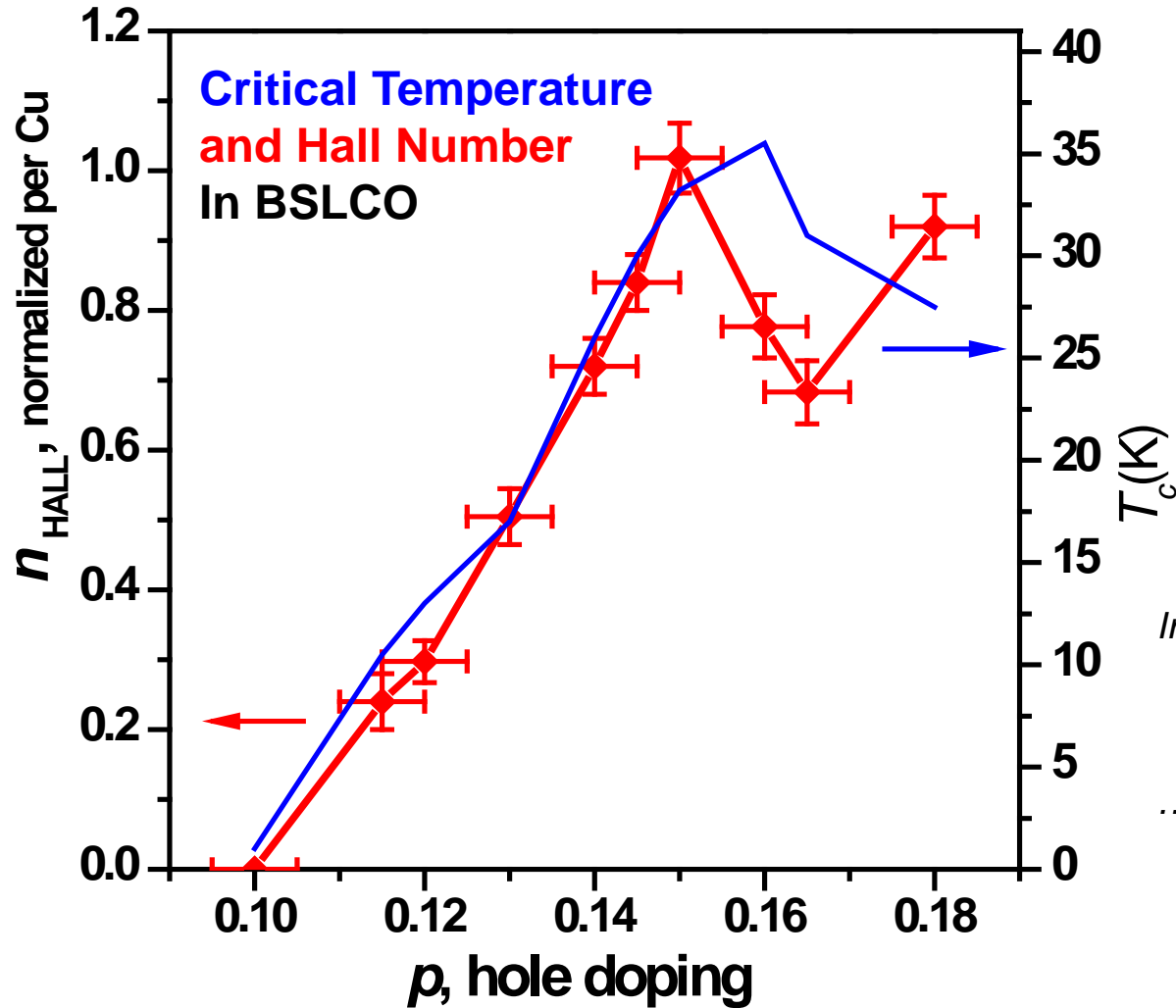
Low-Temperature
Hall Number
in $\text{Bi}_2\text{Sr}_{2-x}\text{La}_x\text{CuO}_{6+d}$

Onset of carriers
yields onset of
superconducting phase

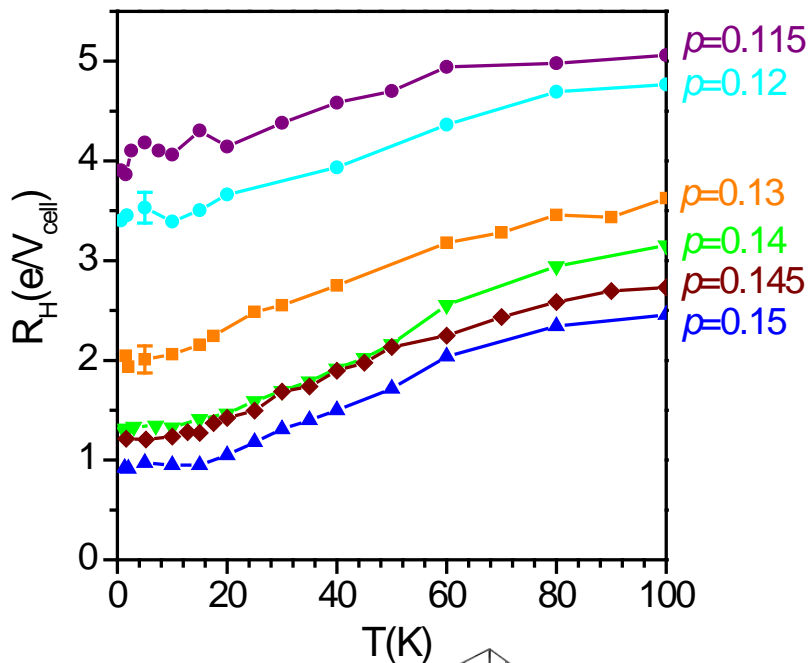
Jump at doping
with Highest T_c



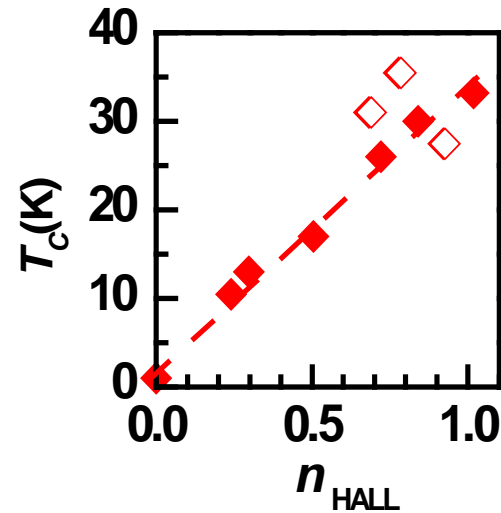
Hall Number is correlated with T_c



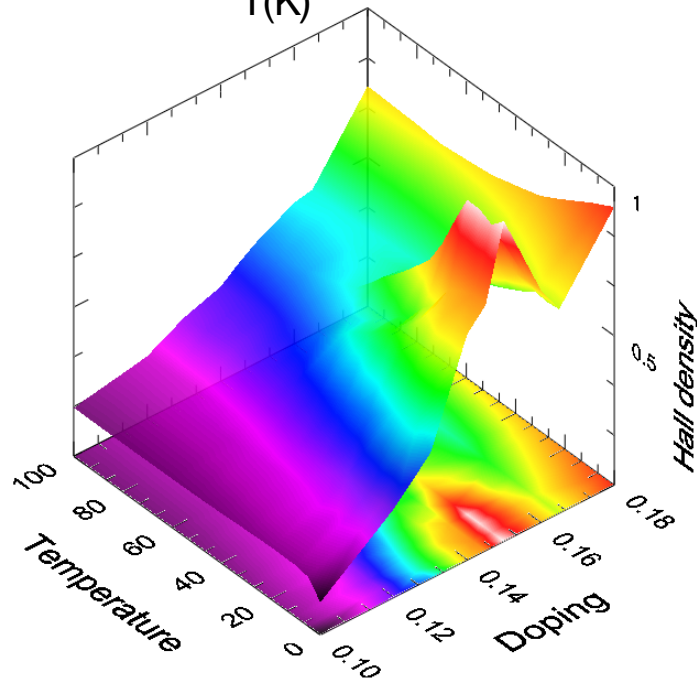
*In the underdoped regime...
 n_{Hall} shows remarkably linear
correlation with T_c
...but not in the overdoped regime...*



Hall coefficient becomes T-independent at low-T near optimum doping in BSLCO
 ---suggesting a measurement of the Hall number.



Linear relation between T_c and the low-T Hall number
 ---suggests phase stiffness governs superconducting transition in underdoped samples



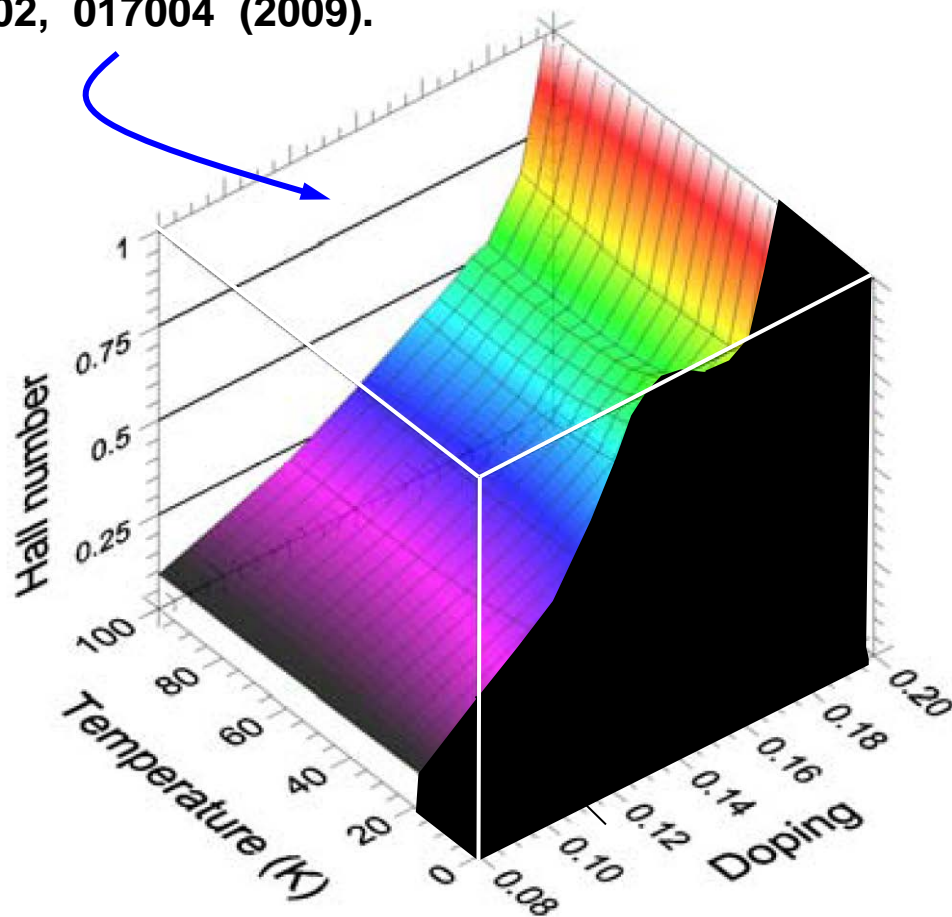
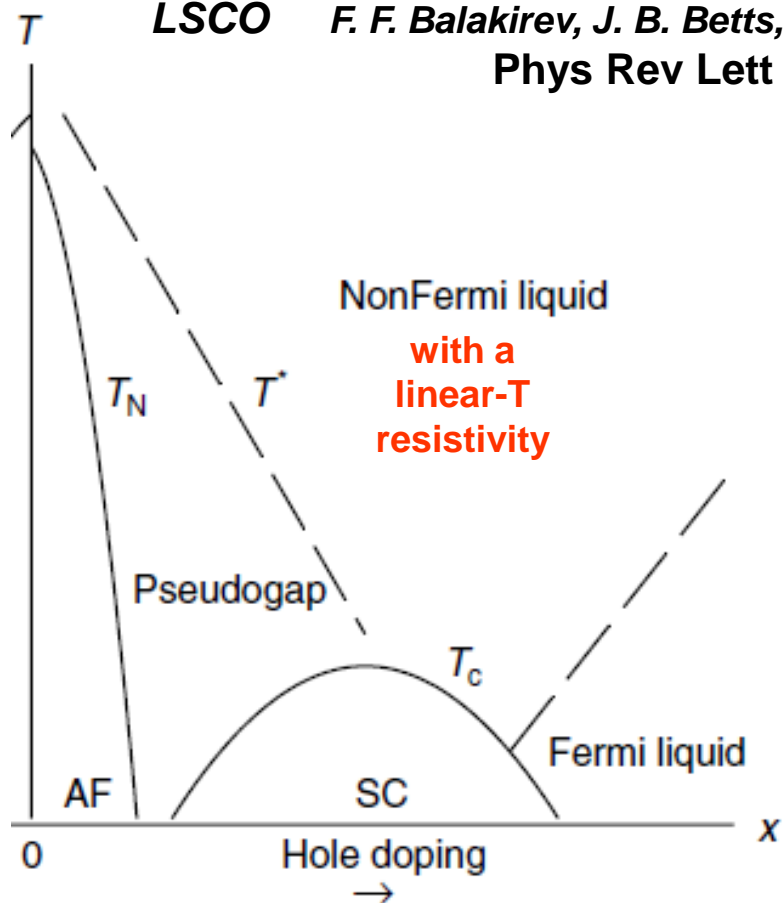
Sharp anomaly in doping dependence of the Hall number at optimum doping
 ---suggesting change in the Fermi Surface

...suggests a Quantum Critical Point governs High- T_c Superconductivity



Quantum Phase Transition at Optimum-Doping: Peak in Hall number also seen in LSCO

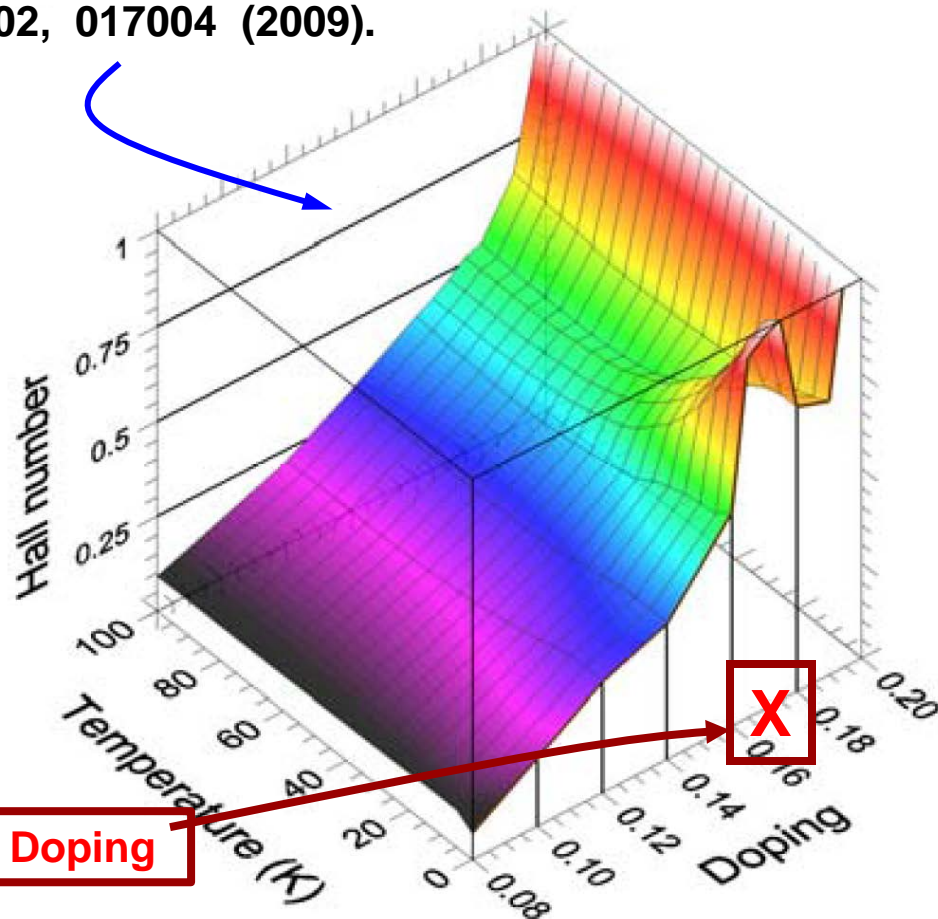
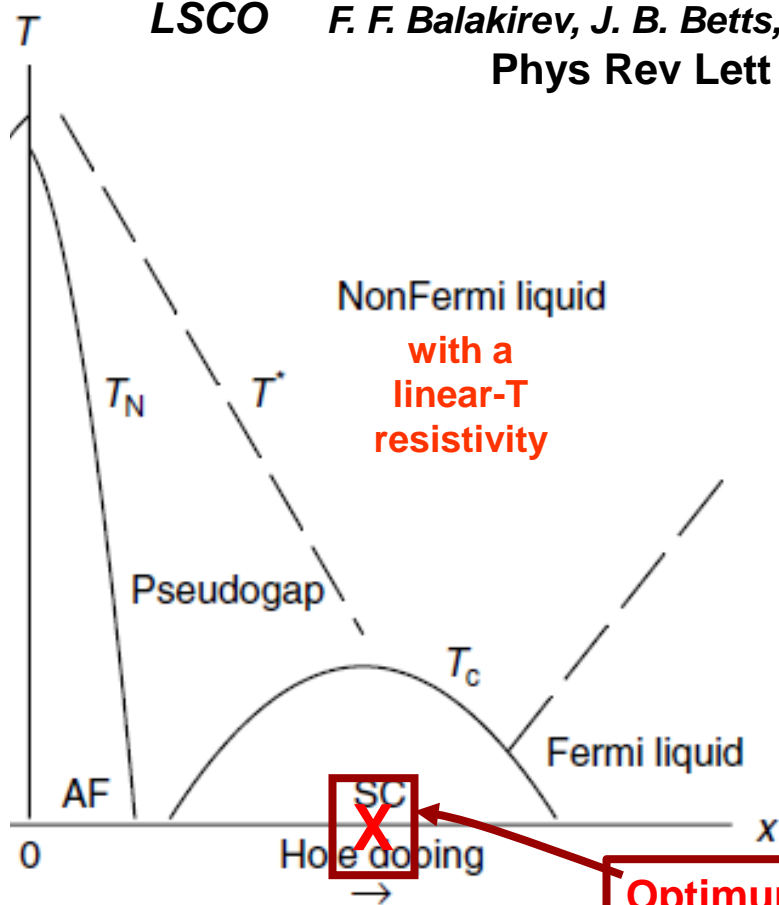
LSCO F. F. Balakirev, J. B. Betts, A. Migliori, I. Tsukada, Yoichi Ando & GSB
Phys Rev Lett 102, 017004 (2009).





Quantum Phase Transition at Optimum-Doping: Peak in Hall number also seen in LSCO

LSCO F. F. Balakirev, J. B. Betts, A. Migliori, I. Tsukada, Yoichi Ando & GSB
Phys Rev Lett 102, 017004 (2009).





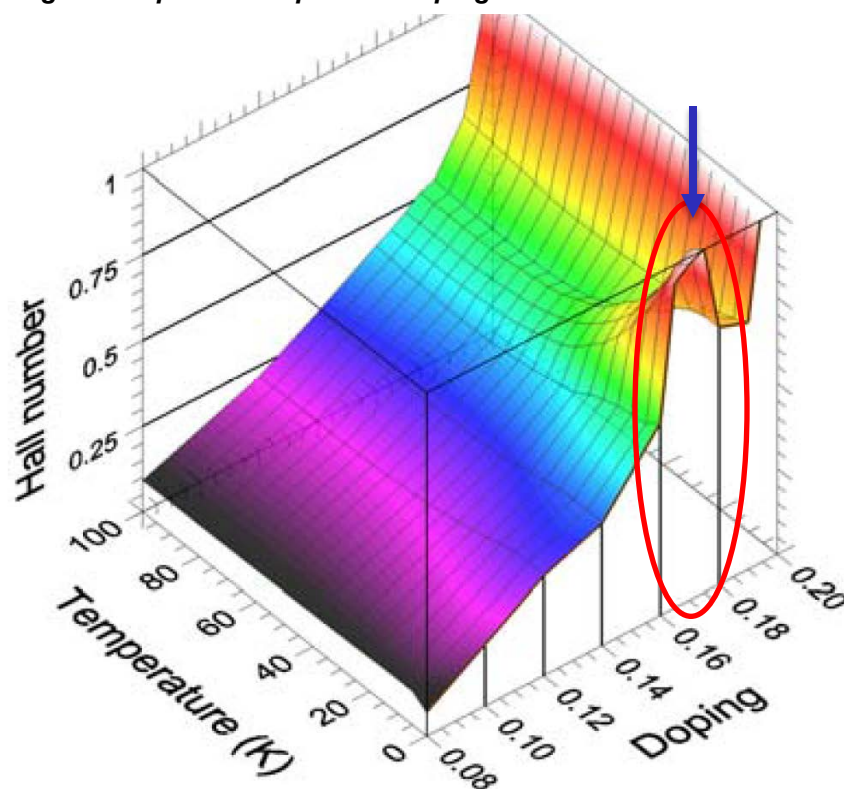
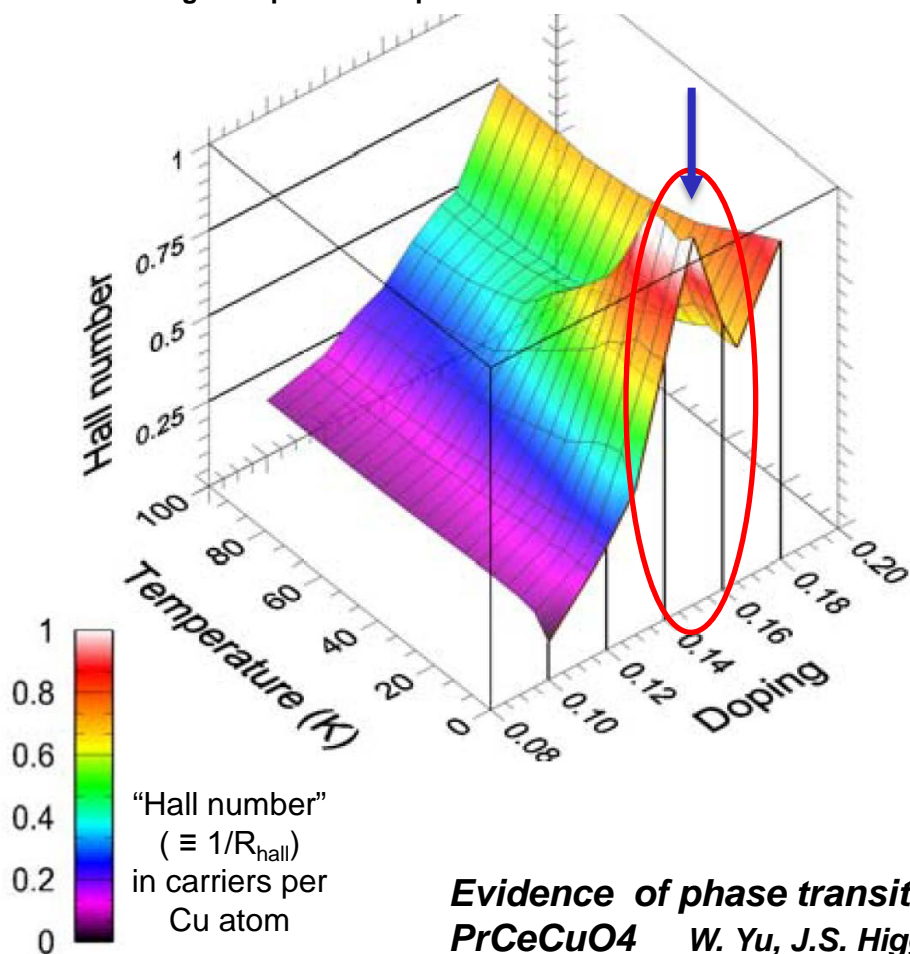
Quantum Phase Transition at Optimum-Doping: Peaks in Hall number seen in two systems

First observed in Bi-2201 in 2003

Fedor F. Balakirev, Jonathan B. Betts, Albert Migliori, S. Ono, Yoichi Ando & Gregory S. Boebinger, *Nature* 424, 912 (2003).
“Signature of optimal doping in Hall-effect measurements on a high-temperature superconductor”

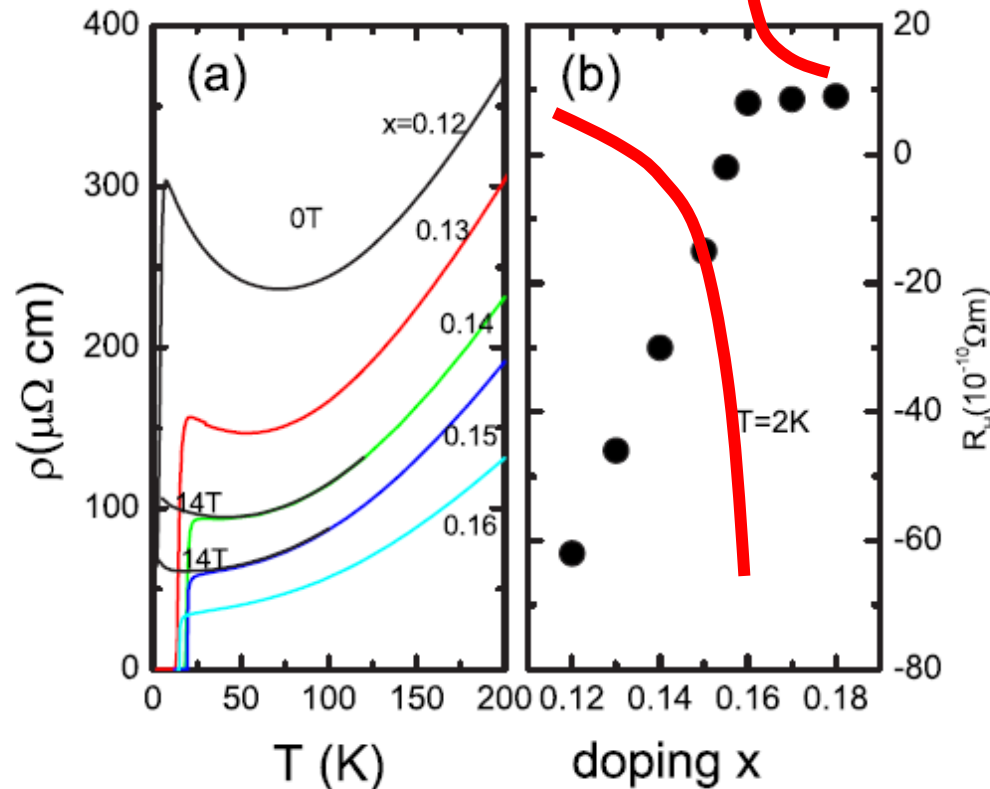
Now confirmed in another high- T_c (LSCO)

F. F. Balakirev, J. B. Betts, A. Migliori, I. Tsukada, Yoichi Ando, G. S. Boebinger, *Phys.Rev.Lett.* 102, 017004 (2009).
“Quantum Phase Transition in the Normal State of High- T_c Cuprates at Optimum Doping.”



Evidence of phase transition (but no peak) also reported in electron doped PrCeCuO4 W. Yu, J.S. Higgins, P. Vach & R.L. Greene, *PRB (RC)* 020503® (2007).

Evidence of phase transition at optimum doping also reported in electron doped PrCeCuO_4 (*M-I transition and Hall changes sign*)



RED LINES
 $\sim 1/R_H$
 $\sim "n_{\text{Hall}}"$

i.e. one gets a divergence in electron-doped samples...

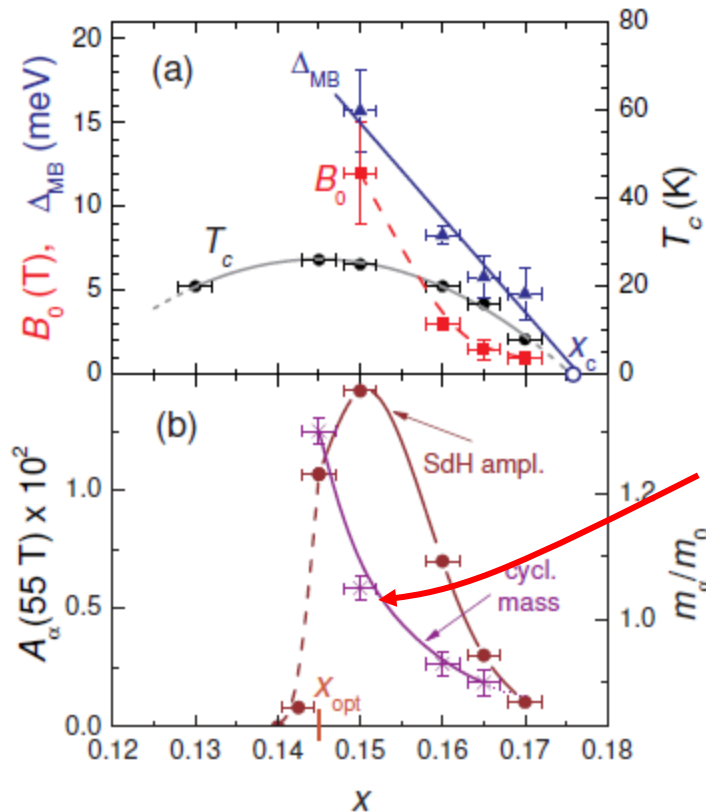
whereas we see a peak in the hole doped samples.

FIG. 2. (Color online) (a) The resistivity of $x=0.12, 0.13, 0.14, 0.15,$ and 0.16 films at zero field and at $\mu_0 H=14T \parallel c$ axis. (b) The Hall coefficient of $0.12 \leq x \leq 0.18$ films ($T=2$ K).

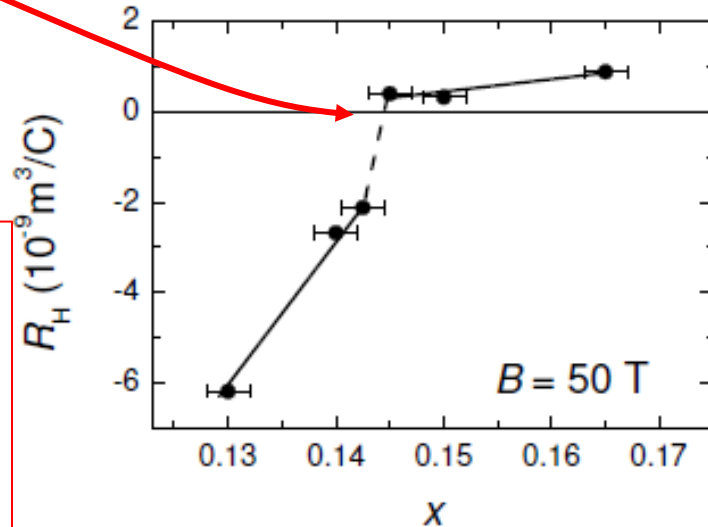
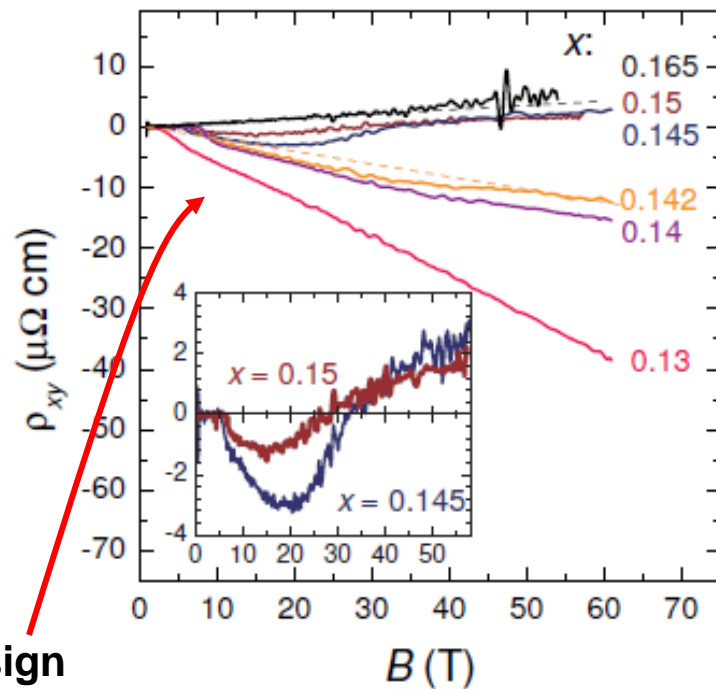
Transport evidence of a magnetic quantum phase transition in electron-doped high-temperature superconductors

W. Yu, J.S. Higgins, P. Vach & R.L. Greene, PRB 76, 020503(R) (2007).

Evidence of phase transition at optimum doping also reported in electron doped $\text{Nd}_{2-x}\text{Ce}_x\text{CuO}_4$ (*M-I transition and Hall changes sign*)



Mass divergence
and Hall changes sign



Correlation between Fermi surface transformations and superconductivity in the electron-doped high- T_c superconductor $\text{Nd}_{2-x}\text{Ce}_x\text{CuO}_4$

T. Helm, M.V. Kartsovnik, C. Proust, B. Vignolle, C. Putzke, E. Kampert, I. Sheikin, E.-S. Choi, J.S. Brooks, N. Bittner, W. Biberacher, A. Erb, J. Wosnitza, and R. Gross
arXiv:1403.7398v1



Back to Zero Magnetic Fields...

(or at least $<30\text{T}$)

The Signatures of the Onset of the Pseudogap

The doping dependence of T^* - what is the real high- T_c phase diagram?

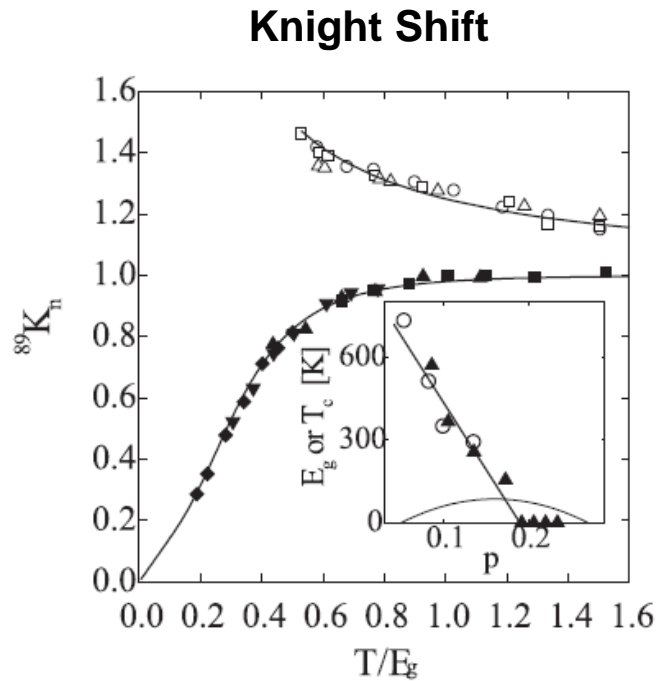


Fig. 3. The ^{89}Y Knight shift for $\text{Y}_{0.8}\text{Ca}_{0.2}\text{Ba}_2\text{Cu}_3\text{O}_{7-\delta}$ with different δ values scaled as a function of T/E_g (\blacklozenge) $T_c = 47.5$, $p = 0.086$; (\blacktriangledown) $T_c = 65.8$, $p = 0.107$; (\blacktriangle) $T_c = 83.2$ K, $p = 0.140$; (\blacksquare) $T_c = 86$ K, $p = 0.160$; (\triangle) $T_c = 72.1$ K, $p = 0.204$; (\square) $T_c = 60$ K, $p = 0.221$; (\circ) $T_c = 47.5$ K, $p = 0.234$). Inset: E_g values obtained from the scaling, 0.1 Ca (\circ) and 0.2 Ca (\blacktriangle).

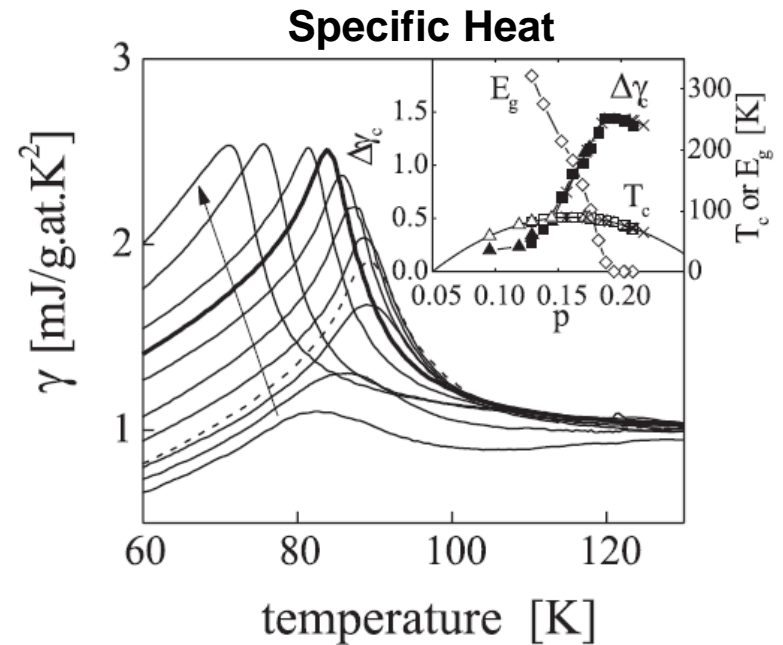


Fig. 5. The T -dependence of $\gamma \equiv C_p/T$ for Bi-2212 with different oxygen contents spanning from underdoped to overdoped (indicated by direction of arrow). The curves for critical and optimal doping are indicated by the bold and dashed curves, respectively. Inset: the doping dependence of the increment in γ for $\text{Bi}_{2.1}\text{Sr}_{1.9}\text{CaCu}_2\text{O}_{8+\delta}$ (\blacksquare), $\text{Bi}_{1.9}\text{Pb}_{0.2}\text{Sr}_{1.9}\text{CaCu}_2\text{O}_{8+\delta}$ (\times) and $\text{Bi}_{2.1}\text{Sr}_{1.9}\text{Ca}_{0.7}\text{Y}_{0.3}\text{Cu}_2\text{O}_{8+\delta}$ (\blacktriangle). In each case, $\Delta\gamma_c$ falls abruptly at $p = 0.19$ with the opening of the pseudogap. E_g values obtained from a scaling analysis are shown by the diamonds.

The doping dependence of T^* -
 what is the real high- T_c phase diagram?

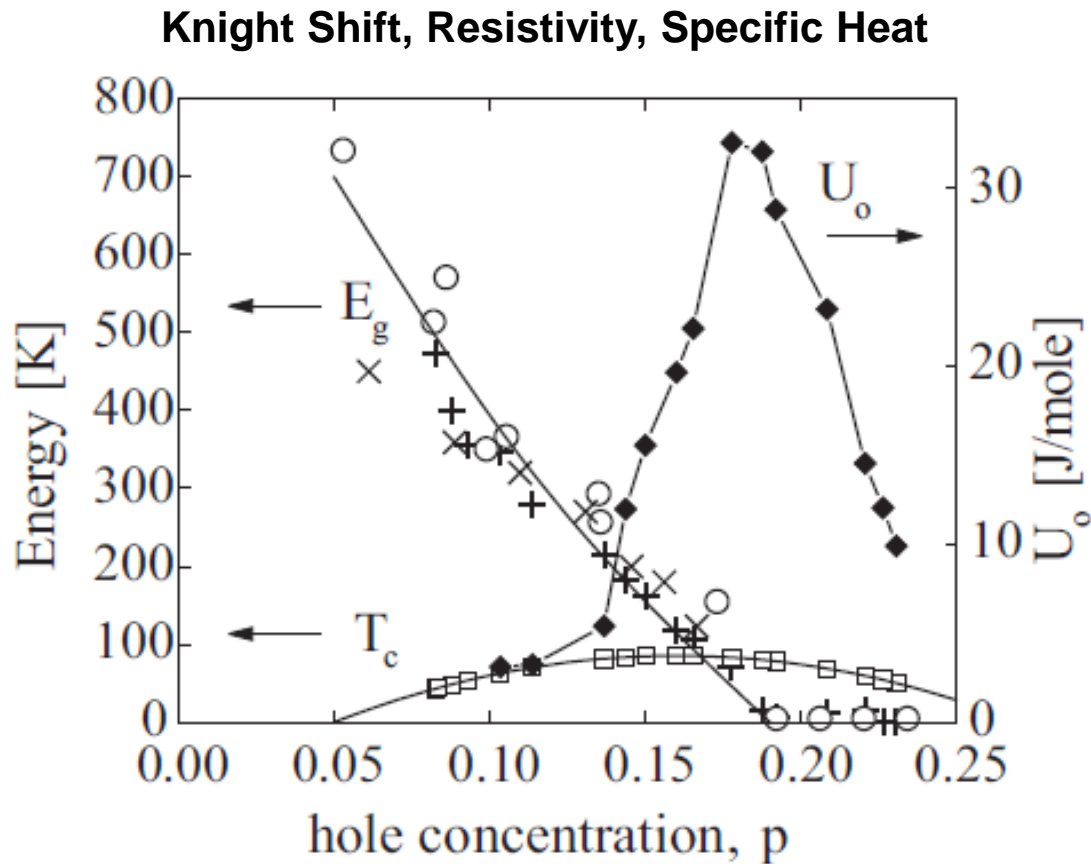
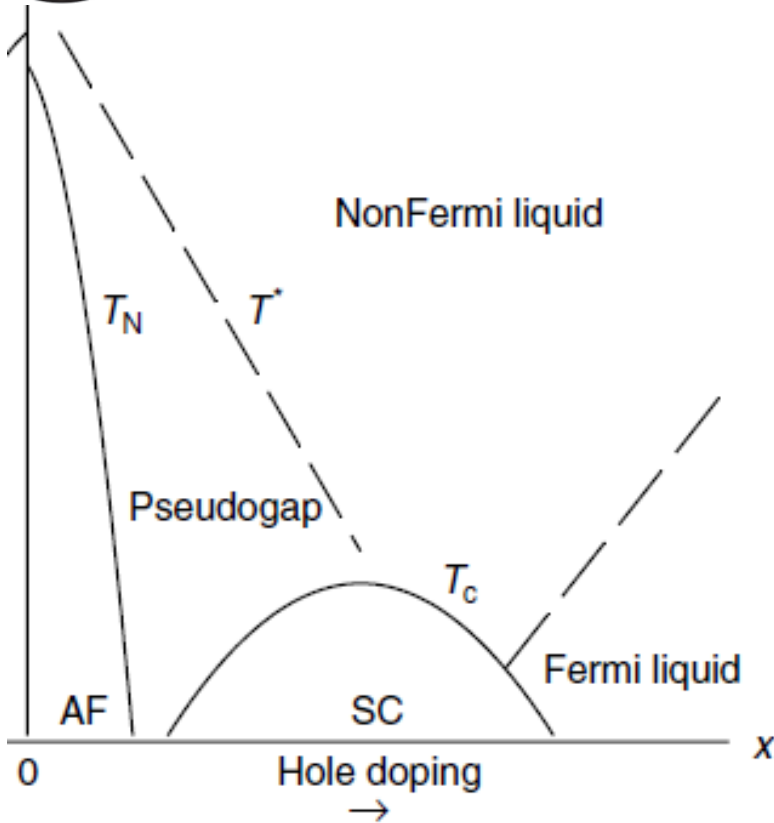


Fig. 4. The doping dependence of E_g for $Y_{0.8}Ca_{0.2}Ba_2Cu_3O_{7-\delta}$ from $^{89}K_s$ (○), from heat capacity (+) and from scaling of the resistivity (×), of the condensation energy U_0 (◆) and of T_c (□).

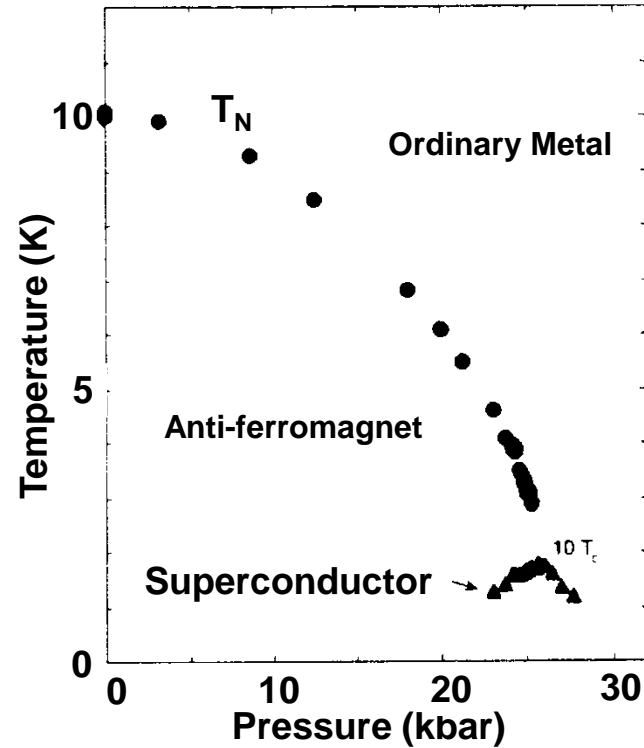


**Superconductivity is Stabilized
Near Quantum Critical Points,
*but no one knows why.***



**Hole-doped High-Temperature
Superconducting Cuprate
Maximum $T_c \sim 40-150\text{K}$**

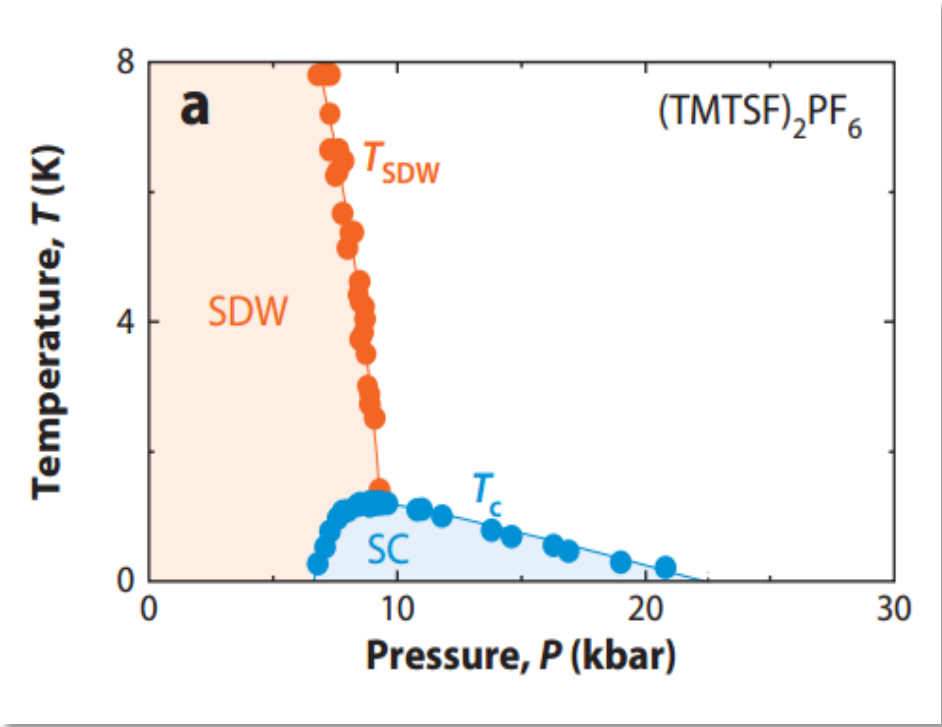
N.D. Mathur et al., Nature **394**, 39 (1998)



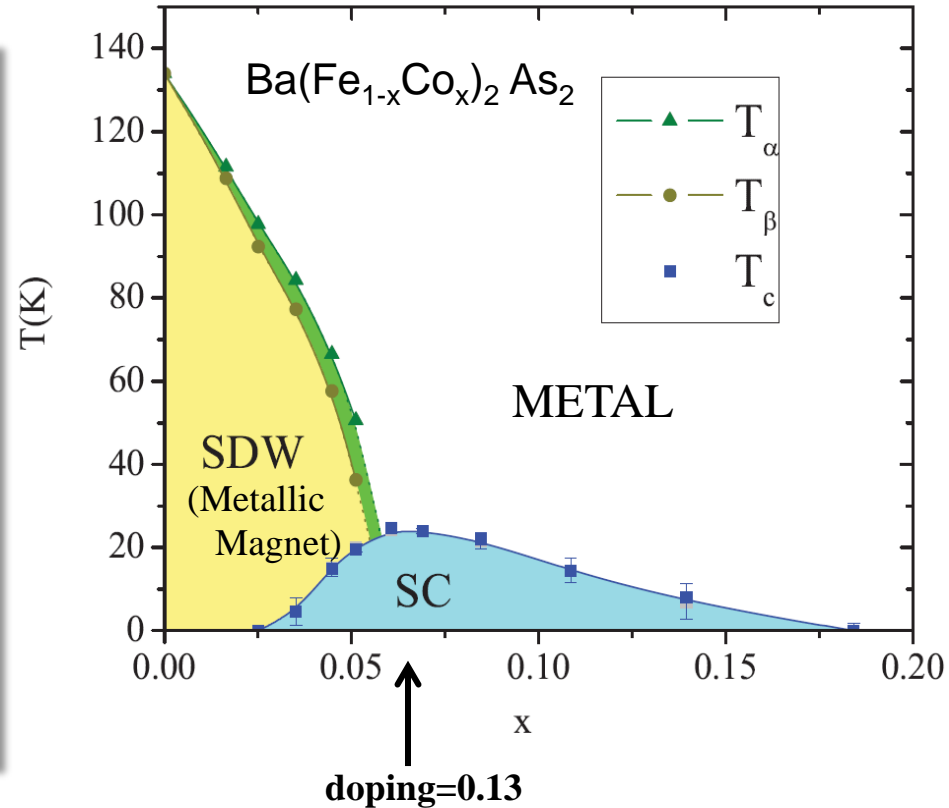
**CeIn_3
a Heavy Fermion Compound
with Superconducting $T_c < 1\text{ K}$**



**Superconductivity is Stabilized
Near Quantum Critical Points,
*but no one knows why.***



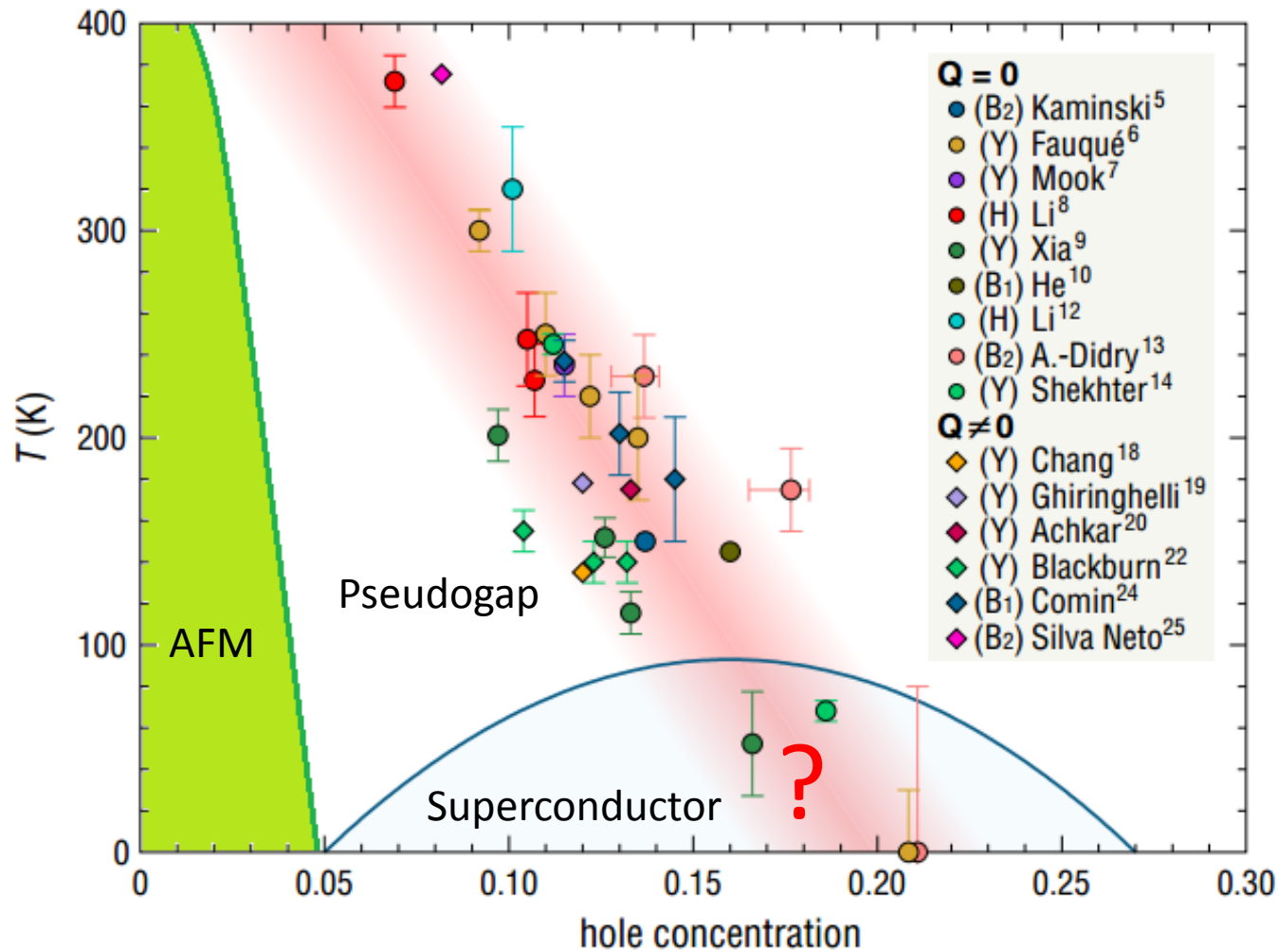
L. Taillefer, Annual Review of Condensed Matter Physics (2010)



Jiun-Haw Chu, James G. Analytis, Chris Kucharczyk, Ian R. Fisher, Phys. Rev. **B 79**, 014506 (2009)
Determination of the phase diagram of the electron doped superconductor $\text{Ba}(\text{Fe}_{1-x}\text{Co}_x)_2\text{As}_2$

As the years go by....

Many Broken Symmetries Discovered at the Pseudogap Onset





Is the Onset of the Pseudogap a Thermodynamic Transition?

“Ultrasound sees all” -Albert Migliori

- Sound speeds depend on compressibility, a thermodynamic susceptibility.
- Any phase transition has a signature in the compressibility.
- Let’s see what a superconductor does (theory by an experimentalist).

energy	$\Delta F _{T_c} = H_c^2(T_c, B, P) = 0$	
volume	$\frac{\partial \Delta F}{\partial P} _{T_c} = \Delta V _{T_c} = H_c \frac{\partial H_c}{\partial P} _{T_c} = 0$	$H_c(T_c) = 0$
stiffness	$\frac{\partial^2 \Delta F}{\partial P^2} _{T_c} = \frac{\partial \Delta V}{\partial P} _{T_c} = \frac{1}{c_{ij}} = H_c \frac{\partial^2 H_c}{\partial P^2} _{T_c} + \left(\frac{\partial H_c}{\partial P} \right)^2 _{T_c}$	This term never zero

There is *always* a step discontinuity at the superconducting transition in elastic stiffness.

Arkady Shekhter, B.J. Ramshaw, Ruixing Liang, W.N. Hardy, D.A. Bonn, Fedor F. Balakirev, Ross McDonald,
 Jon B. Betts, Scott C. Riggs, Albert Migliori,

Nature 498, 75 (2013)

doi:10.1038/nature12165

Resonant Ultrasound Spectroscopy is simple

Resonant ultrasound spectroscopy (RUS) uses the mechanical resonances of small samples to extract all the components of the elastic tensor at the same time.

RUS and other ultrasound techniques measure the *adiabatic* moduli-typically within 1% of isothermal moduli in solids.

Only RUS measures the true thermodynamic attenuation, independent of defects and scattering, transducer misalignment.

PROOF COPY 232512RSI

REVIEW OF SCIENTIFIC INSTRUMENTS 76, 1 (2005)

Implementation of a modern resonant ultrasound spectroscopy system for the measurement of the elastic moduli of small solid specimens

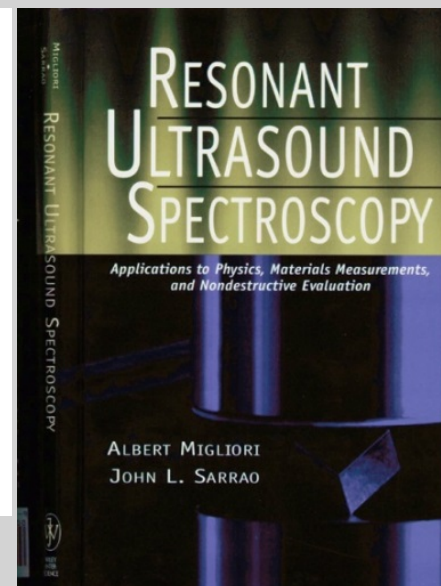
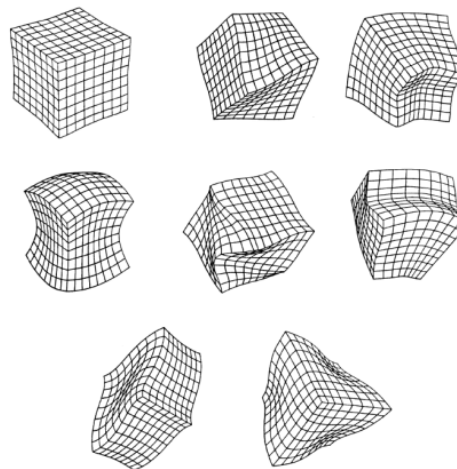
Albert Migliori
National High Magnetic Field Laboratory of the Los Alamos National Laboratory, Los Alamos, New Mexico 87545

J. D. Maynard
The Pennsylvania State University, University Park, Pennsylvania 16802

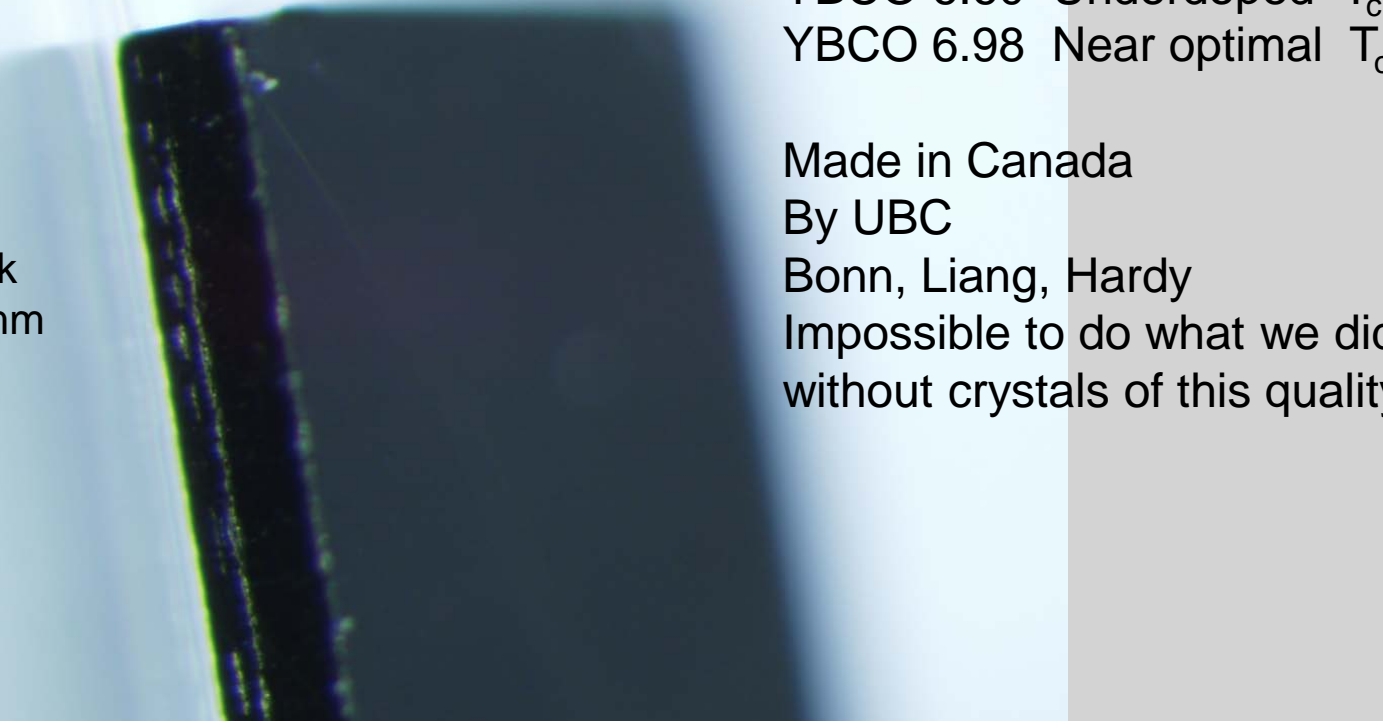
(Received 8 August 2005; accepted 24 October 2005)

The use of mechanical resonances to determine the elastic moduli of materials of interest to condensed-matter physics, engineering, materials science and more is a steadily evolving process. With the advent of massive computing capability in an ordinary personal computer, it is now possible to find all the elastic moduli of low-symmetry solids using sophisticated analysis of a set of the lowest resonances. This process, dubbed "resonant ultrasound spectroscopy" or RUS, provides the highest absolute accuracy of any routine elastic modulus measurement technique, and it does this quickly on small samples. RUS has been reviewed extensively elsewhere, but still lacking is a complete description of how to make such measurements with hardware and software easily available to the general science community. In this article, we describe how to implement realistically a useful RUS system. © 2005 American Institute of Physics.

[DOI: [10.1063/1.2140494](https://doi.org/10.1063/1.2140494)]



Tiny single detwinned crystals are *required*

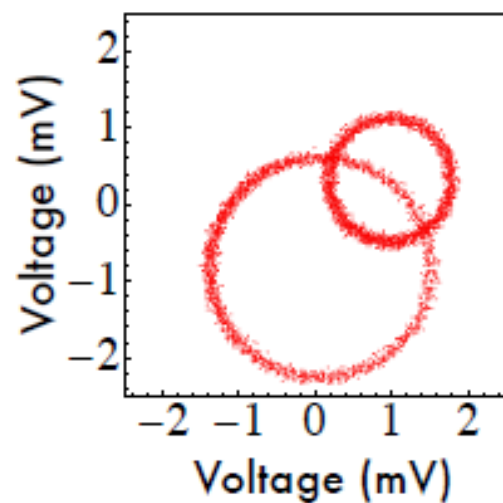
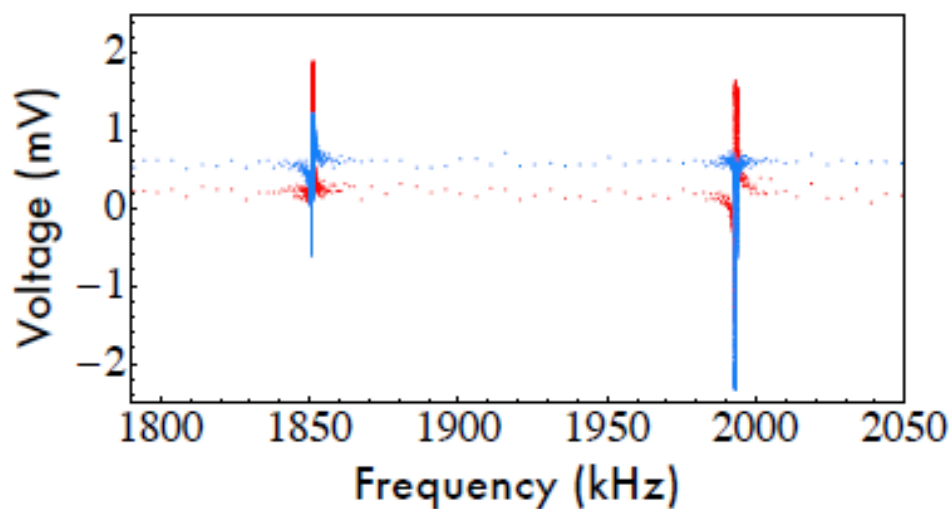
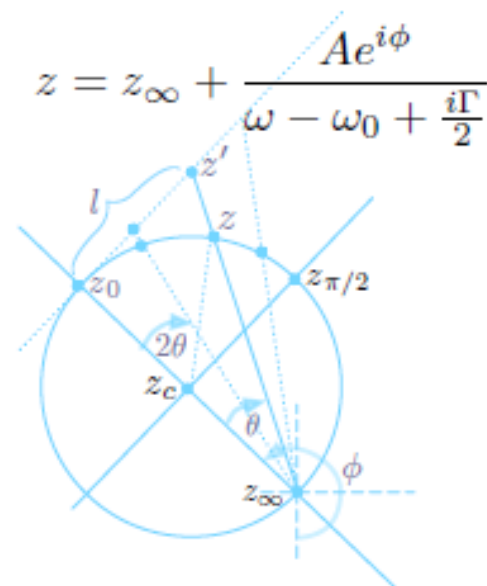
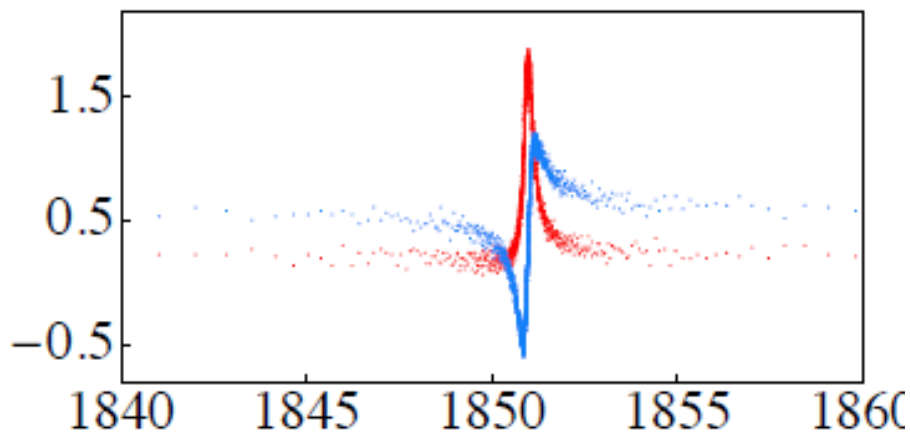


205 μ m thick
1.03 x 1.2mm
1.62 mg

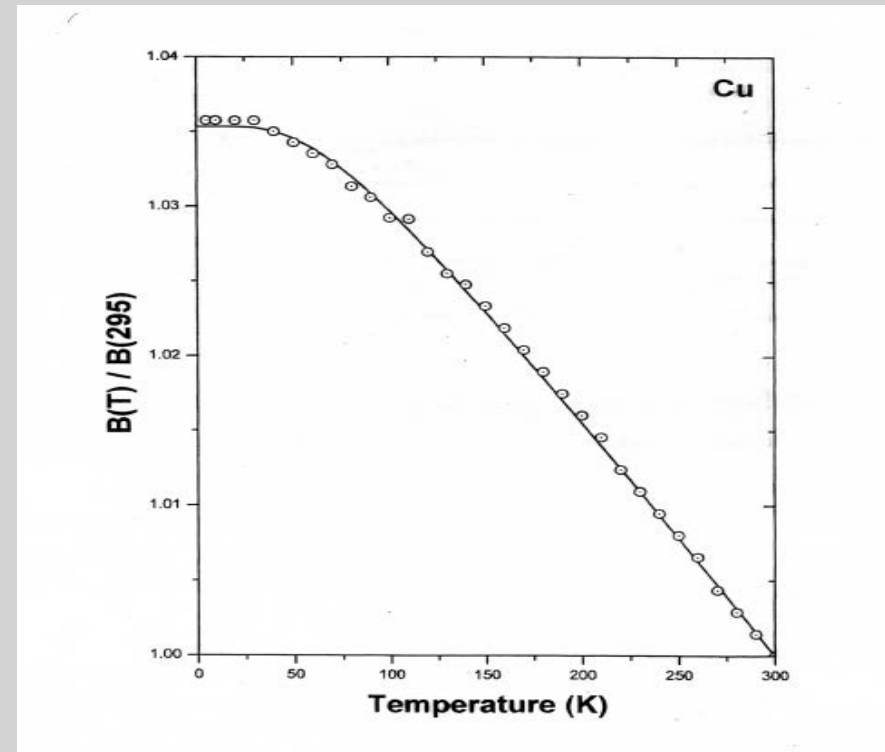
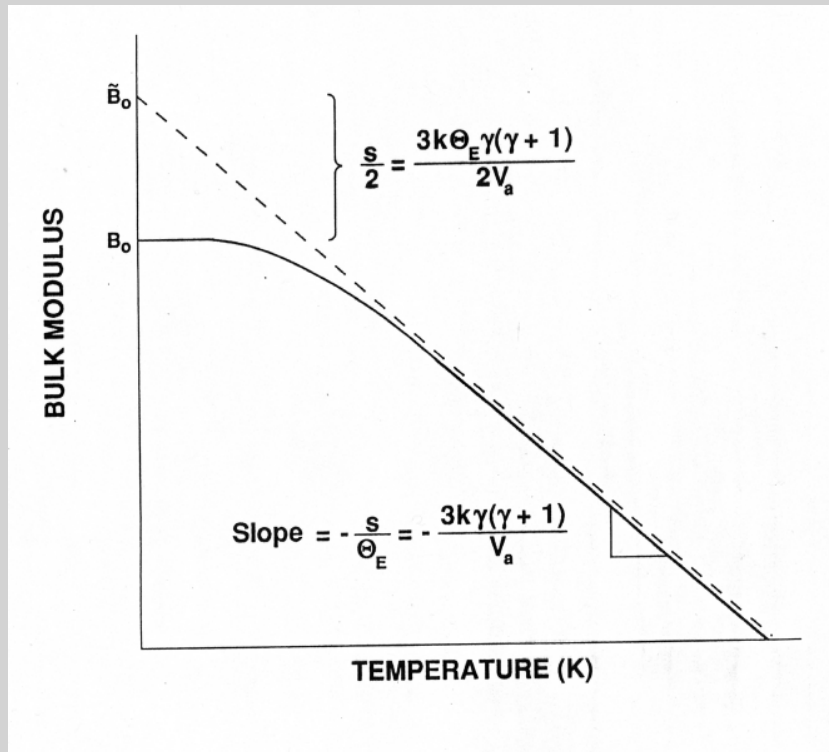
YBCO 6.60 Underdoped $T_c=61.6$ K
YBCO 6.98 Near optimal $T_c=88.0$ K

Made in Canada
By UBC
Bonn, Liang, Hardy
Impossible to do what we did
without crystals of this quality

Resonant Ultrasound Spectroscopy — technique

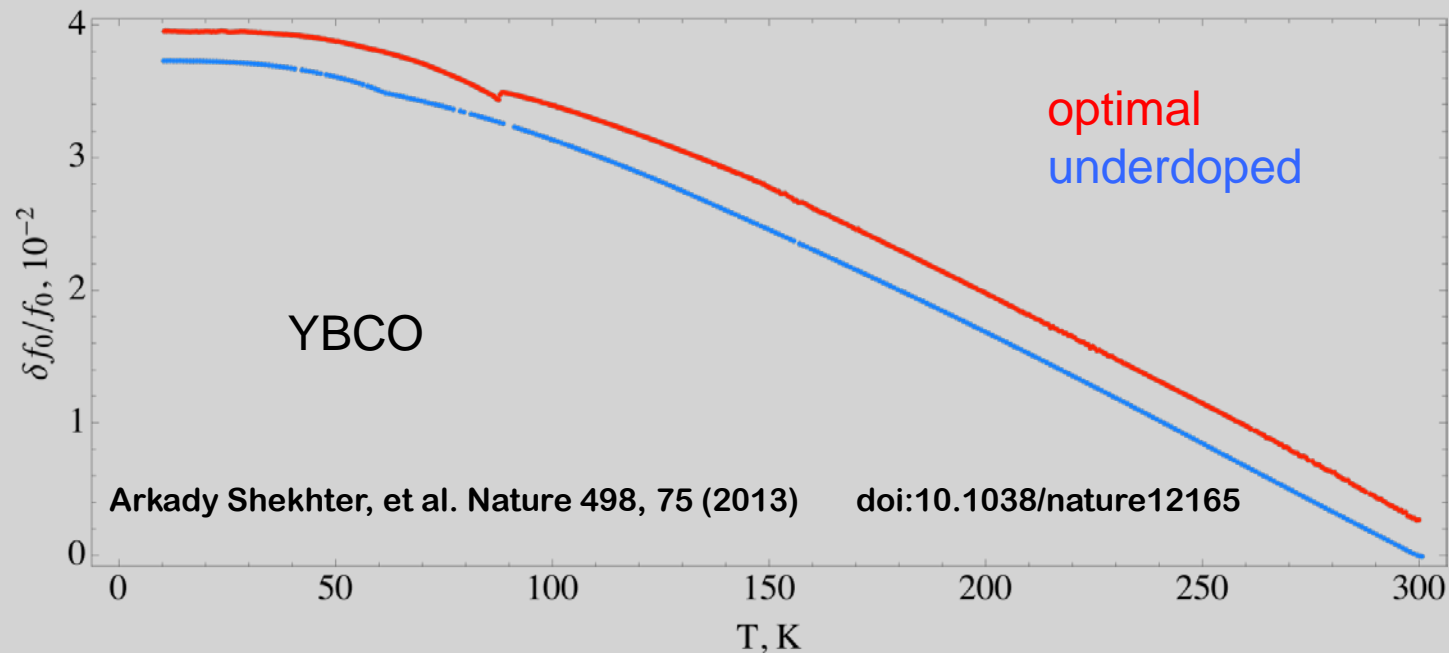
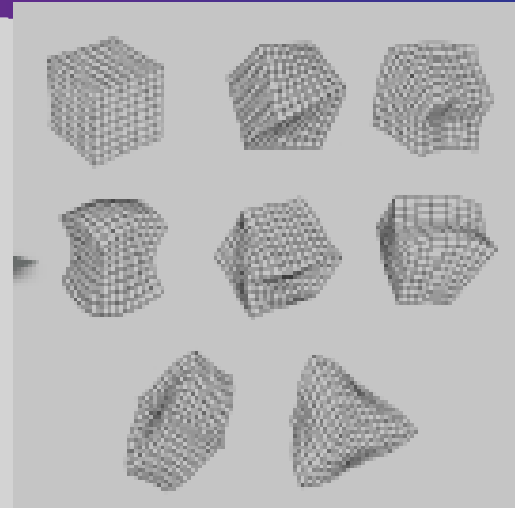
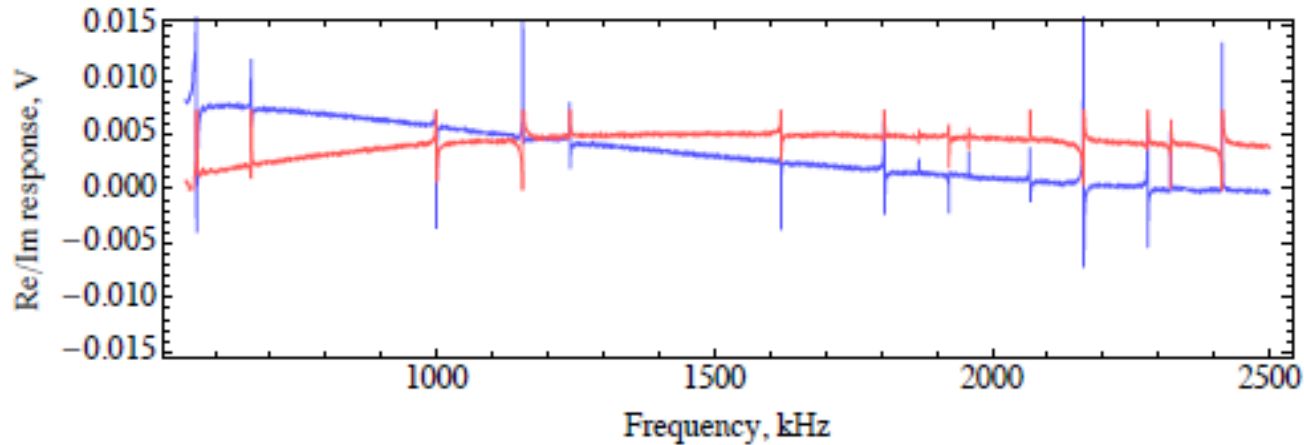


What is normal?

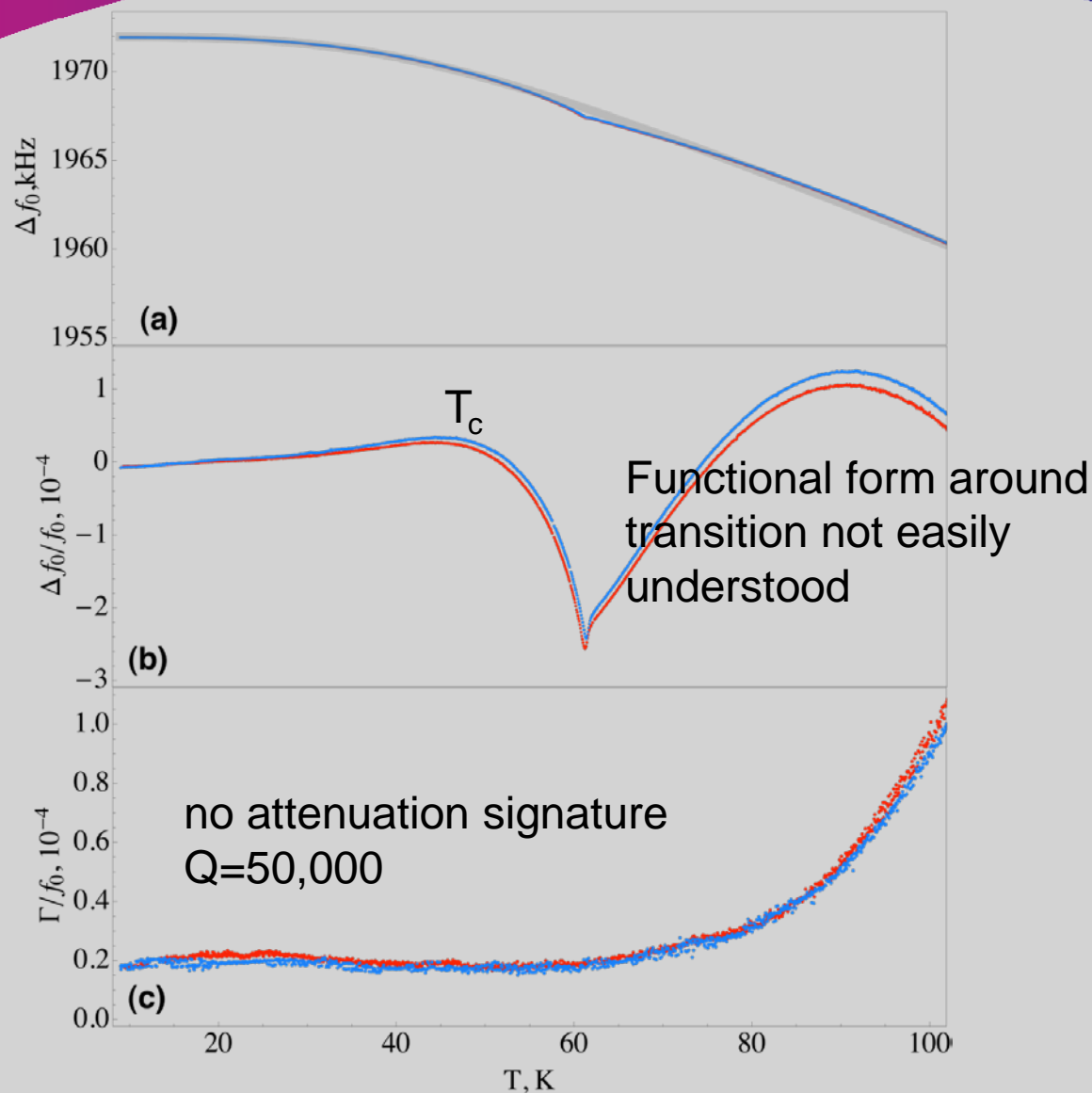


Overall smoothness and normal behavior

mechanical resonances of a macroscopic crystal



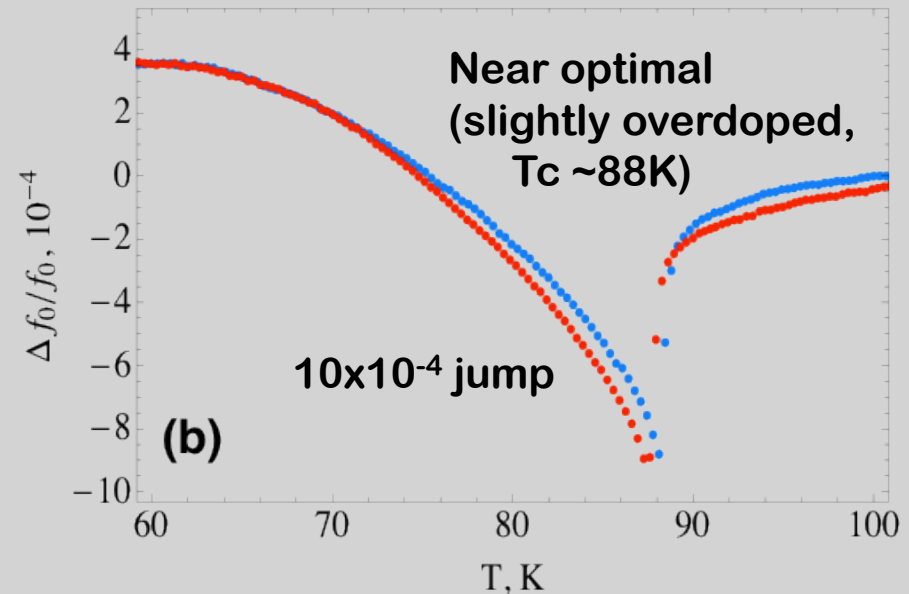
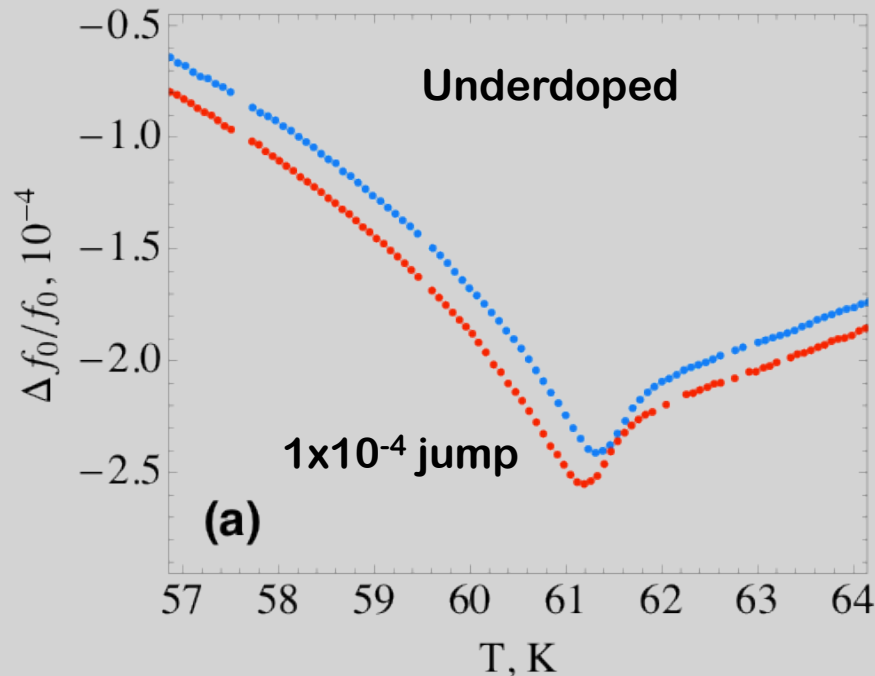
Elastic moduli and attenuation in **underdoped** YBCO at superconducting transition through the looking glass



Arkady Shekhter, et al.
Nature 498, 75 (2013)
doi:10.1038/nature12165

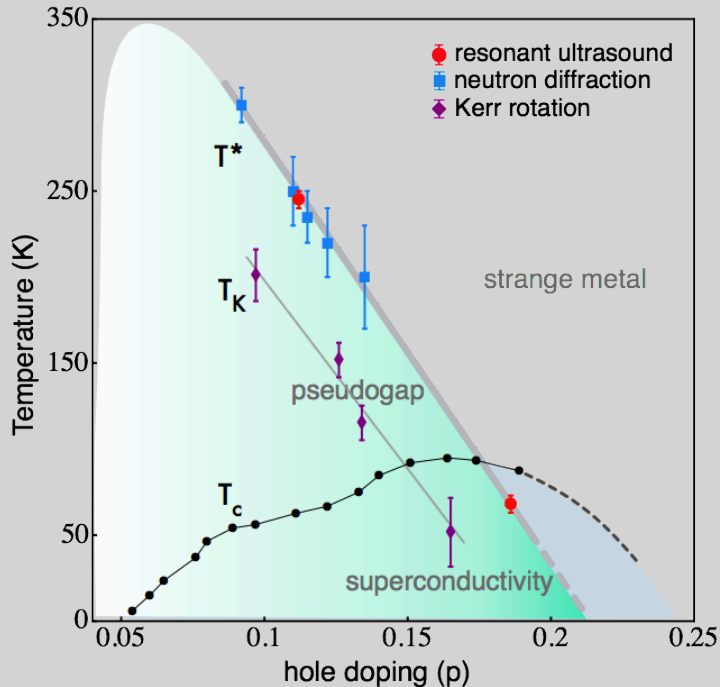
Detail of the superconducting transition seen through even stronger looking glass

- Step size depends on superconducting fraction.
- Transition width is sharper than most observations of YBCO.
- Size of jump makes sense if we observed **full thermodynamic signature: $(T_c/T_f)^2$ (no preformed pairs)**.



Pseudogap boundary in YBCO 6.98 (overdoped) $T_c=88.0\text{K}$

Perform a linear component analysis of the temperature dependence of multiple resonances

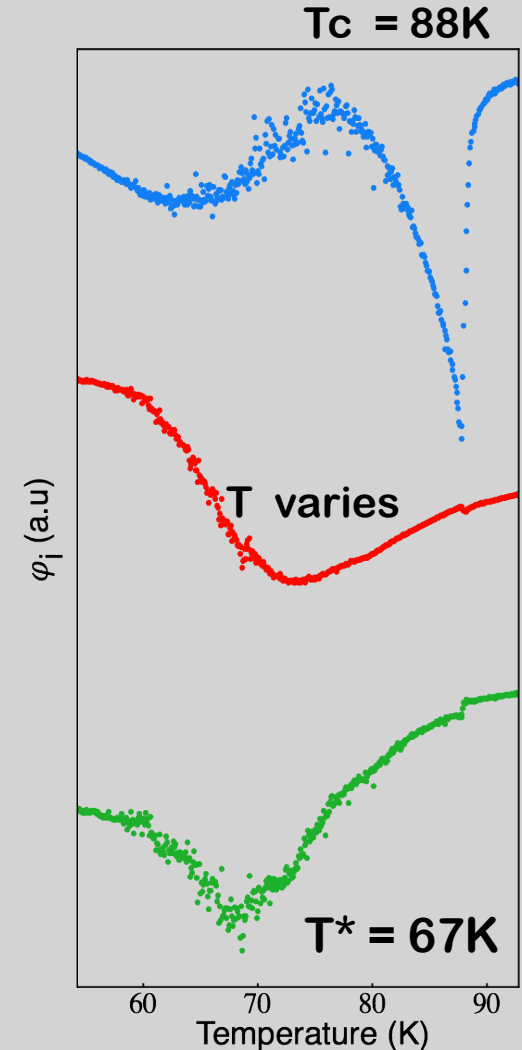


- Each resonance is a combination of the thermal response of several elastic moduli.
- Deconvolution produces the three types of thermal responses shown at right.

Superconductivity
(this feature appears at the same temperature for all resonances)

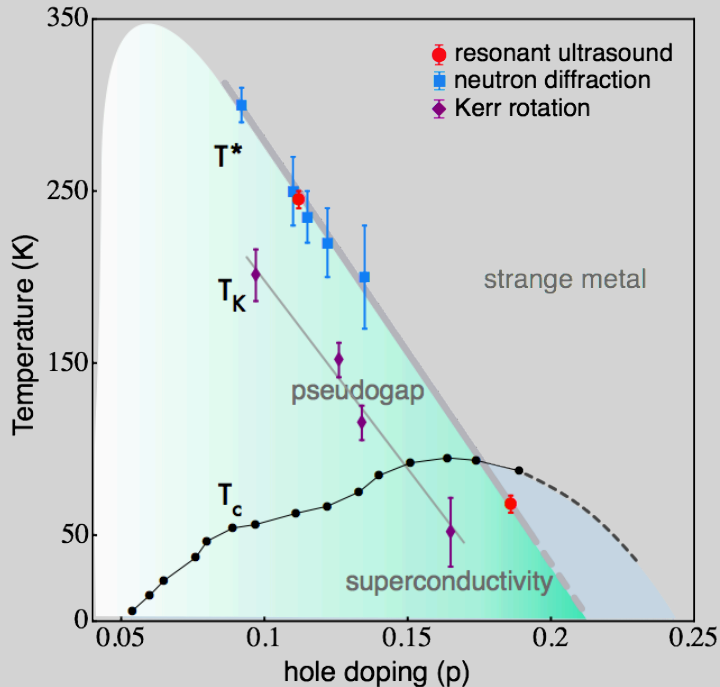
Dissipation feature at temperatures that track frequency of each resonance
(thus not a phase transition)

Pseudogap
(this feature appears at the same temperature for all resonances)



Pseudogap boundary in YBCO 6.98 (overdoped) $T_c=88.0\text{K}$

Perform a linear component analysis of the temperature dependence of multiple resonances

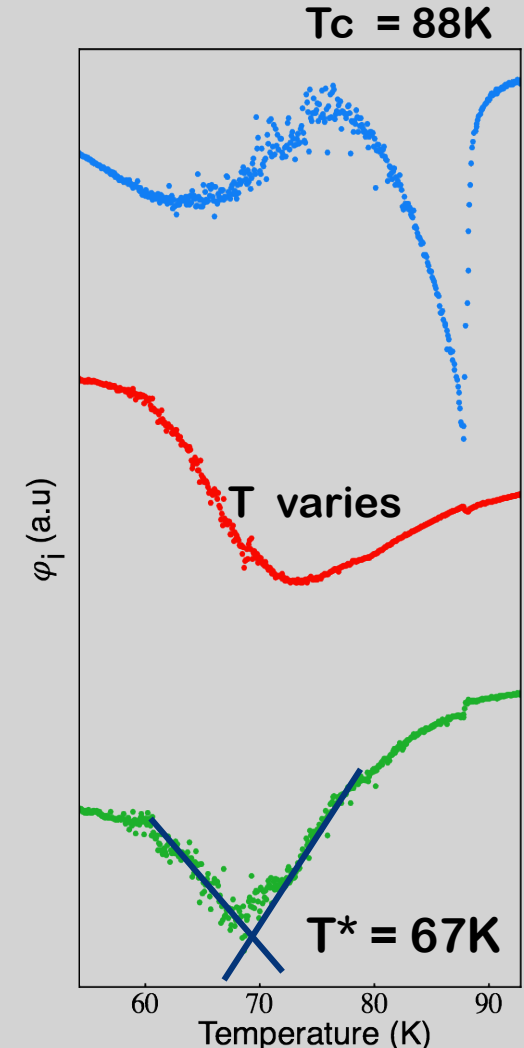


- Each resonance is a combination of the thermal response of several elastic moduli.
- Deconvolution produces the three types of thermal responses shown at right.

Superconductivity
(this feature appears at the same temperature for all resonances)

Dissipation feature at temperatures that track frequency of each resonance
(thus not a phase transition)

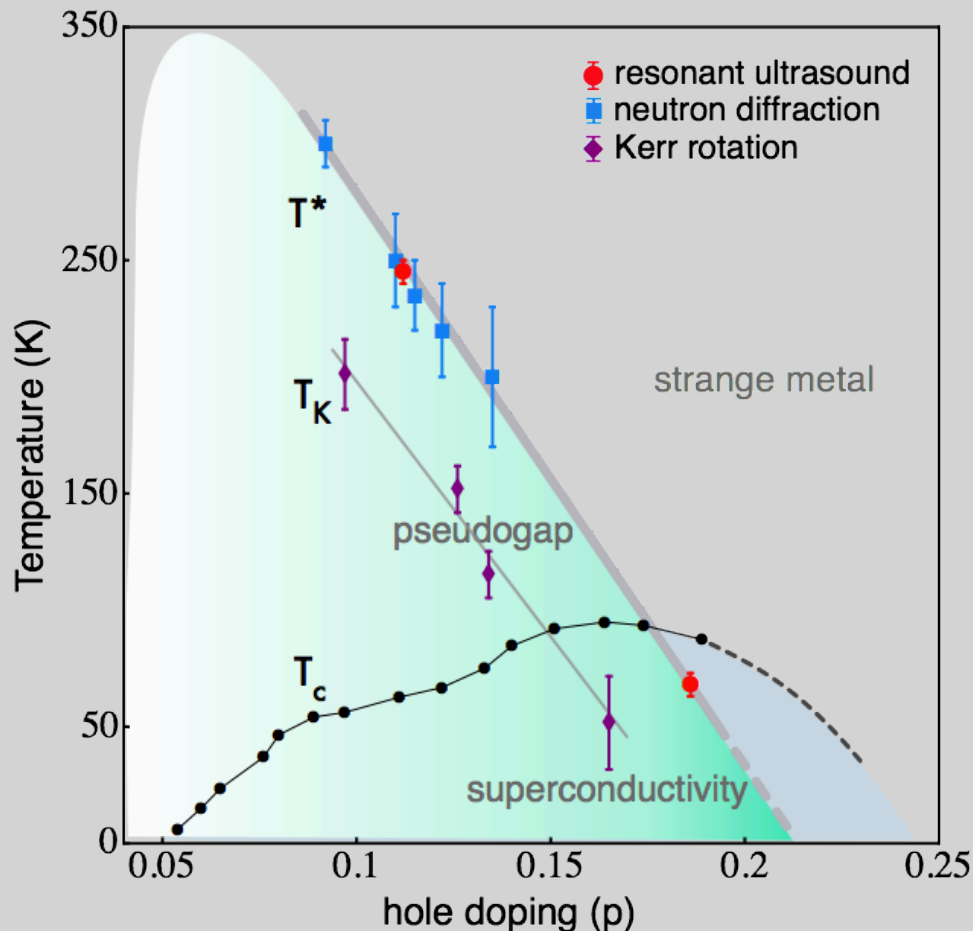
Pseudogap
(this feature appears at the same temperature for all resonances)



The precision in determining T^* is determined by the sharpness of the change in slope

Conclusions from Resonant Ultrasound Spectroscopy

- Pseudogap onset IS a thermodynamic phase transition, conjectured to be second order with a magnetic order parameter.
- Observed evolution of the pseudogap phase boundary from underdoped to overdoped establishes the presence of a quantum critical point inside the superconducting dome.
- This suggests a quantum-critical origin for both the strange metallic behavior and the glue mechanism of superconducting pairing.



Arkady Shekhter, et al.
Nature 498, 75 (2013)
doi:10.1038/nature12165



Back to High Magnetic Fields...

(up to 60T)

to see Quantum Oscillations



Large Fermi Surface in $Tl-2201$ in the overdoped regime

Original measurement using Angle-Dependent Magneto-resistance Oscillations:

N.E. Hussey, M. Abdel-Jawad, A. Carrington, A.P. Mackenzie, L. Balicas,

“A coherent three-dimensional Fermi surface in a high-transition-temperature superconductor” *Nature* 425, 814 (2003)

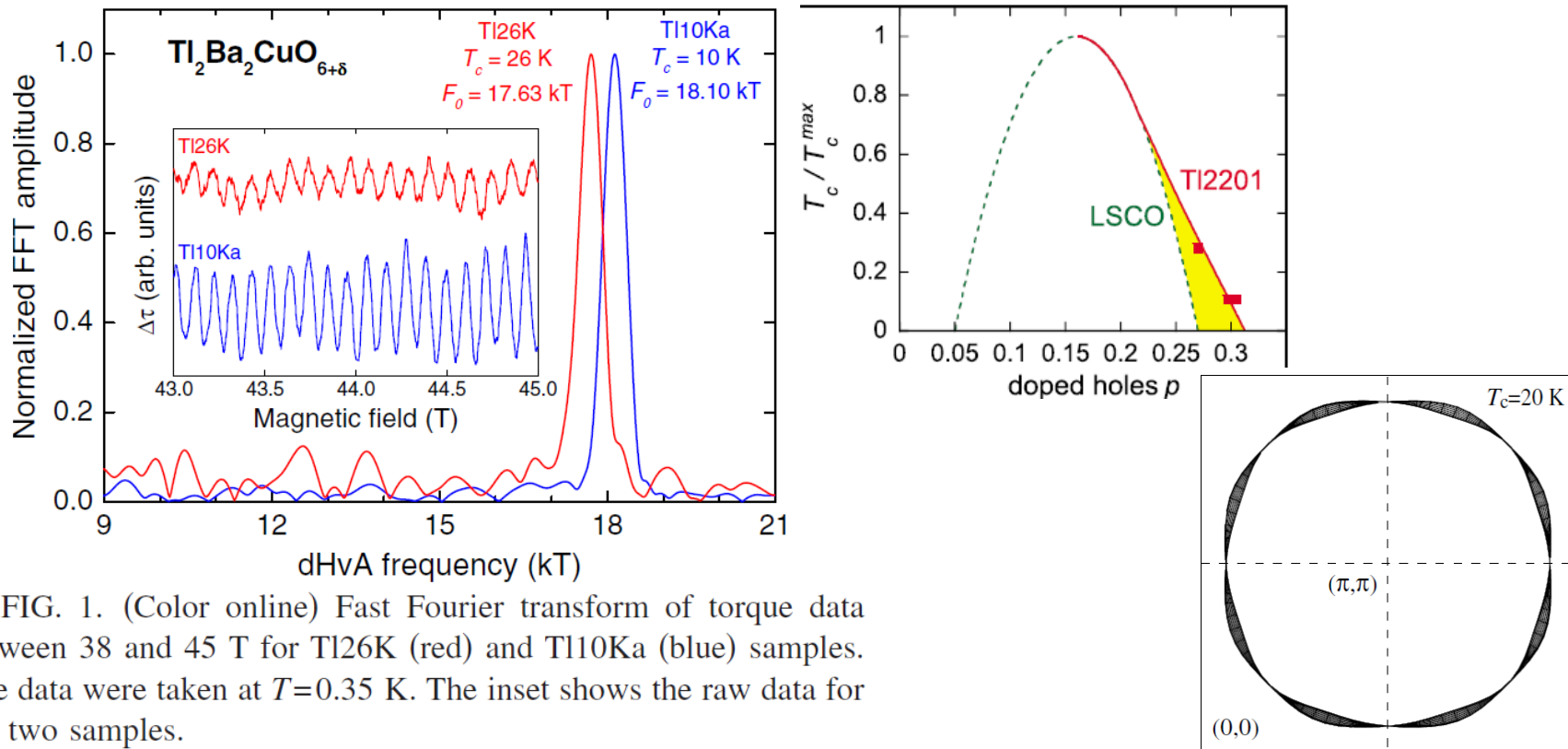
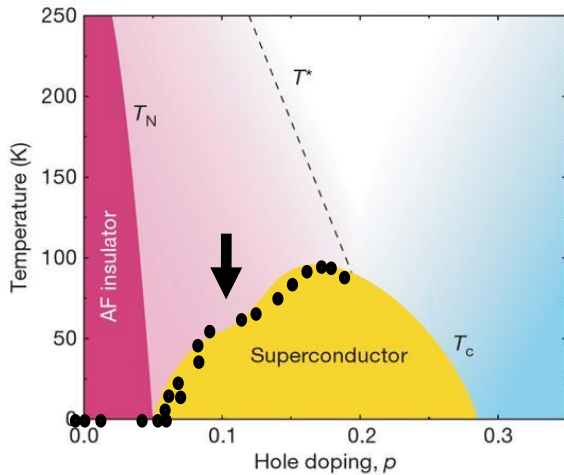


FIG. 1. (Color online) Fast Fourier transform of torque data between 38 and 45 T for Tl26K (red) and Tl10Ka (blue) samples. The data were taken at $T=0.35$ K. The inset shows the raw data for the two samples.

A.F. Bangura, P.M.C. Rourke, T.M. Benseman, M. Matusiak, J.R. Cooper, N.E. Hussey, and A. Carrington
Fermiology and electronic homogeneity of the superconducting overdoped cuprate $Tl_2Ba_2CuO_{6+\delta}$ revealed by quantum oscillations
Phys. Rev. B 82, 140501(R) (2010)

2007: Small Fermi Surface in the Underdoped YBCO – The Pseudogap State Looks like an Ordinary Fermi Liquid !

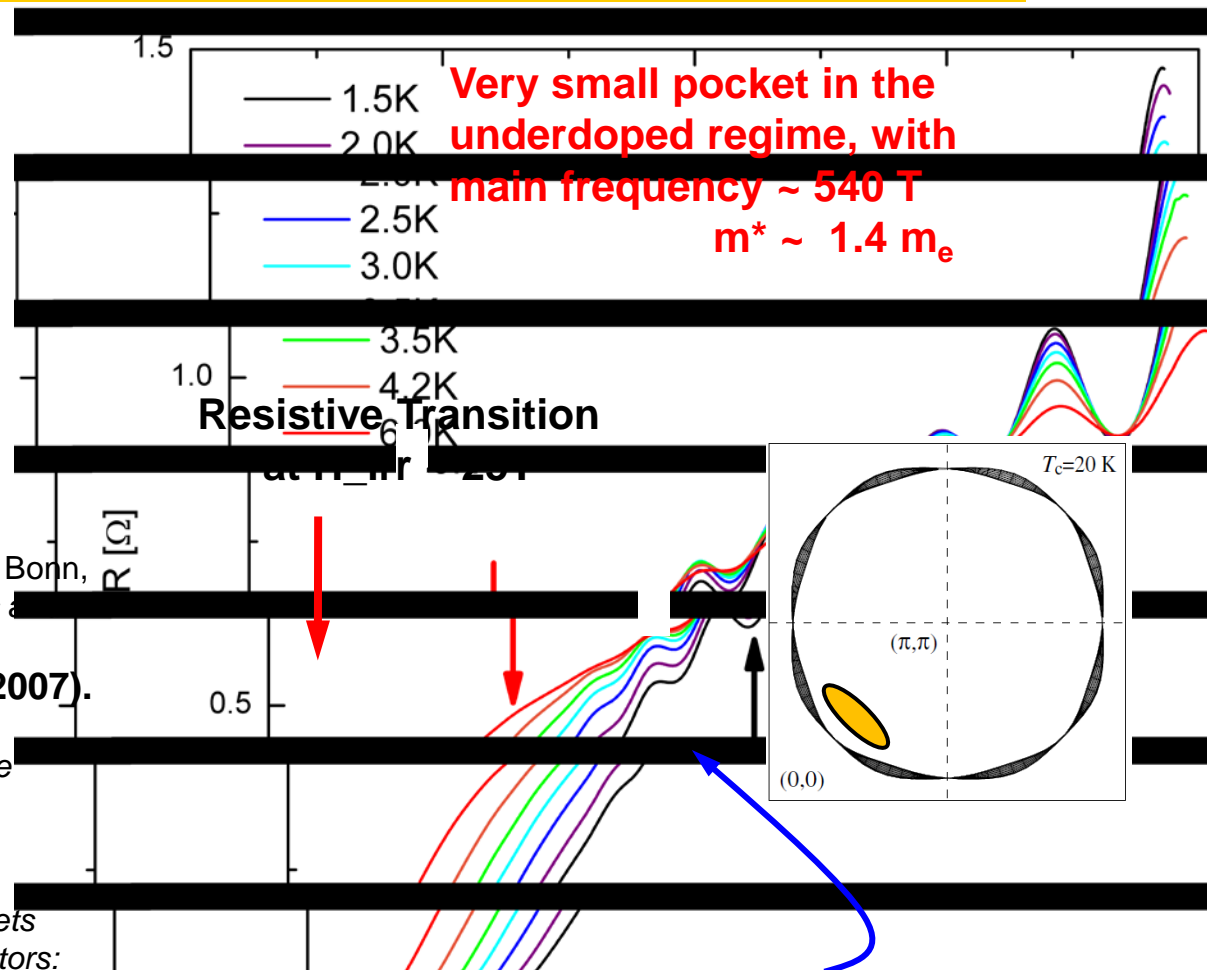


N. Doiron-Leyraud, C. Proust, D. LeBoeuf, J. Levallois, J-B Bonnemaïson, R. Liang, D.A. Bonn, W.N. Hardy, L. Taillefer, "Quantum oscillations at the Fermi surface in an underdoped high- T_c superconductor." **Nature 447, 565-568 (2007).**

Yelland, E. A. *et al.* Quantum oscillations in the underdoped cuprate $YBa_2Cu_4O_8$. **Phys. Rev. Lett. 100, 047003 (2008).**

Bangura A. F. *et al.* Small Fermi surface pockets in underdoped high temperature superconductors: observation of Shubnikov-de Haas oscillations in $YBa_2Cu_4O_8$. **Phys. Rev. Lett. 100, 047004 (2008).**

Jaudet C. *et al.*, de Haas–van Alphen oscillations in the underdoped high-temperature superconductor $YBa_2Cu_3O_{6.5}$. **Phys. Rev. Lett. 100, 187005 (2008).**



B.J.Ramshaw, B. Vignolle, J. Day, R. Liang, W.N. Hardy, C. Proust, D.A. Bonn, Angle dependence of quantum oscillations in $YBa_2Cu_3O_{6.59}$ shows free spin behavior of quasiparticles **Nature Physics 7, 234 (2010)**

Suchitra E. Sebastian *et al.* A multi-component Fermi surface in the vortex state of an underdoped high- T_c superconductor. **Nature 454 200 (2008)**



Doping Dependence of Quasiparticle Number

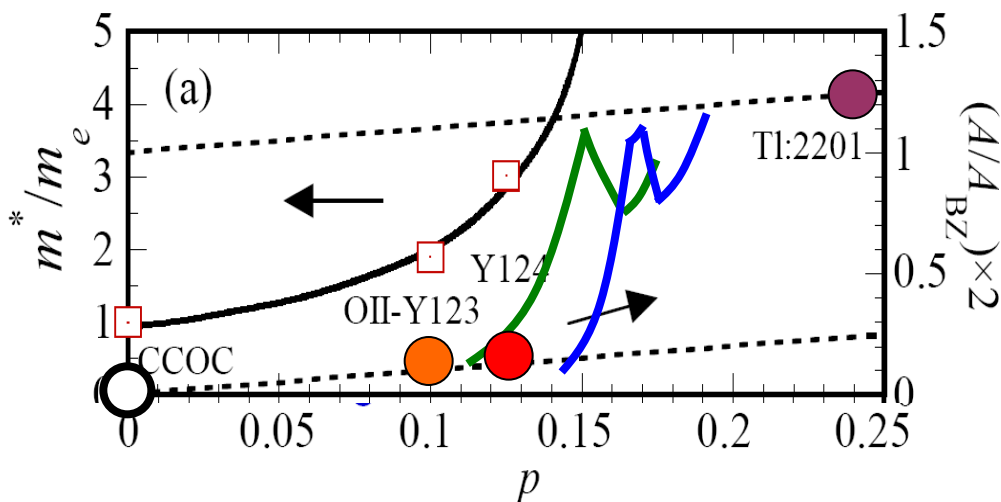
Hall Effect in Single Layer BSLCO

F. F. Balakirev, J. B. Betts, A. Migliori, S. Ono, Y. Ando, and G S. Boebinger, *Nature* **424**, 912 (2003).

Hall Effect in Single Layer LSCO

F. F. Balakirev, J. B. Betts, A. Migliori, I. Tsukada, Yoichi Ando, G.S. Boebinger *Phys.Rev.Lett.* **102**, 017004 (2009)

Effective Mass and Quasiparticle Number



Hussey et al, *Nature* **425**, 814 (2003)

Doiron-Leyraud, et al *Nature* **447** 565 (2007)

Yelland *et al.*, *PRL* **100**, 047003 (2008)



Turning it up to “11”...

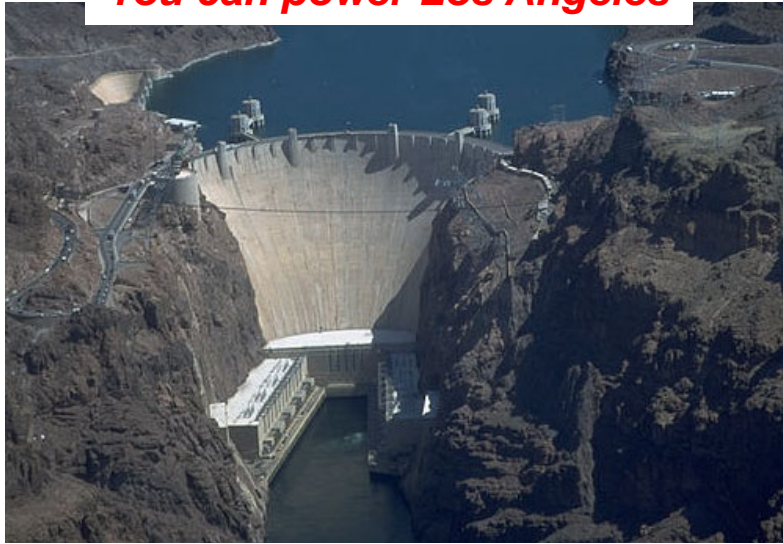


**(Achieved 100T in 2012 for the first time
without blowing something up)**

What can you do with 1,400,000,000 Watts ?

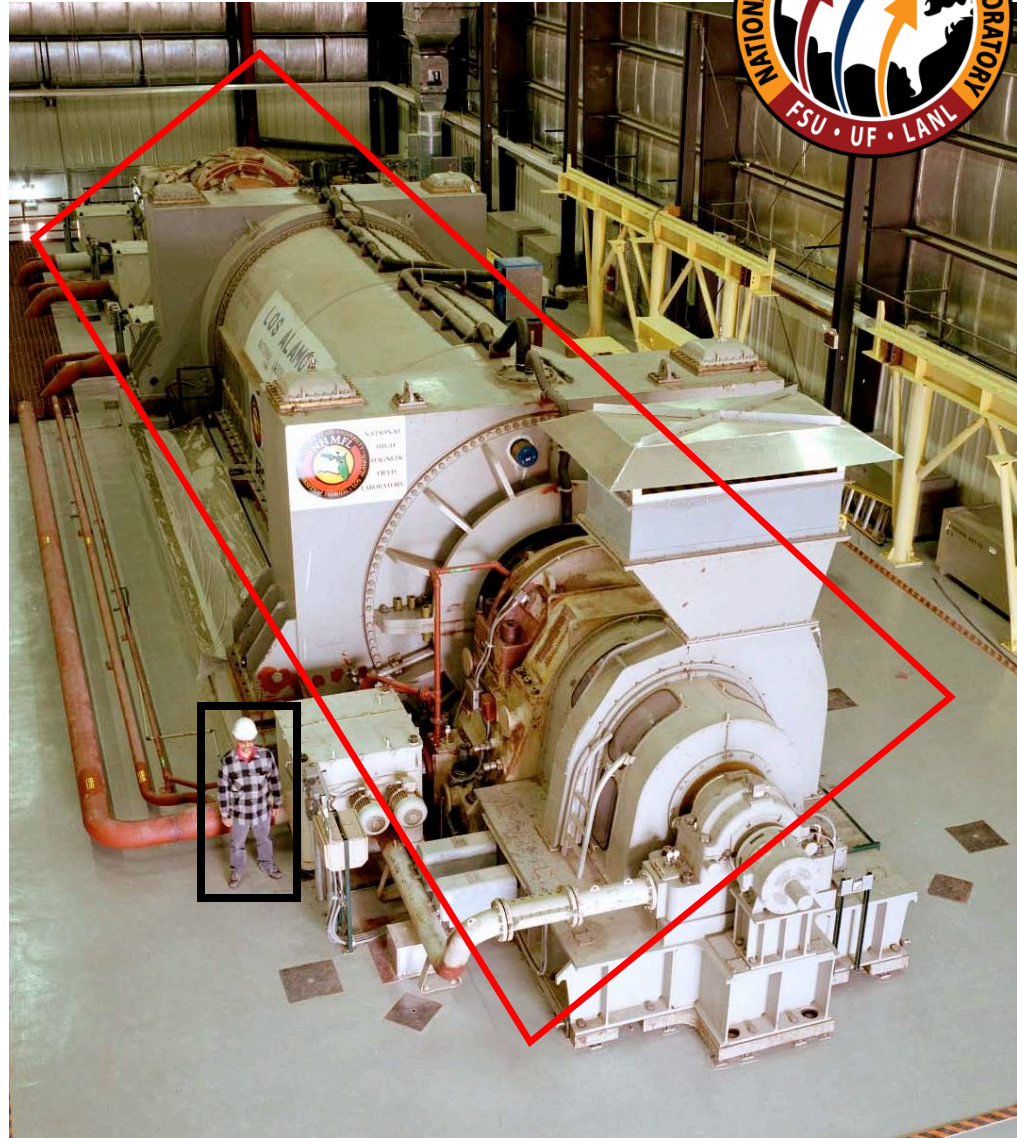


You can power Los Angeles

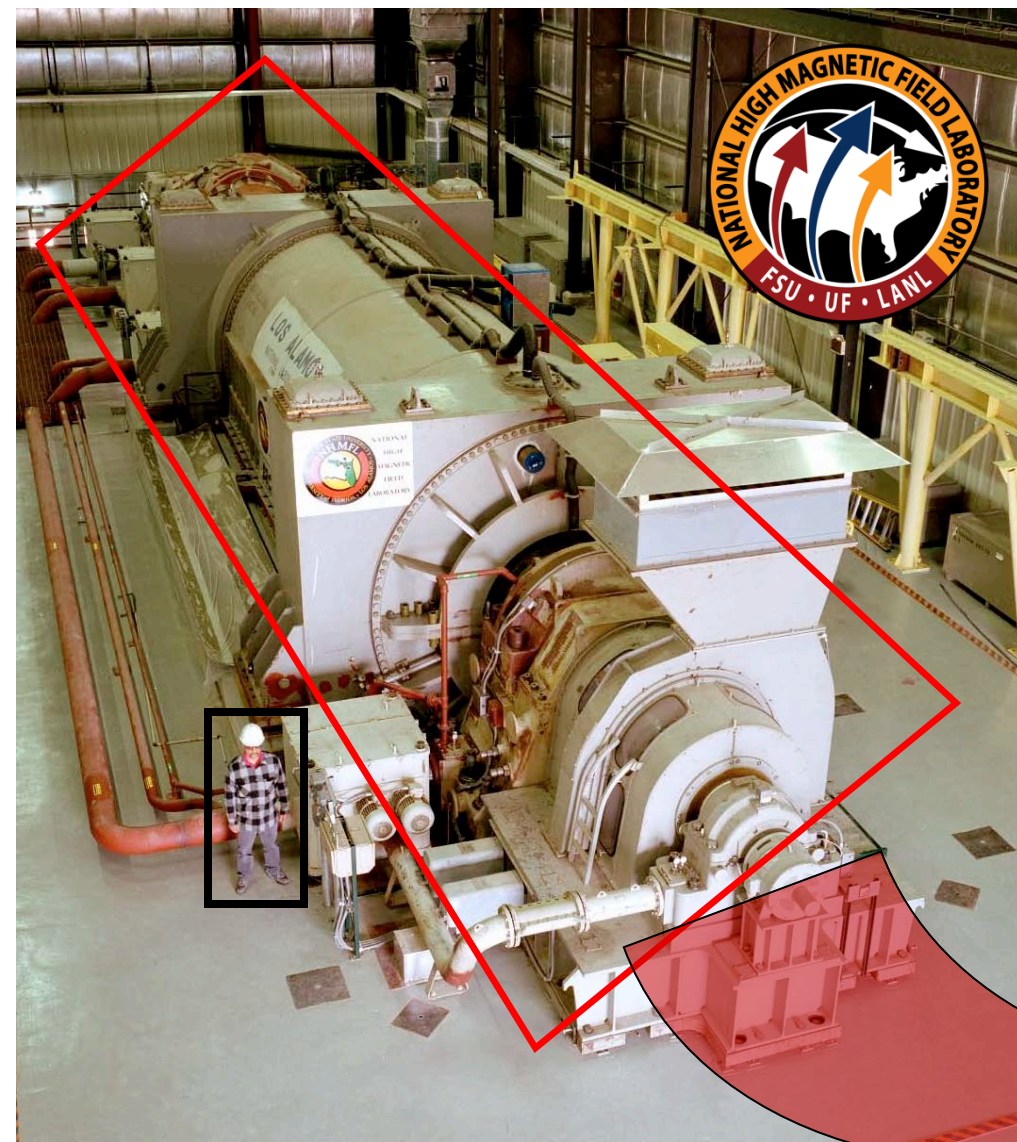


You can go...

BACK TO THE FUTURE



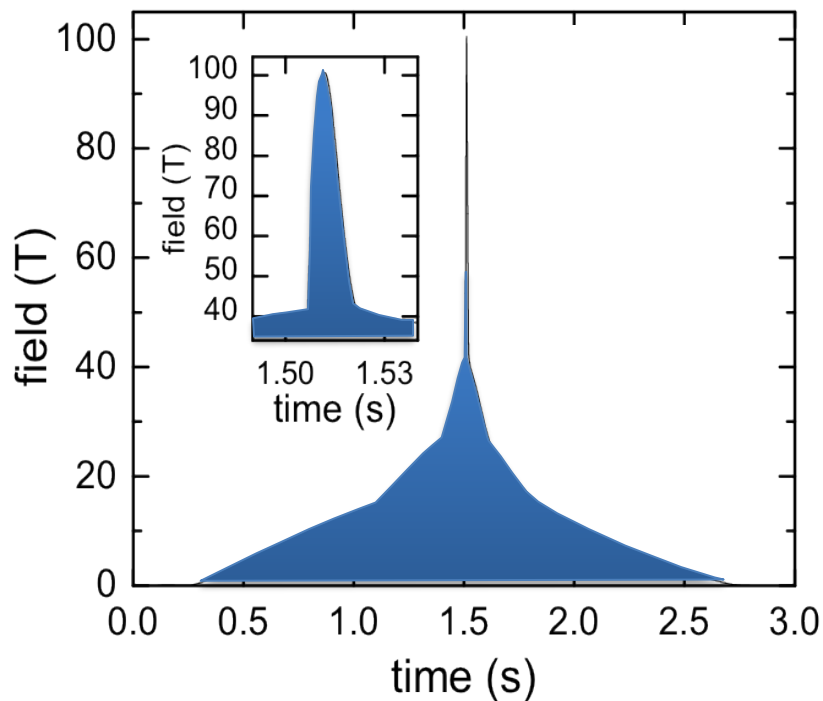
...or you can pulse one magnet



250 Mega Joules = 500 STICKS OF DYNAMITE

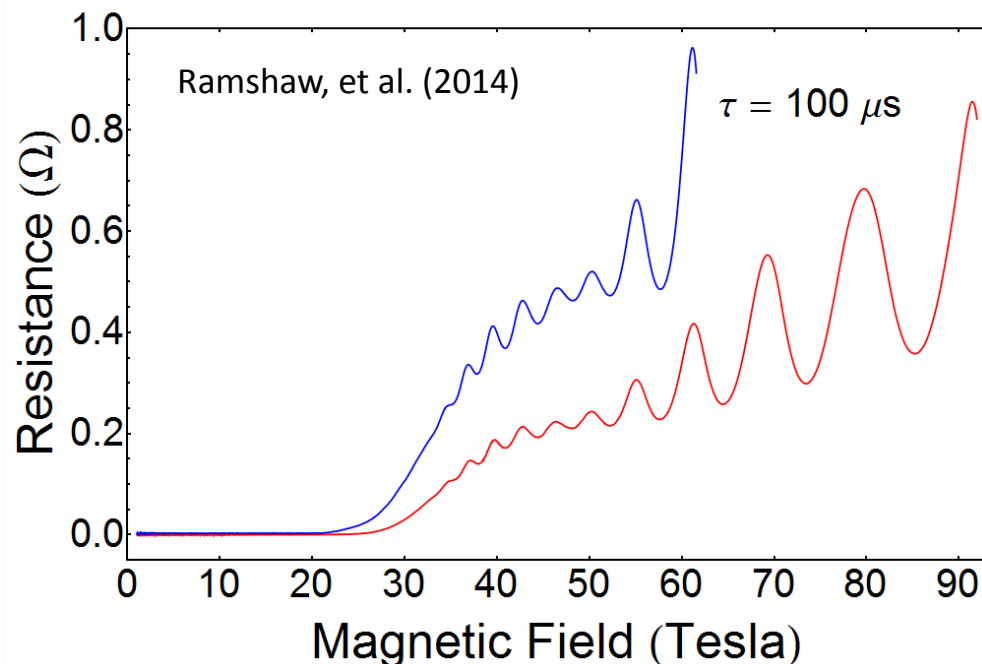


March 22, 2012: 100.7T Pulse (Non-destructively!)

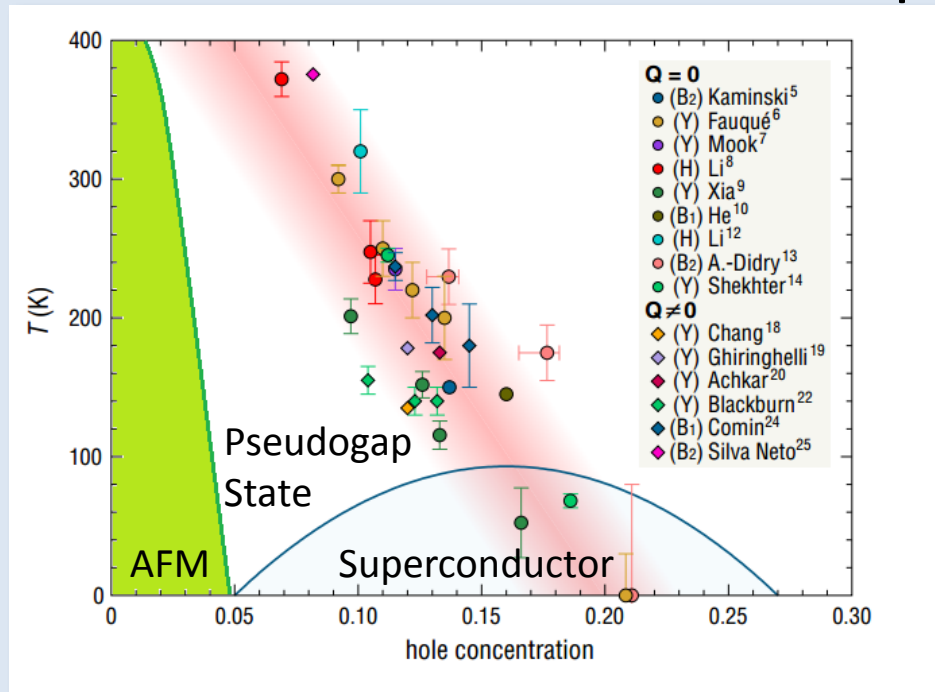


YouTube: Search for "100 tesla magnet"

Many groups have used the 100T magnet to study quantum oscillations in cuprates. We will focus on recent unpublished work by Ramshaw, et al. that is relevant to the question of a critical point at optimum doping.



There IS a Quantum Critical Point Near Optimum Doping



K. Fujita *et al.*,
arXiv (2014)

IN THE UNDERDOPED REGIME:

***Magneto-transport finds a low-density metal ... with logarithmic scattering or localization.
ARPES finds arcs.***

THE ONSET OF THE PSEUDOGAP :

***... is a thermodynamic phase transition, from Resonant Ultrasound Spectroscopy
... is accompanied by many symmetry-breaking phenomena***

AT THE TERMINATION OF THE PSEUDOGAP LINE NEAR OPTIMUM DOPING,

***The linear- T resistivity persists to lowest temperatures
There are anomalies in the Hall number.***

The quasiparticle mass appears to diverge... evidencing enhanced electron interactions

IN THE OVERDOPED REGIME:

***Magneto-transport finds a high-density metal.
ARPES finds a complete Fermi surface.***

Thank You !

Inducing insulating behavior in optimally doped $Y_{1-x}Pr_xBa_2Cu_3O_{7-\delta}$ by increasing disorder. (Don't know if this will be log-T)

Resistivity vs T for (a) $Y_{1-x}Pr_xBa_2Cu_3O_{7-\delta}$. For increasing Pr the T_c drops and the residual resistivity increases, (b) Ion damaged $YBa_2Cu_3O_{7-\delta}$. After bombardment of 1-MeV Ne^+ ions at fluences of (0, 0.1, 2.5, 4.0, 10.0, 15.0, 20.0, and 22.0) $\times 10^{13}$ ions/cm². For increasing ion damage the behavior is similar for increasing Pr in (a).

Electron tunneling and transport in the high- T_c superconductor $Y_{1-x}Pr_xBa_2Cu_3O_{7-\delta}$

PHYSICAL REVIEW B 50, 3266 (1994)
A. G. Sun, L. M. Paulius, D. A. Gajewski, M. B. Maple, and R. C. Dynes

